Heavy Rain Events in Svalbard Summer and Autumn of 2016 to 2018

Ola Bakke Aashamar

UNIS

The University Centre in Svalbard

Thesis submitted for the degree of Master of Science in Meteorology

Department of Geosciences
Faculty of Mathematics and Natural Sciences
University of Oslo

Department of Arctic Geophysics
The University Centre in Svalbard

August 15, 2019

“ Når merket vel dere byfolk her i deres stengte gater selv det minste pust av den frihet som tindrer over Ishavets veldige rom? Sto en eneste av dere noensinne ensom under Herrens øyne i et øde av snø og natt? Stirret dere noen gang opp i polarlandets flammende nordlys og forstod de tause toner som strømmet under stjernene? Hva vet dere om de makter som taler i stormer, som roper i snøløsningens skred og som jubler i fuglefjellenes vårskrik?
Ingenting. “

- *Fritt etter John Giæver, Ishavets glade borgere (1956)*

Acknowledgements

First of all, I am forever grateful to my main supervisor Marius Jonassen, who with his great insight and supportive comments gave me all the motivation and help I needed along the way towards this master thesis.

Big round of applause to all the amazing students and staff at UNIS who I was lucky to meet during my stays in Svalbard, and the people at MetOs in Oslo. The times shared with you inspire me both personally and professionally, and I will always keep the memories!

Then I want to thank Grete Stavik-Døvle, Terje Berntsen, Frode Stordal and Karl-Johan Ullavik Bakken for admitting and guiding two lost NTNU students into studies at UiO. If not for you, who knows what would have happened.

Thanks also to my co-supervisors Chris Borstad and Rich Moore, who with their 'American spirit' saw potential in my project idea, but unfortunately had to leave during the process.

And to the co-supervisor who didn't leave (!) , Kjetil S. Aas, for good support from Oslo, solid feedback and keeping up with my ever-changing motivation and ideas.

Kiitos! to Siiri Wickstrøm for her positivity, good ideas, and general helpfulness with everything.

And a most well earned praise goes out to PhD candidate, Eirik Amadeus Aasmo Finne, for being the ultimate field assistant and best friend.

Around seventy thousand thanks to Jan Christensen's Legat, UNIS Geophysical department and the Department of Geosciences at UiO who funded this project, and to Christian Thoresen who helped with the accounting afterwards.

Many thanks to the helpful amigos John Hult, Thomas V. Schuler and Stefan Claes who assisted me with loggers, cabinets and batteries for the stations. And, of course, Andy Hodson for his inspiring attitude towards field work, and for lending me tools and his field computer without hesitation.

Thanks to Gunnar-Kurt Liahjell and Linn Høeg Volstad with help in assembling and taking down the stations, and Marcos Porcires and Martin Molde Eriksen for skillful boat-driving in a fjord full of ice.

Thanks to Morten Køltzow and Teresa Valkonen at MET for support and guidance in the sometimes confusing world of model data, and for giving me the ECMWF HRES data. And to meteorologist Ine-Therese Pedersen for good discussions about Svalbard weather, and showing me the secrets of the Geonor-200!

I am also thankful to Justyna Wodziczko who gave me the opportunity of working as a forecasting meteorologist at MET, and to my colleagues at VNN for moral support through the final months of thesis writing.

Finally, I am very thankful for the decent upbringing I got from my mom and my dad, and the love and support I have received from them, my siblings and the rest of my family through the years.

And of course Ingvild, who brought me to Svalbard in the first place, and whom I look forward to sharing the rest of my life with!

Abstract

Heavy rain events in the Arctic archipelago Svalbard can have a high impact on nature and settlements, and are predicted to become more frequent and intense in the coming decades. This thesis work focuses on heavy rain events (> 10 mm/24 hr) in summer and autumn season of 2016, 2017 and 2018. Heavy rain events in this period were found to be most common during southwesterly synoptic air flow over the archipelago.

By comparing observations of heavy rain events with precipitation forecasts from the operational weather models AROME Arctic and ECMWF IFS HRES, the ability of AROME Arctic to predict such heavy rain events is evaluated. Both models are found to underestimate heavy rain events for the West-Coast stations Hornsund, Isfjord Radio and Ny-Ålesund, while for Longyearbyen there is a slight overestimation. By evaluating precipitation metrics from a model grid point box, spanning a larger area around the stations, the mean error and mean absolute error are substantially lowered.

To complement the measurements from official MET stations measuring precipitation in Svalbard, six additional automatic weather stations with precipitation instruments were built and set up in the remote Tempelfjorden area, and around Longyearbyen, in the summer and autumn of 2018. The results from the field campaign show that it is possible to make reasonable measurements of heavy rain events in Svalbard from a relatively low-cost field campaign.

In the observation period, the field campaign rain gauges measured one heavy rain event (19. August 2018 - 13 mm) with a maximum hourly intensity of 5 mm/hr. Additionally, a positive precipitation gradient of ~10 % per 100 m elevation was calculated based on field campaign observations. In Tempelfjorden, there seems to be a relation between the direction of large scale synoptic air flow, and when the model is underestimating or overestimating precipitation. Through the field period a persistent undercatchement was found for the official precipitation instrument in Adventdalen, the Geonor T-200B, when compared with field campaign measurements.

Contents

Chapter 1
Introduction

The autumn of 2016 was one of the warmest and wettest autumns ever recorded in Longyearbyen, Svalbard (Heiberg et al. 2016). In October, heavy rainfall in combination with thawing permafrost caused a mudslide that blocked a road and almost wiped out a century old cemetery. In November, more than 90 students were evacuated from their housing in Nybyen due to the forecasted heavy rainfall. During that rain storm, on the 8th of November 2016, 41.7 mm rain was measured over 24 hrs in Longyearbyen, making it the second largest 24 hr precipitation amount ever recorded there.

Heavy rain events of such magnitude are currently a relatively rare occurrence in Svalbard, but the impact on society and nature can be large when they do strike (Dobler et al. 2019). It is therefore important to assess how well the operational weather models forecast such extreme rain events (Køltzow et al. 2019b). In this thesis the ability of the operational weather model AROME Arctic to correctly forecast heavy rain events in Svalbard in the summer and autumn of 2016-2018 is evaluated. Central parts of this evaluation include a comparison against *in-situ* observations from the Norwegian meteorological office's (MET) weather stations, and the coarser global high resolution forecasts (IFS HRES) model from the European Centre for Medium Range Weather Forecasting (ECMWF).

The recently published Svalbard Climate 2100 report, which nicely summarizes the current knowledge of Svalbard climate, states that heavy rain events are likely to be more frequent and intense in Svalbard in the coming century (Hanssen-Bauer et al. 2019). To understand the changes in precipitation that are likely to occur in Svalbard, a key factor is to have a good understanding of the past and present conditions. Currently, precipitation measurements in Svalbard are all conducted in low-elevation locations close to settlements or research stations on the West-Coast of Spitsbergen, and at the smaller remote islands of Bjørnøya and Hopen (Vikhamar-Schuler et al. 2019). In an attempt of balancing this geographic bias, and expand the current knowledge about heavy rain events in Svalbard, a field campaign involving several automatic weather stations measuring precipitation was conducted in remote parts of central Spitsbergen and around Longyearbyen as part of this thesis, in the summer and autumn of 2018.

The main goal of this master thesis is to answer the following questions:

1. How well did the operational weather forecast model AROME Arctic predict heavy rain events in Svalbard, in the summer and autumn of 2016 to 2018?

2. What added knowledge can be gained from a field campaign in the central parts of Spitsbergen with simple rain gauge stations measuring precipitation through a summer and autumn season?

In an attempt to answer these questions, several data sources have been used. These range from *in-situ* measurements from automatic weather stations (AWS) including rain gauges, through remote sensing satellite data from space, to output from the AROME Arctic and ECMWF IFS HRES weather prediction models.

The remainder of this thesis is structured as follows: In Chapter 2, important theoretical concepts for the scope of the thesis are introduced and explained. Chapter 3 gives an introduction to the study areas in Svalbard. In Chapter 4, the different weather stations, NWP models, and the subsequent data handling procedures are described. As this thesis aims to answer two separate, but connected main questions, heavy rain observation statistics, model evaluation and field campaign results are presented and discussed separately in Chapter 5. Finally, in Chapter 6, conclusions are drawn and future outlook is discussed.

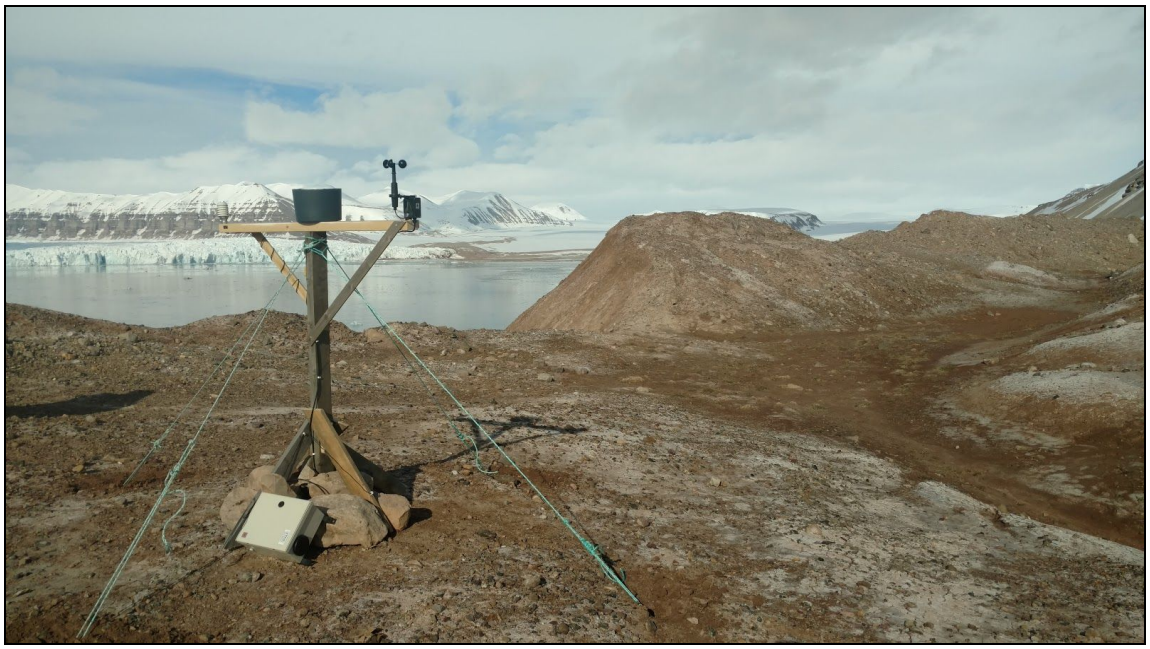

Figure 1.1: *One of the automatic weather stations set up for this thesis, overlooking Tunabreen.*

Chapter 2
Theory

2.1 Precipitation

Precipitation is an important, albeit difficult, meteorological variable to predict, as its existence depends on a complex interplay of micro- and thermophysics in clouds. Precipitation occurs when water vapour condenses onto cloud condensation nuclei (CCN) in the air and further accumulates into drops or crystals that are heavy enough to fall towards the ground (Wallace and Hobbs 2006). The main driver of this condensation process is often rising motion of air, which causes the air to expand in lower ambient pressure, and subsequently cool sufficiently enough for water vapour to condense.

Precipitation Processes

Precipitation is often differentiated based on which physical process that causes the air to rise. Large-scale, or frontal, precipitation occurs from the rising motion along cold or warm fronts of extratropical cyclones. Convective precipitation, or showers, are often less prolonged in time and space but more intense than frontal precipitation, and occurs when the atmosphere is in an unstable state, where warmer air rises through colder air due to differences in density caused by the differences in temperature. This process is often generated by air that is warmed by the surface and starts rising through colder air aloft, but additional lift can be generated by turbulence or large scale lifting caused by upper level troughs. As is often the case for the chaotic atmosphere, these physical mechanisms causing precipitation are not always easy to separate. Convective cells are for example often found along cold fronts or embedded in occluded fronts.

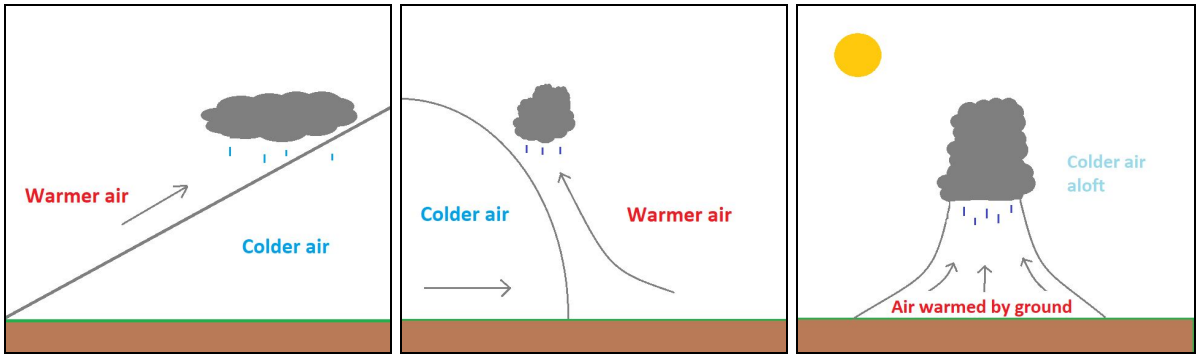

Figure 2.1: *General concepts of how precipitation is caused by warm fronts (left panel), cold fronts (central panel) and convection (right panel). Arrows indicate general air motion.*

Orographic Precipitation

Orographic precipitation occurs when the rising motion is caused by mountains that force air to rise over the topography, when advected towards them. Additional mechanisms that help to intensify orographic precipitation are the low level clouds (stratus) often found over mountains under these conditions. These clouds contain small drops that function as feeder drops for the larger rain drops falling through them from higher parts of the cloud deck. Additionally, the short distance from cloud base to the ground, leaves little time for the rain drops to evaporate before reaching the ground (Førland et al. 1997). In connection to orographic precipitation it is also worth mentioning the spillover effect, or lee side precipitation, and the rain shadow effect. The spillover effect is when orographic lifting is causing increased precipitation on the leeward side of the mountain range that caused the initial lifting (Milne and Wallmann 2007). The opposite is the rain shadow effect, where the moisture has already precipitated out of the atmosphere on the windward side before reaching far beyond the mountain ranges (Milne and Wallmann 2007). What determines if an event exhibits spillover or rain shadow characteristics is a complex question, and can be linked to several variables such as wind speed, wind direction, mountain waves and atmospheric stability (Milne and Wallmann 2007). Orographic precipitation is often seen in combination with frontal systems or atmospheric rivers (Neiman et al. 2013). In Svalbard, studies have shown that orography plays an important role for precipitation in Svalbard (Førland et al. 1997), and precipitation elevation gradients (increased precipitation with increasing elevation) of between 4-28 %, with an average of 14%, have been proposed for the Svalbard area by different studies (Killingtveit et al. 2003).

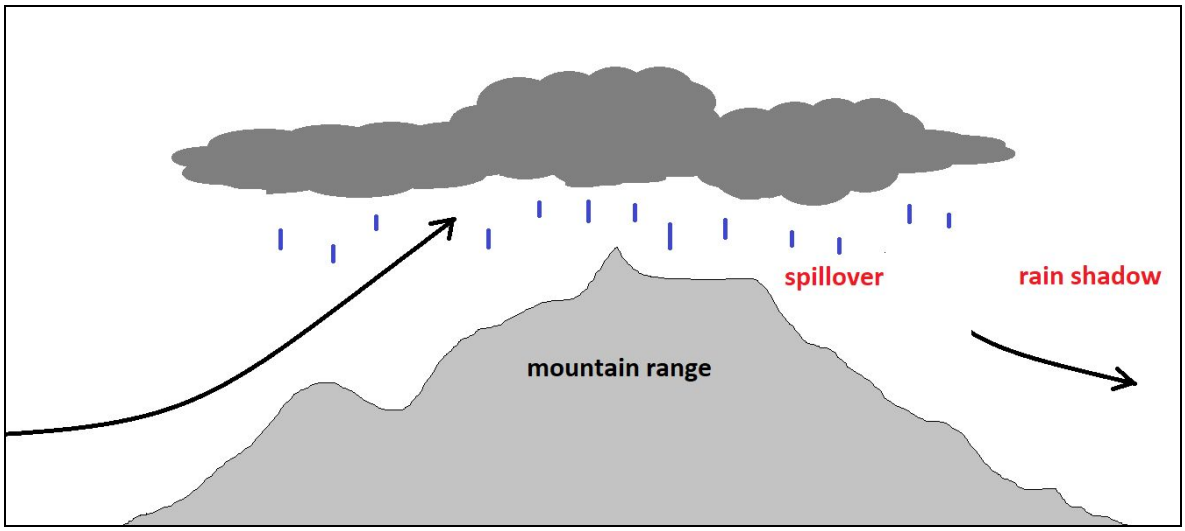

Figure 2.2: *General concept of orographic precipitation. Two areas where the spillover and rain shadow effect is in place in this example, are also denoted.*

Precipitation States

Precipitation can reach the ground in several different states such as liquid (rain), solid (snow, hail) or a combination (sleet). The state of precipitation reaching the ground depends both on the temperature in the cloud and in the underlying air. Several studies have shown that with climate change there will likely be more rain than snow in the Arctic at the end of the century (Bintanja and Andry 2017). In Svalbard, such a shift might already be in progress (Vikhamar-Schuler et al. 2019).

Observations of Precipitation

Precipitation is a challenging meteorological variable to measure correctly, mainly due to wind affecting the hydrometeors, but also the wide range of different instrument types used for measurements. Traditionally, observations have been conducted by measuring the accumulated amount of precipitation in a certain time span. For manual measurements this is normally done once or twice a day, in the morning at 06Z and the evening at 18Z, which results in 24 or 12 hours accumulated precipitation values. If a precipitation event happens to occur around the time of measuring the accumulated amount, it might split into two separate observations, and some heavy precipitation events can thus be hidden in daily precipitation data sets. Today, automated rain gauges easily provide hourly precipitation values, and even more novel measuring techniques such as radars or optical sensors can give instantaneous precipitation values. In Svalbard there are unfortunately no operational precipitation detecting radars, and only one station with an optical precipitation sensor (see Section 4.1.1).

Model Representation of Precipitation

In numerical weather models, physical processes involved in precipitation, and the subsequent precipitation rate itself, are parameterized based on variables such as temperature, and cloud water (ECMWF 2018). As mentioned, these variables often depend on the vertical velocity in the air, and there are generally two ways of calculating this. The method used in many regional models is the so-called non-hydrostatic scheme, which allows for vertical motion and convection in the models' dynamical scheme. More widely used in global weather forecast, or climate, models, as it requires less computation and spatial and temporal resolution, is the hydrostatic scheme where the vertical momentum equation is not solved and instead the hydrostatic approximation is applied. (ECMWF 2018). Also worth noting, is that in many reanalysis datasets precipitation is one of the few important meteorological variables for which observations are not assimilated (e.g. Dee et al. 2017).

Chapter 3
Study Area and its Precipitation Climate

3.1 Svalbard

Svalbard is an archipelago located in the high Arctic between 74 - 81 degrees north, and 10-30 degrees east. It is situated in the northernmost parts of the Atlantic Ocean, between Greenland and the Barents Sea, at the end of the Atlantic cyclone track (Humlum 2002). The most intense cyclones in this area occurs in autumn and winter (Humlum 2002; Hanssen-Bauer et al. 2019) Svalbard consists of several islands, with Spitsbergen being the largest island where the largest settlements Longyearbyen, Barentsburg and Ny-Ålesund are located. In addition, there are manned meteorological stations at the smaller islands of Hopen and Bjørnøya, and a manned research station in Hornsund (Fig. 3.1).

The climate of Svalbard is considered tundra (ET) in the Geiger-Köppen climate classification, with cold temperatures year around, and in general little precipitation (Eckerstorfer and Christiansen 2011). Despite this, it is one of the warmest areas at its latitude, due to the relatively warm waters of the North Atlantic Ocean current flowing along its western coast as the West Spitsbergen Current (Teigen et al. 2010). In the winter and spring, the islands are often surrounded by sea ice in the north and east. Sea ice cover plays an important role for climate in this region, as it strongly influences heat and moisture exchange between the atmosphere and the ocean (Isaksen et al. 2016), although with regards to heavy rain events it is not that important.

The mean annual precipitation at the MET stations (1971-2000) varies from just below 200 mm/year in Longyearbyen to above 400 mm/year at Ny-Ålesund and Hornsund, respectively (Dobler et al. 2019). For the stations with the longest running time series there is an increase in mean annual precipitation for all stations, with the largest increases occurring in the autumn season (Dobler et al. 2019). There appears to be some decadal variations in the mean annual precipitation, but it is not as clear as for the mean annual temperature signal, and it is not in phase at the different stations. Interestingly, regional climate models do not necessarily show a similar increase as observations in annual precipitation levels for the total land area of Svalbard (Vikhamar-Schuler et al. 2019). It is therefore proposed that some of the observed increase might be due to a shift in precipitation phase that accompanies the increasing temperatures, and causing less undercatchement by the rain gauges (Vikhamar-Schuler et al. 2019).

Heavy rain events are not very common in Svalbard, but occur most frequently in autumn and winter. Interestingly, the maximum 24hr accumulated precipitation record for Svalbard (98 mm, 30. January 2012, Ny-Ålesund) is higher than for Finnmark (78.2 mm), Østfold (89 mm) and Akershus (95 mm) based on measurements up until 2016 (*"Fylkesvis oversikt over høyeste registrerte nedbørsmengde (mm) for ulike varigheter"* n.d.)

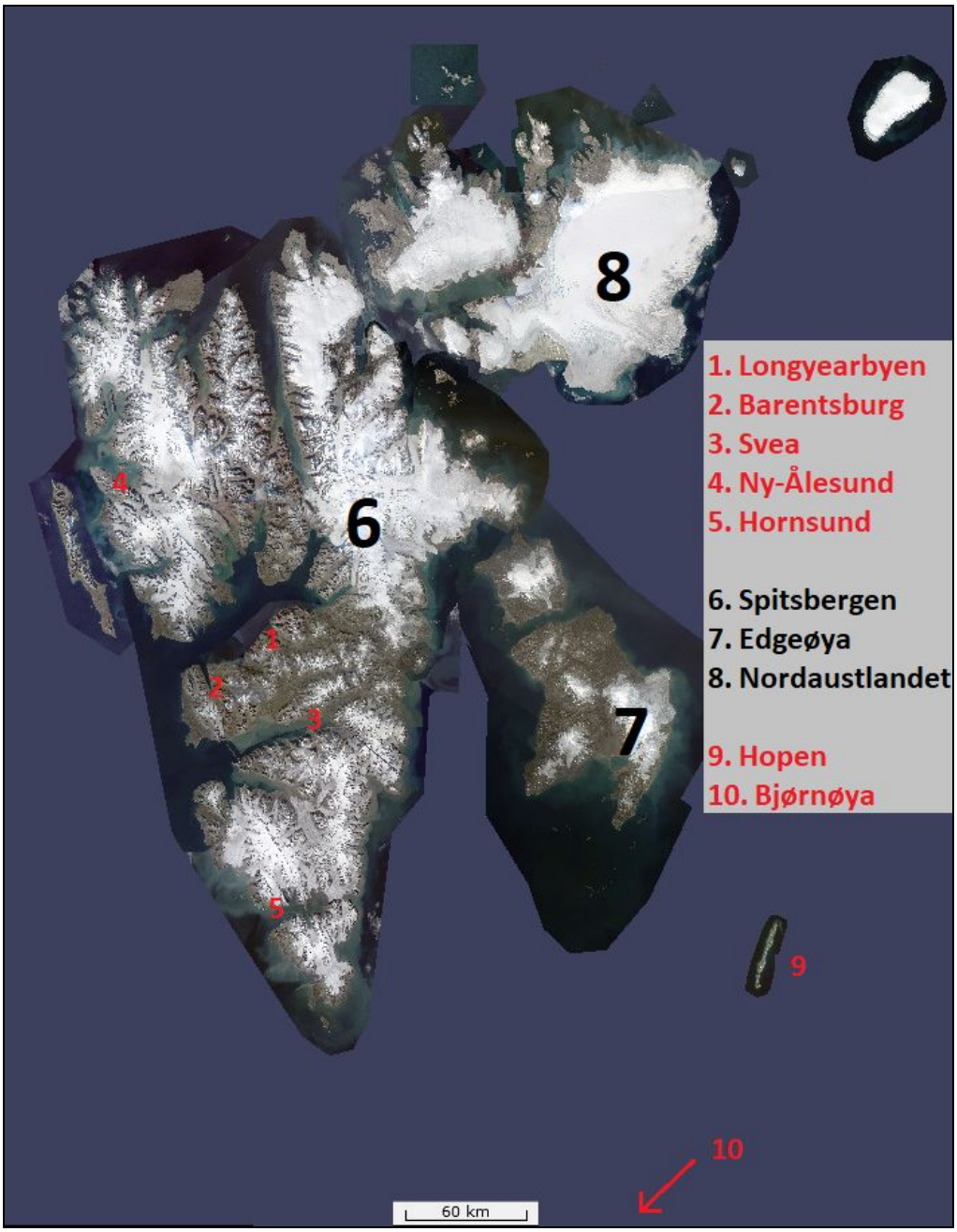

Figure 3.1: *Composite satellite image of Svalbard in summertime, with important place names included. Source: Norwegian Polar Institute, toposvalbard.npolar.no.*

3.2 Longyearbyen and Adventdalen

Longyearbyen is the largest settlement in Svalbard, located on the southeast side of Isfjorden, in the central parts of Spitsbergen. It has around 2000 inhabitants and is located in a valley with surrounding mountains reaching from 400 - 1000 m.a.s.l, mainly south of the settlement (Fig. 3.1, Fig. 3.2)

Figure 3.2: *Longyearbyen as seen from Hiorthfjellet (~900 m.a.sl.), towards the south. Important place names are included.*

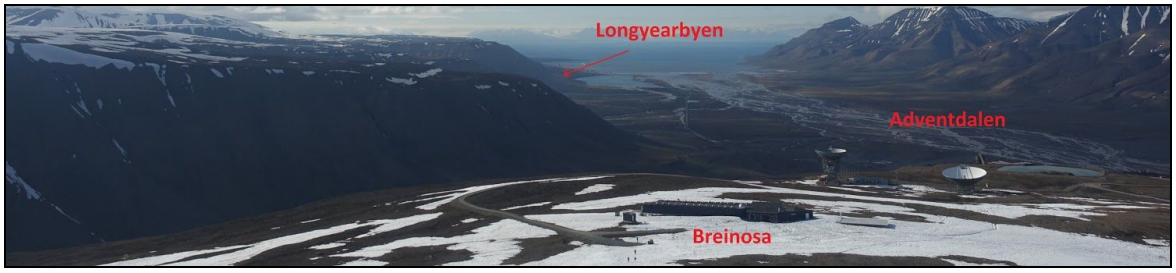

Figure 3.3: *Adventdalen as seen from Breinosa (~500 m.a.s.l.). Important place names are included.*

There is in general relatively little precipitation falling in Longyearbyen, with a mean annual precipitation recorded at Longyearbyen Airport of around 200 mm (Dobler et al. 2019), the lowest of the precipitation measuring stations in Spitsbergen. On average, there are just 8 days per year in Longyearbyen where the daily observed precipitation exceeds 5 mm. Since measurements started (1964) there has been an increase in annual precipitation of approx 4 %, with the largest increase in summer and autumn (Dobler et al. 2019). Although, as mentioned, some of this increase might be due to a shift from snow to rain leading to more catchment by the rain gauges. The strongest heavy rain event recorded here was the 5.August 1981 with 43.7 mm in one day, and the 08.November 2016 event being the second strongest with 41.7 mm (Dobler et al. 2019).

Adventdalen is one of the largest valleys in central Svalbard, around 30 km long and up to 5 km wide. Longyearbyen is located in the westernmost side valley, and in the middle runs Adventdalen river (Fig. 3.3). The valley is often channeling winds from the east toward the Longyearbyen Airport, and on some occasions sand-storms formed by wind and fine sediment can be present in the valley.

A more detailed description of the climate in the Longyearbyen area can be found in the newly released Svalbard 2100 report, and its background reports, which sums up the current knowledge about Svalbard and Longyearbyen climate in a detailed way (Dobler et al. 2019; Hanssen-Bauer et al. 2019; Vikhamar-Schuler et al. 2019).

3.3 Tempelfjorden and Tunabreen Area

Tempelfjorden is a side fjord on the northeast side of the larger Isfjorden, in central parts of Spitsbergen. With the surging tidewater glacier Tunabreen at its northeastern end it is considered a hotspot for climate research and is studied by several scientific campaigns by UNIS, and other institutes (e.g. Ericson et al. 2019; Flink et al. 2015; Fleming et al. 2013; How et al. 2019; Sevestre et al. 2015).

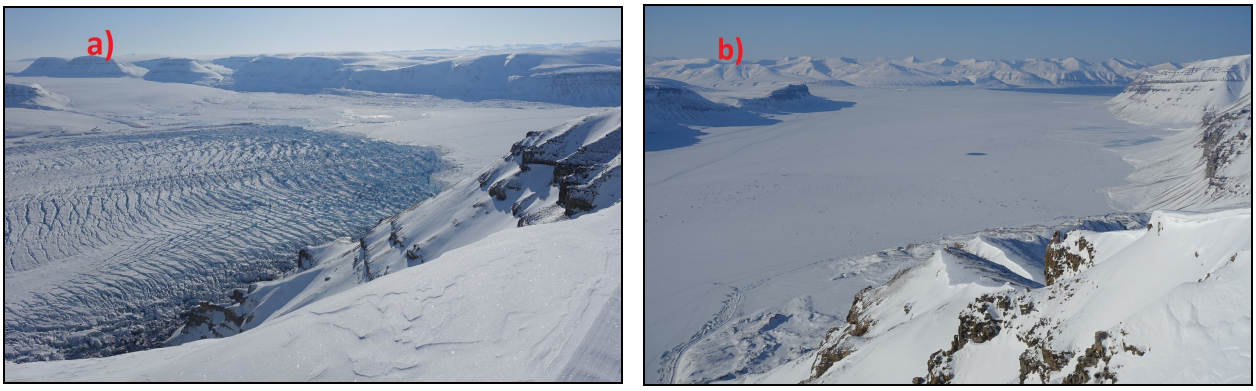

Figure 3.4: *a) The glacier tongue of Tunabreen seen from Ultunafjella (600 m.a.s.l.), towards south. b) The Ice-covered Tempelfjorden seen from Ultunafjella, towards southwest.*

Tempelfjorden is a relatively narrow fjord 30 km across, with mountains to the northwest, and southeast reaching 600 - 800 m.a.s.l (Fig 3.4). From the end of Tempelfjorden, it is only 35 km to the East-Coast over the Fimbulisen glacier cap (~700 m.a.s.l.). Few measurements of precipitation have been done in the area around Tempelfjorden, the closest measurements are possibly the ones conducted in Pyramiden from 1948 - 1957, 33 km further northwest (Ivanov et al. 2014).

Tunabreen is one of the most active surging glaciers in the world, with four surges occuring in the last century. In November 2016 satellite images again showed that a surge had started in Tunabreen, around 20 years earlier than expected (Borstad 2017). Only one heavy rain event was measured in the Tempelfjorden area by the field campaign of the present study, but the dataset still remains interesting as few precipitation observations are being conducted in these parts of Svalbard.

Chapter 4
Data and Methods
4.1 Measurements and Weather Stations

In Svalbard, including the islands Bjørnøya and Hopen, 18 official meteorological stations are currently (2019) operated by the Norwegian Meteorological office (MET). Of these, only nine measure precipitation. The standard automated rain gauge used by MET, Geonor T-200B, requires a power source to melt the collected snow before measuring it, and since Svalbard consists mostly of remote areas with little or no infrastructure, MET measures precipitation in Svalbard only at manned stations or in proximity to settlements.

To complement the nine MET stations utilized in this thesis, a total of six field campaign rain gauge stations were assembled and deployed in central Spitsbergen for the summer and autumn of 2018. Two of these stations were installed next to existing MET stations, while four stations were placed at locations close to Tunabreen and on a mountain plateau by Adventdalen.

The following sections will give an overview of the MET stations in Svalbard and the field campaign rain gauge stations deployed there through summer 2018, which together provided the precipitation measurements that were used in this study.

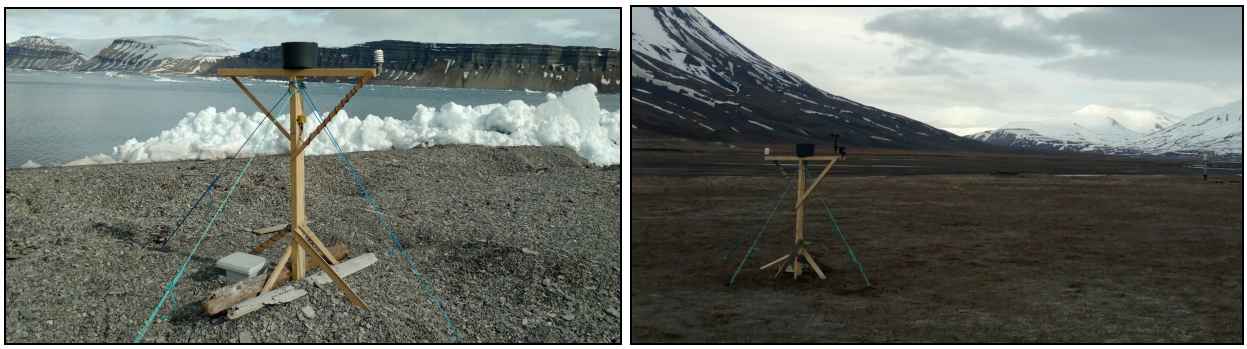

Figure 4.1: *The Bjonapynten station set up by Tempelfjorden for the field campaign (left). The semi-permanent station set up close to the Geonor T-200B in Adventdalen (right).*

4.1.1 MET Weather Stations

The MET stations in Svalbard span a large area, from Bjørnøya at 74N to Ny-Ålesund at 79N, which is a distance of more than 500 km. There are also considerable differences among the stations' localities with respect to environmental factors such as adjacent topography, ocean influence, and instrumentation for measuring precipitation. In Table 4.1, some specifications are given for these MET stations.

Table 4.1: *MET Stations in Svalbard with specifications.*

Station Name	Location	Operating Since	Instrument	Measuring interval
Longyearbyen Airport	N78 E16	1964	Manual rain gauge	daily
Adventdalen	N78 E16	Nov 2016	Geonor T-200B	hourly
Platåberget III	N78 E15	Mar 2018	Optical sensor	hourly
Sveagruva II	N78 E17	Nov 2016	Geonor T-200B	hourly
Isfjord Radio	N78 E14	2015	Geonor T-200B	hourly
Hornsund	N77 E16	1985	Manual rain gauge	daily
Ny-Ålesund	N79 E12	1974	Manual rain gauge	daily
Hopen	N77 E25	1944	Manual rain gauge	daily
Bjørnøya	N75 E19	1910	Manual rain gauge	daily

Ideally, all the MET stations would have the same instruments and temporal resolution output to make their data series as comparable as possible, but this is not the case. Out of the nine MET stations used in this study, five stations are manned and measure precipitation manually on a daily (24hr) basis from a standard rain gauge collector at around 06Z every day (Table 4.1). The remaining four stations are fully automated and measure precipitation at hourly intervals. Three of the automated stations are equipped with the Geonor T-200B ("Geonor T-200B datasheet" n.d.) heated precipitation bucket, while Platåberget III uses an optical precipitation sensor ("Thies Laser Precipitation Monitor datasheet" n.d.).

For the discussion and analysis, it is beneficial to group the precipitation measuring MET stations by their locations. The stations can be divided into three main geographic areas: West-Coast, Central Spitsbergen and Island stations, as can be seen in Figure 4.2

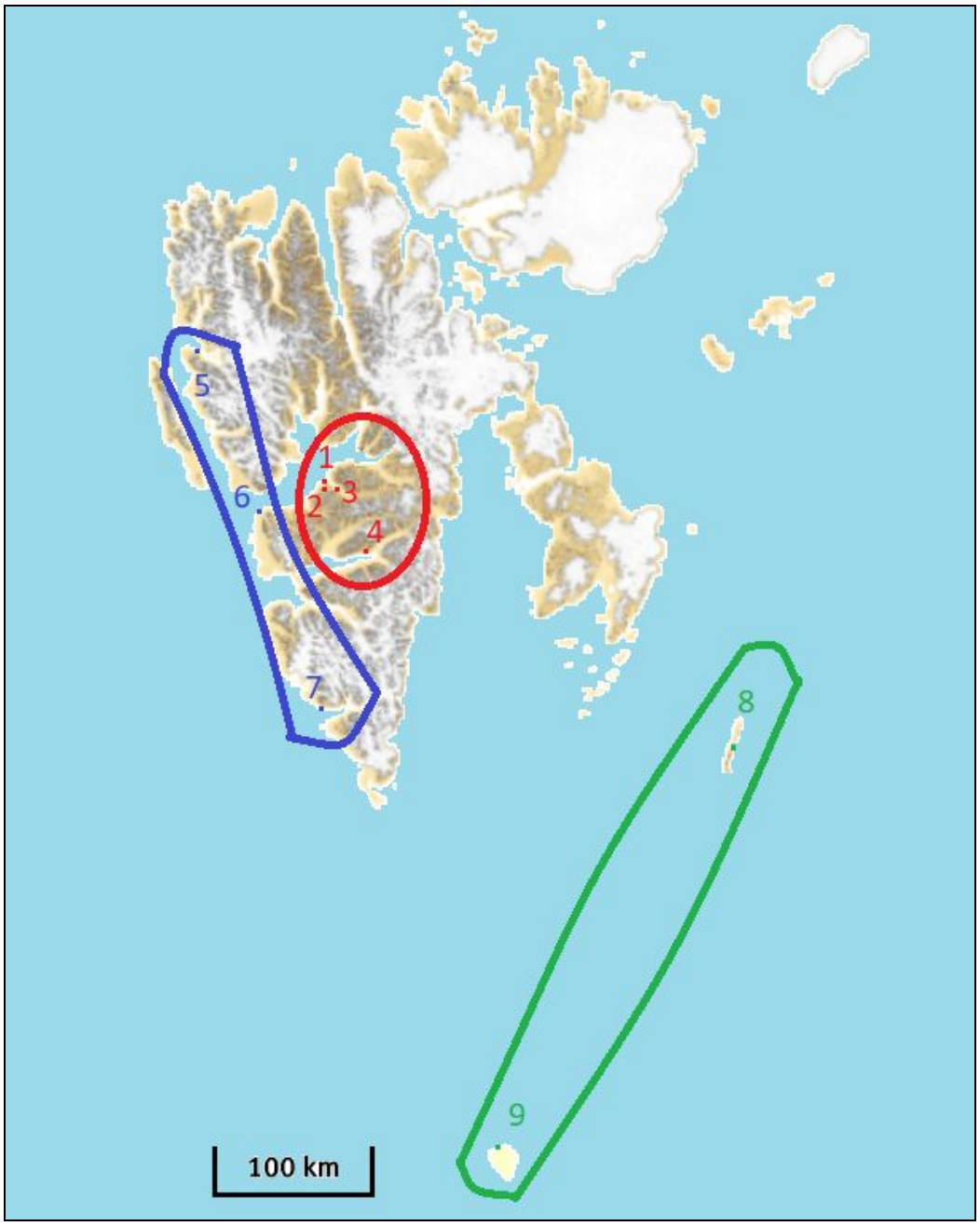

Figure 4.2: *Map of the Svalbard Archipelago, with official precipitation stations numbered. Blue, red and green lines highlight the West-Coast, Central Spitsbergen and Island station regions, respectively. 1 = Longyearbyen Airport, 2 = Platåberget III, 3 = Adventdalen, 4 = Svea II, 5 = Ny-Ålesund, 6 = Isfjord Radio, 7 = Hornsund, 8 = Hopen, 9 = Bjørnøya.*
Source: Norwegian Mapping Authority, norgeskart.no

West Coast Stations

The West-Coast stations Hornsund, Isfjord Radio and Ny-Ålesund, are spread along the West-Coast of the main island Spitsbergen.

Figure 4.3: *Birds-eye view of the West-Coast stations, seen from the west.*
Source: NPI, toposvalbard.npolar.no

Hornsund is located on the north side of the Hornsund fjord (Fig. 4.3), and is the southernmost station measuring precipitation on Spitsbergen. Northeast of the station are the mountains of Wedel Jarlsberg land (~700 m.a.s.l.).

Isfjord Radio is located on the south side of the mouth of Isfjorden, situated just northwest of the mountain range Linnéfjella (~750 m.a.s.l.).

Ny-Ålesund, is the northernmost MET station measuring precipitation in Svalbard. It is located on the south side of Kongsfjorden, northeast of the mountain ranges of both Brøggerhalvøya and Prins Karls Forland (Fig. 4.3).

The coastal stations are all affected by relatively warm ocean surface waters of the West Spitsbergen Current (WSC) that runs northward along the West-Coast of Spitsbergen (Hanssen-Bauer et al. 2019) . The topography adjacent to the stations is also of importance, as it makes orographic induced precipitation likely during south or southwesterly flow, with moist air impinging on the West-Coast mountain ranges (Førland et al. 1997).

Central Spitsbergen Stations

The Central Spitsbergen stations are located in and around the two settlements of Longyearbyen and Svea. In the Longyearbyen area there are three stations: Longyearbyen airport, Adventdalen and Platåberget III. In Svea there are two MET stations, but only Svea II measures precipitation.

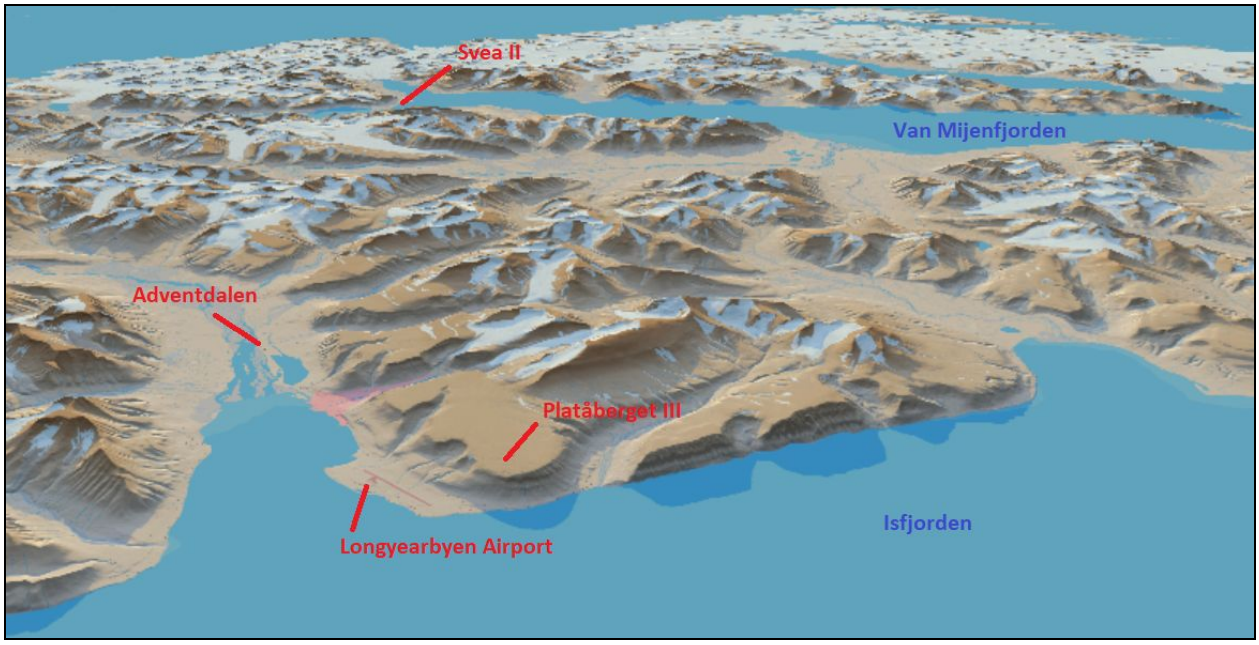

Figure 4.4: *Birds-eye view of the central Svalbard stations seen from northwest. MET station names included. Source: NPI, toposvalbard.npolar.no*

Longyearbyen Airport meteorological station is located at Hotellneset on the southeast side of Isfjorden, four kilometers northwest of Longyearbyen city center.

Platåberget III station is located 2.5 km southwest of the airport (Fig. 4.4). This is the newest official MET station operating in Svalbard, since March 2018, and the only station with an optical precipitation sensor. It is also the highest located MET station in the archipelago, at ~450 m.a.s.l.

Adventdalen station is located 9 km to the east of Longyearbyen, in the middle of the valley Adventdalen. Despite being only eight kilometers from the shore of Adventfjorden (Fig. 4.4), Adventdalen is the MET station in Svalbard farthest from the ocean. Since starting measuring in 2016, this station has captured noticeably less precipitation than Longyearbyen airport throughout the year. If there is an actual climatological difference between the two stations, or instrumentation problems is discussed further in Section 5.3.5.

Around 40 kilometers southeast of Longyearbyen lies the station Svea II, in the now abandoned mine settlement of Svea. The station has been operating since November 2016, and is located in the northeastern end of Van-Mijen fjord. It is the easternmost MET station measuring precipitation on Spitsbergen and it lies closer to the East-Coast than the stations around Longyearbyen.

Although the central parts of Spitsbergen receive less precipitation than the coastal regions (Vikhamar-Schuler et al. 2019), the stations here are important due to their location close to the main settlements and infrastructure in Svalbard, and in an area of frequent outdoor activity. The central Spitsbergen stations are also surrounded by mountain ranges, and are consequently not as exposed to the open ocean as the other stations.

Island Stations

The two island stations, Hopen and Bjørnøya, are located 200 km east and 240 km south of the main island Spitsbergen, respectively.

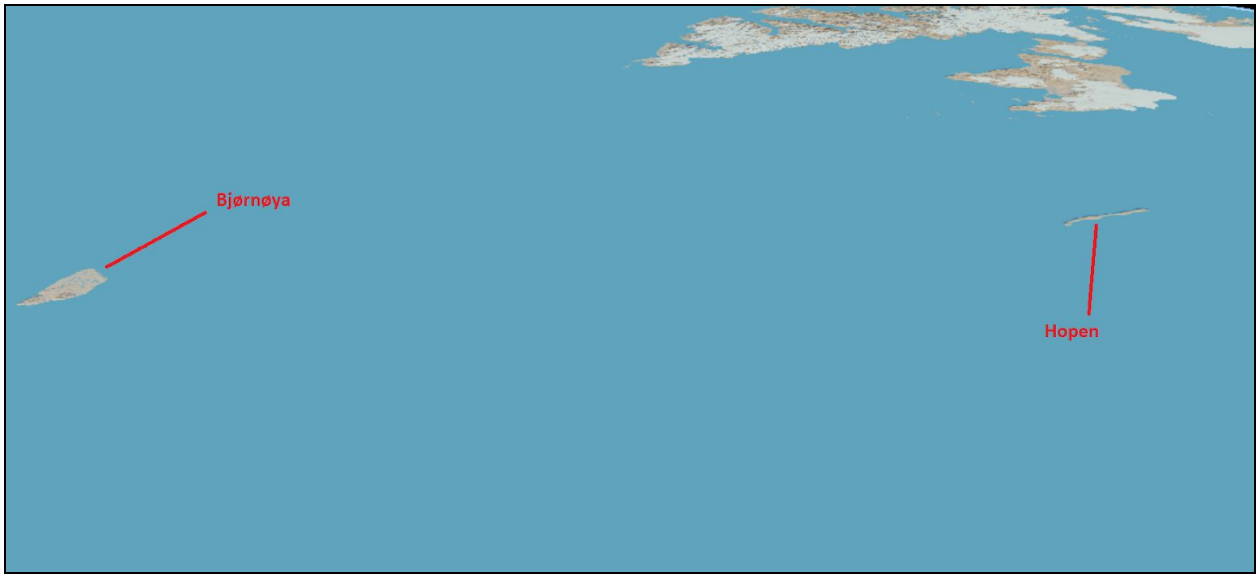

Figure 4.5: *Birds-eye view of the central Svalbard stations seen from southeast.*
Source: NPI, toposvalbard.npolar.no

Hopen is the easternmost station that measures precipitation in Svalbard (Fig. 4.5 and 4.2). It is an elongated remote island in the western parts of the Barents Sea. The island consists of an approximately two kilometers wide and 300 m high mountain range, stretching 30 km north-south. The MET station itself is located in the middle of the island, on the eastern side.

Bjørnøya is the southernmost station included in this study, and is located midway between Northern Norway and Svalbard (Fig. 4.5 and 4.2). The island is relatively small (178 km²) with the highest peak reaching 500 m.a.s.l., but most of the island being below 100 m height.

The two island stations do not have any massive topography in their proximity, and are located so that they often experience different weather conditions than Spitsbergen.

4.1.2 Field Campaign Rain Gauge Stations

In addition to the nine MET stations measuring precipitation in Svalbard, six field campaign rain gauge stations were built and deployed in the Tunabreen/Tempelfjorden area and around Longyearbyen during the summer and autumn of 2018. This was done mainly as an attempt to measure heavy rain events similar to the ones in 2016 in other areas than where MET stations are located, but they also turned out to be useful in evaluating measurements from the MET stations around Longyearbyen and for evaluating the operational weather forecast model AROME Arctic.

Figure 4.6: *Large rain gauge station (left) and small rain gauge station (right). Student (174 cm) for scale. The manual precipitation gauge at Longyearbyen airport MET station is seen in the background of the right image.*

The stations were low-cost and built on wooden frames. They had various constellations of meteorological instruments (see “Rain Gauge Station Overview” in Appendix), but common for

all of them were the ECRN-50 tipping spoon rain gauge for measuring precipitation (Fig. 4.7). As the main goal of the field campaign was to measure heavy rain events with a limited budget, the ECRN-50 tipping bucket rain gauge had a relatively coarse measurement resolution of 1 mm ("ECRN-50 datasheet" n.d.). As a result of this, hourly precipitation values less than 1 mm may not have been measured before evaporating, or measured at a later time with additional precipitation tipping the spoon. However, for the heavy rain events that was the focus of this study, they were found to have sufficient accuracy.

Four of the stations were larger semi-permanent stations, while two were smaller easy-deployable stations. Images of both types can be seen in Fig. 4.6 and their locations in Fig. 4.8. Observing period and measured variables can be found in Table 4.2. Due to the lack of transmitting capabilities, data from the stations needed to be collected by accessing the loggers directly.

Figure 4.7: *Close-up image of the ECRN-50 rain gauge instrument (white) inside its windshielding (dark grey) in a semi-permanent station. Left image is from deployment of the Bjonapynt station (11.Jun 2018). Right image is from retrieval of the station at Tuna South (10.Oct 2018), at a point where the rain gauges were clogged by snow.*

Table 4.2*: The field campaign rain gauge stations deployed in summer and autumn of 2018. (WS = Wind speed, T2 = Temperature 2m, RH = Relative humidity 2m, GT = Ground temperature, precip. = precipitation)*

Station Name	Operating	Measured variables
Tuna South	11 Jun. - 10 Oct.	WS, T2, RH, precip.
Bjonapynten	11 Jun. - 10 Oct.	T2, RH, precip.
Murdoch	15 Aug. - 18. Aug	T2, GT, precip.
Adventdalen	11 Jun. - 10 Nov.	WS, T2, RH, precip.
Longyearbyen airport	23.Aug - 09.Sep	precip.
Breinosa	23.Aug - 09.Sep	precip.

Figure 4.8: *Map of all AWS stations in Longyearbyen/Adventdalen and Tempelfjorden area. Numbered, Light blue (MET), green (UNIS), and red dots (Field campaign rain gauge stations) indicate the locations of AWS in the Longyearbyen/Adventdalen and Tempelfjorden area.*

Tempelfjorden and Tunabreen Stations

In Tempelfjorden, a total of three semi-permanent stations were put up during two field excursions in summer 2018. Tuna South and Bjonapynten (Fig. 4.8) stations measured throughout the summer from 11th June to 10th October, while the Murdoch station (Fig. 4.8) unfortunately collapsed only two days after deployment 15th August, either by strong winds or a polar bear encounter.

Tuna South station was located three kilometers southwest of the Tunabreen glacier front (Fig. 3.4, Fig. 4.8), on a small ridge (30 m.a.s.l.) on the south side of Tempelfjorden. On the second field trip the 15th of August the ice conditions in Tempelfjorden made it impossible to reach the Tuna South station by boat, and it stood unsupervised through the summer, but seemed to be in good shape before disassembling, on the 10th of October.

Bjona station was set up on the north side of the mouth of Tempelfjorden, close to the permanent UNIS weather station Tempelfjorden, which does not have instruments to measure precipitation. Due to their co-location, the UNIS station data could be used to validate the measurements done by the temperature sensor on the rain gauge station, and give complementary wind speed and direction data. The UNIS station also had a webcam pointed towards the rain gauge station, which made it possible to follow the state of the rain gauge station through the field period, and to verify if the precipitation measurements were somewhat reasonable given the weather conditions seen in the webcam images (e.g Fig. A16, Appendix). The webcam was unfortunately only operative until 15.August 2018, and the UNIS station was taken down sometime after the field campaign, due to restrictions from Sysselmannen.

Longyearbyen and Adventdalen Stations

The remaining three stations were deployed in the Longyearbyen-Adventdalen area in different periods from June to November 2018 (Table 4.2). The two small easily-deployable stations Longyearbyen airport station and Breinosa station was put up the 23.August, and taken down and used for fieldwork in the AGF-213 UNIS course from 10.September to 21.September. During this fieldwork, one station was unfortunately destroyed during deployment, most likely by an animal. This caused the data from the field campaign rain gauge at Longyearbyen Airport to be lost, and the small stations were not put up again around Longyearbyen after that.

The fourth semi-permanent rain gauge station was put up in Adventdalen (11.June - 10.Oct) by the old Aurora station, close to the official MET station in Adventdalen, to compare the ability of the ECRN-50 rain gauge and the Geonor T-200B to capture heavy rain events. This rain gauge station was taken down due to below zero temperatures and snow in late October 2018.

4.2 Numerical Weather Prediction Models

In this thesis, data from the two operational models used at MET that cover the Svalbard archipelago has been analysed, namely the regional AROME Arctic model which is maintained and run by MET, and the coarser ECMWF IFS HRES model which is run and maintained by the European Center for Medium range Weather Forecast (ECMWF). Here, the models are briefly described.

4.2.1 AROME Arctic

AROME Arctic is the operational weather forecast model run by MET for Svalbard, the surrounding seas and Northern Scandinavia. It has been operational since March 2015, and produces the data presented at MET's online weather portal yr.no for the Svalbard region, up to 66 hours ahead.

The model is based on the HARMONIE-AROME (HIRLAM–ALADIN Research on Mesoscale Operational NWP in Euromed–Application of Research to Operations at Mesoscale) configuration (Bengtsson et al. 2017) of the ALADIN–HIRLAM NWP system. It is a convective permitting model that is forced with data from ECMWF HRES at its lateral boundaries. It has a horizontal resolution of 2.5 kilometers, and 65 vertical model levels.

For representing surface processes, HARMONIE-AROME uses the Externalized Surface (SURFEX) parameterization package (Masson et al. 2012). The ISBA force-restore scheme is used to parameterize land surfaces (Boone et al. 1999) with three layers and a single-layer snow model (Douville et al. 1995) is also implemented. Open ocean is defined by a prescribed sea surface temperature field and for parameterizing sea ice cover a one-dimensional thermodynamic scheme is used (Batrak et al. 2018). The temperature and humidity at 2 m and wind speed at 10 m are all diagnostic outputs from the SURFEX scheme.

The OCND2 scheme (Müller et al. 2017; Bengtsson et al. 2017) is used for parameterizing precipitation and cloud microphysical processes using the prognostic variables precipitating rain, ice, hail and snow as well as cloud fraction and cloud water.

The model is run deterministically at 00Z, 06Z, 12Z and 18Z every day with a forecast range of 66 hours. Hourly lateral boundary conditions are provided by the European Centre for Medium Range Weather Forecasting high resolution forecasts (ECMWF IFS-HRES). During its operational period (2015-2018) new model cycles have been implemented, but as this thesis

focuses on the operational model output, all AA data is treated independent of model cycle in the model evaluation part (Section 5.2).

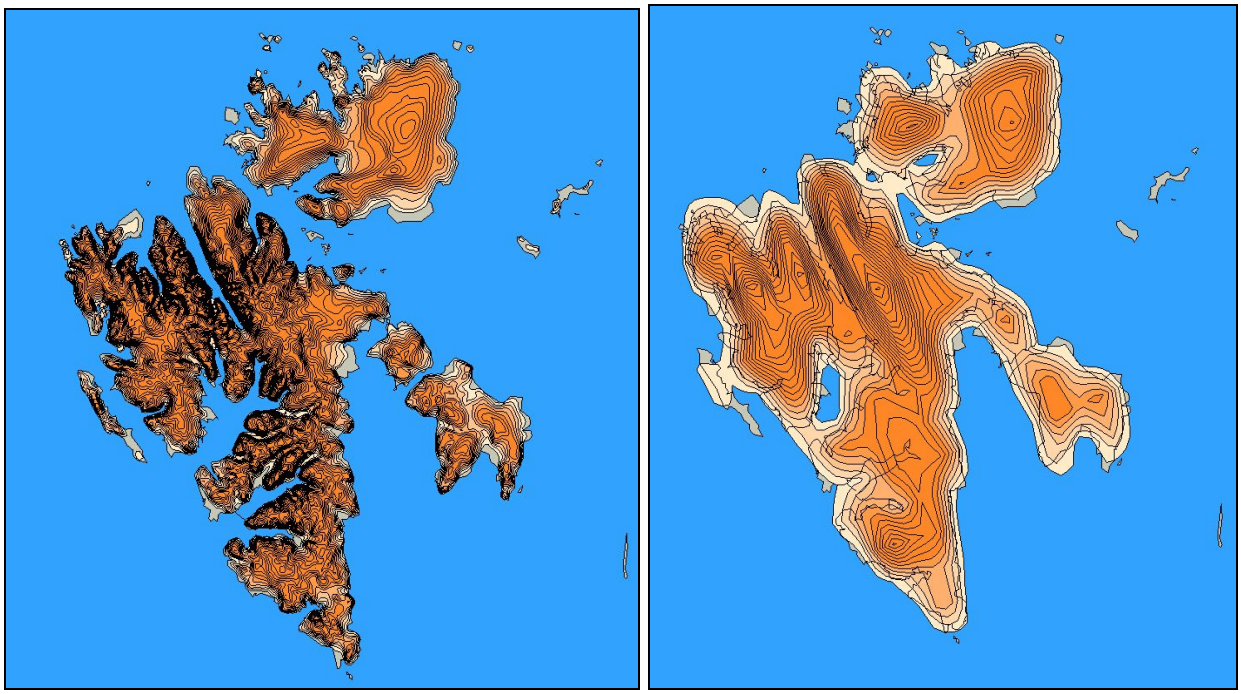

Figure 4.9: *How the topography of Svalbard is represented in the AA model (left panel) and the EC model (right panel) for comparison. Darker orange tones indicate higher elevation.*

4.2.2 ECMWF IFS HRES

The ECMWF IFS HRES model is an acronym for European Centre for Medium range Weather Forecast Integrated Forecast System High RESolution model. As it is used by MET, in addition to AA, as an operational forecasting model for Svalbard and the Norwegian Arctic, it is the most reasonable model to compare AA performance with.

The ECMWF IFS HRES is the high resolution configuration of the ECMWF IFS, run by the ECMWF consortium every 12 hrs (00Z, 12Z). As with AA it has undergone updates/cycles in the period of study (2016-2018), but as with AA data, the operational EC data is treated independent of model cycle.

The scheme used for parameterizing precipitation and cloud microphysical processes is basically the same as introduced for large scale weather models in the 90's (Tiedtke 1993), but has been steadily improved since then (ECMWF 2018). From hereon the ECMWF IFS HRES will be

referred to as EC, or the EC model. The most obvious differences from AA are the spatial resolution, and that EC has a hydrostatic dynamical core (ECMWF 2018).

4.3 Data Acquisition and Handling

4.3.1 Observational MET Data

Observational data from the MET stations was downloaded from MET's online data portal eklima ("Eklima data portal" n.d.). Datasets with both daily and hourly values were used. The 24hr values are quality checked according to the WMO standard, while the hourly dataset values are not, and should be handled with some caution ("Eklima data portal" n.d.). The precipitation variables subsequently used for daily and hourly analysis, are the ones named *RR_24* and *RR_1* by MET in eklima. See Table 4.1 for which stations that measures precipitation manually and which measures with automatic instruments.

4.3.2 Field Campaign Rain Gauge Station Data

The hourly measurements from the field campaign rain gauge stations in the 2018 summer/autumn season were stored in Campbell Scientific loggers ("CR10 datasheet" n.d.; "CR200 datasheet" n.d.) and collected during and after the field period.

Precipitation rates were measured with the ECRN-50 rain gauge, with 1 mm resolution ("ECRN-50 datasheet" n.d.). Temperature and relative humidity were measured by TinyTags, with a 0.01 °C and ± 3 % accuracy for temperature and relative humidity readings, respectively ("TinyTag Sensor datasheet" n.d.). Wind speed was measured by a Campbell Scientific wind sensor, with a ± 0.5 m/s accuracy ("Campbell Wind Sentry datasheet" n.d.). All variables were measured on an hourly basis.

To make 24 hr values, the hourly data was subsequently added (precipitation) or averaged (wind, temperature and humidity) from 07Z - 06Z each day.

4.3.3 AROME Arctic Data

The AA data was downloaded from MET's publicly available thredds service ("Thredds data server" n.d.) where they are stored as NetCDF files. The precipitation variables that were used in this work were the *precipitation*, *precipitation high estimate* and *precipitation low estimate* variables from the post processed NetCDF files publicly available at MET's thredds server.

As parts of this study consider how model performance varies with the model run lead time, an explanation of how model run lead time is defined follows. Here the lead time is defined after how many hours into a model run the first hour of daily accumulated precipitation is found (Fig. 4.10).

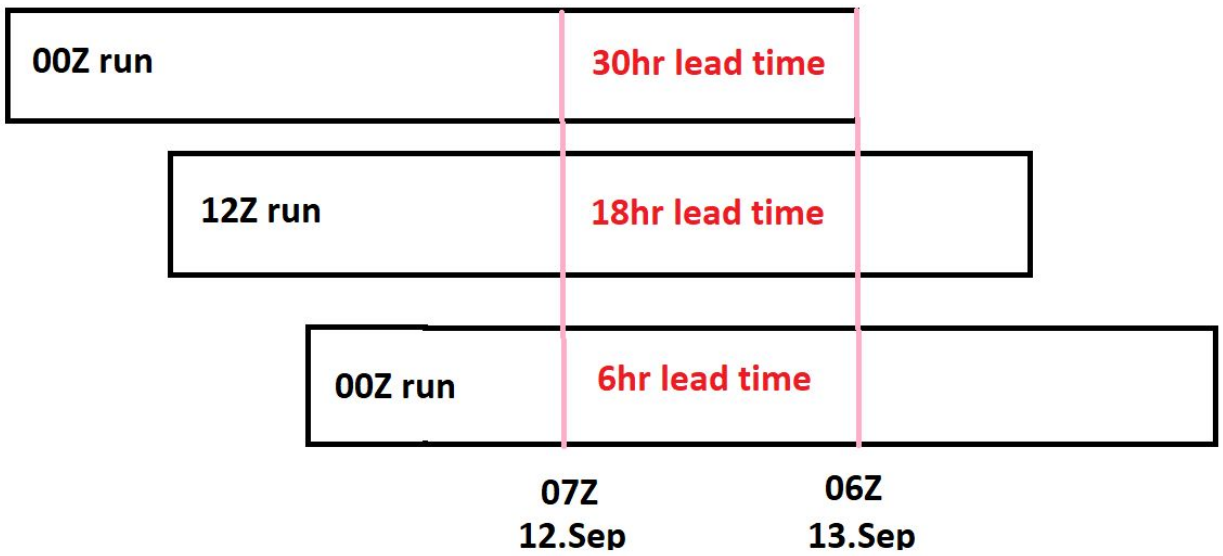

Figure 4.10: *Conceptual idea of how lead times are defined when dealing with an accumulated value such as precipitation. Every black box represents the time span of a model run. Pink lines indicate the start and end time of precipitation data to be included in (for this example) the 24 hr precipitation for 13.September.*

Similar to the field campaign rain gauge data, the hourly AA data was added (precipitation) or averaged (wind, temperature and humidity) from 07Z - 06Z each day for 24 hr values (Fig 4.10).

For some part of the analysis (Fig 5.9 and Fig 5.10) AA precipitation data have been accumulated, and AA 2m temperature data have been averaged, for each day from September 2012 to December 2017.

4.3.4 ECMWF IFS HRES Data

The EC data was kindly provided by researchers Morten Køltzow and Teresa Valkonen at MET, for use in this project. The precipitation variable from the EC files that was used in this study was the *precipitation_amount_acc*. This hourly variable is the accumulated precipitation, in each grid point, so far in the model run.

From this variable, to calculate the 24hr precipitation between 06Z and 06Z, which is analysed in this study, the value at 07Z from the previous day was subtracted from the 06Z value.

Unfortunately, there are some heavy rain event days in the study period for which one or more of the three daily (one for each lead time, each day) EC files are corrupted. These events were discarded from the model evaluation part (Section 5.2), hence the differences in numbers of events in Section 5.1 and Section 5.2. For the stations included in Section 5.2, Longyearbyen and Isfjord Radio had one discarded event, Hornsund had three and Ny-Ålesund had four.

4.3.5 Flow Type Dataset

The extensive flow type dataset used in this study has in the later years have been widely used in atmospheric studies with focus on Svalbard (Isaksen et al. 2016; Førland, et al. 1997). It has been manually created by the Polish scientist Dr. Tadeuz Niedźwiedź. Based on daily synoptic weather charts made by the German weather service, a general synoptic flow type, or atmospheric circulation, is decided for Svalbard for each day since December 1950 (Isaksen et al. 2016).

The flow types are divided into cardinal and ordinal directions based on where the air is advected from (e.g. north, northeast, south, etc), and further subdivided into what pressure system that governs the advection. If a cyclonic (low pressure) system is the main driver of the flow, there is no addition to the direction abbreviation. Flows driven by anticyclonic (high pressure) systems get an additional ‘a’ at the end (e.g. SWa). Additionally, there are the flow categories: Bc = cyclonic through, Cc = Cyclone over Svalbard, Ka = Anticyclonic ridge, X = unclassified flow. In total this makes 21 flow types to classify the flow over Spitsbergen. In the following, the synoptic flow type directions will be denoted by their abbreviations.

As 24hr precipitation is measured at 06Z every morning, 18 of the 24 hours that make up the observation period for daily precipitation are actually part of the previous day. In the analysis in Chapter 5, the atmospheric circulation type from the day before each heavy rain event is defined as the flow type for the event.

4.3.6 Event Filtering

In this thesis, a heavy rain event is considered to be when *more than 10 mm precipitation has accumulated in 24 hours, and the mean temperature was above 2°C for that 24hr period***.** This may seem like a small amount, but compared to the climatological rainfall at Svalbard stations it is considerable for single events (Dobler et al. 2019). The chosen heavy rain event threshold is

based on discussions with experienced AROME Arctic researchers at MET (Morten Køltzow and Teresa Valkonen, MET, Personal Communication), and following the limit that has been used in other studies (Dobler et al 2019; Køltzow 2019a). In addition, one study found that if the upper layer of the permafrost is sufficiently thawed, hourly rain intensities of more than 2.5 mm per hour can cause heavy mudslides in Longyearbyen (Larsson 1982). This makes even the events in the size-range of 10 mm/24 hr interesting for this study.

In this study, it was decided to not choose events based on forecasted precipitation values. The strength of this method is that the same events for all models and lead times is used in the statistical analysis, and that the method indeed evaluates how well the models perform during observed extreme events. The general drawback is that episodes where the models predict extreme levels of precipitation, which do not occur, a so-called false alarm event, are not included. The skill-score results presented in Table 5.2, must therefore be treated with caution.

4.3.7 Mean Error and Mean Absolute Error

Mean error (ME) and mean absolute error (MAE) are the central variables in the model evaluation part of this thesis, and are calculated by the following equations:

$$ME = \frac{\left(\sum^{n} (r_f - r_o) \right)}{n} \quad (1)$$

And

$$MAE = \frac{\left(\sum^{n} |(r_f - r_o)| \right)}{n} \quad (2)$$

Where n is the number of heavy rain events, r_f is the forecasted 24 hr precipitation amount and r_o is the observed 24 hr precipitation amount for the same heavy rain event.

4.3.8 Model Grid Point Boxes

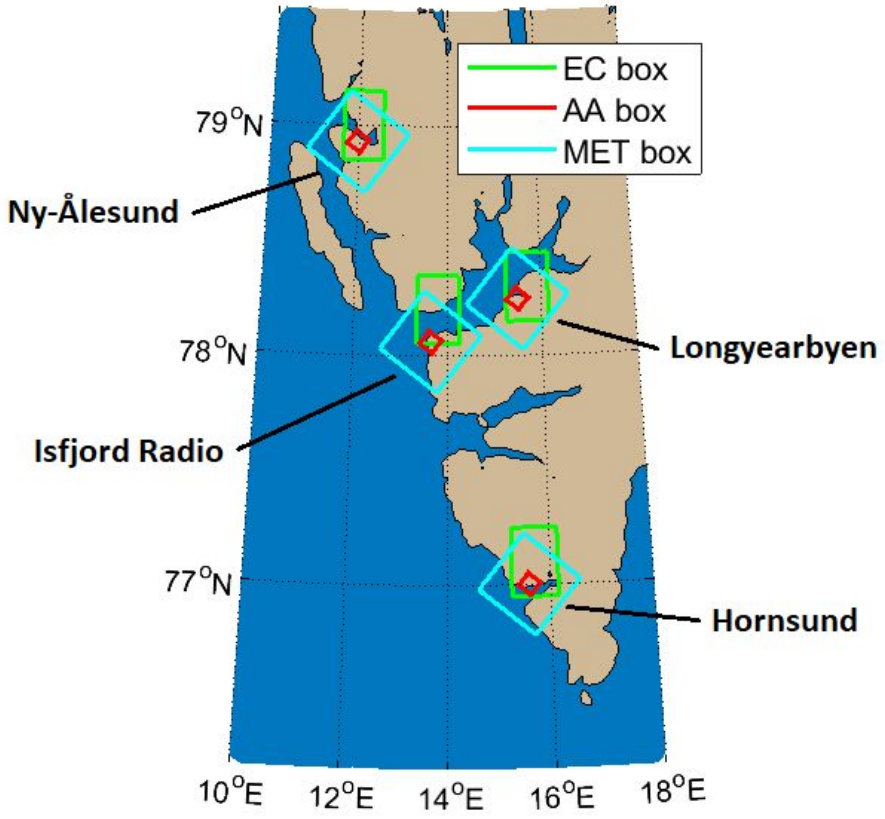

Figure 4.11: *A map of West-Coast and Central Spitsbergen showing the areas spanned by the different grid point boxes used for further analysing the model performances at the different stations.*

As mentioned, precipitation is a complex variable to simulate in models. Subsequently, there are several complex methods to evaluate model performance taking into account spatial and temporal correctness of the forecast (Wolff et al. 2014). Some of these methods base their evaluation on radar data (e.g. Shahrban et al. 2016), but since there currently are no precipitation radars in Svalbard, a relatively simple method of model grid boxes is used to further look into spatial variability and the role of topography in the forecasted precipitation.

From the AA output MET calculates, as part of their post-processing procedures, hourly high and low estimates by using a 15 x 15 grid point box centered on each grid point (light blue boxes, Fig. 4.11). The high estimate is the upper 85th percentile (of all the 225 grid points included in

the box), and the low estimate is the lowest 15th percentile. To make a 24hr accumulated precipitation value for the MET high and low estimates, each hourly value in the observation period was added together.

Inspired by this grid point box method, a smaller 3 x 3 grid point box centered at each station grid point was made for this study (red box, Fig. 4.11). From this, several box metrics have been calculated, (listed in Table A1, Appendix). Unlike the MET high and low estimates, the accumulated 24hr value for each grid point in the box was used to calculate the different metrics.

Similarly, a 3 x 1 grid point box was introduced for the EC data (green box, Fig. 4.11). The dimensions of this box were chosen so the EC box would not cover too large an area around the station, and to be as similar as possible in size as the large MET box. The metrics from the EC box were calculated in the same way as for the AA box.

Chapter 5
Results and Discussion

5.1 Heavy Rain Event Observations
5.1.1 General Statistics

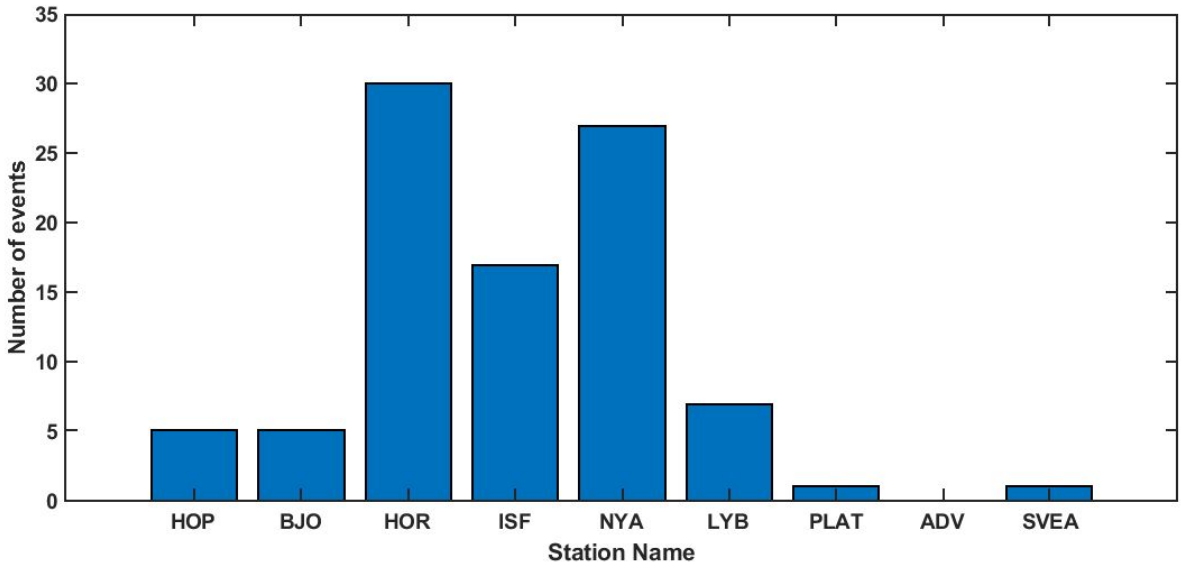

Figure 5.1: *Total number of observed heavy rain events (>10 mm per 24 hr) in the period Jun-Nov 2016-2018, at the different MET stations.*

As mentioned in Section 4.3.6, events that are classified as heavy rain events are those when the measured precipitation is more than 10 mm in 24 hours, accumulated from 06Z one day, to 06Z next day. An additional criterion of a mean temperature above 2°C over the same period is applied to minimize the number of snow readings. Figure 5.1. shows the total number of such events at each MET station in the study period (Jun-Nov, 2016-2018).

Although some stations only measured during two seasons (Svea, Adventdalen) and one season (Platåfjellet), it is clear that the three West-Coast stations (Hornsund, Isfjord Radio, Ny-Ålesund) experienced the highest number of heavy rain events in the study period. This is also in line with the higher annual amount of precipitation that these stations generally observe (Vikhamar-Schuler et al. 2019) Figure 5.2. shows the number of heavy rain events per station per year, indicating that 2016 and 2018 were the years with the highest number of events, for most of the stations.

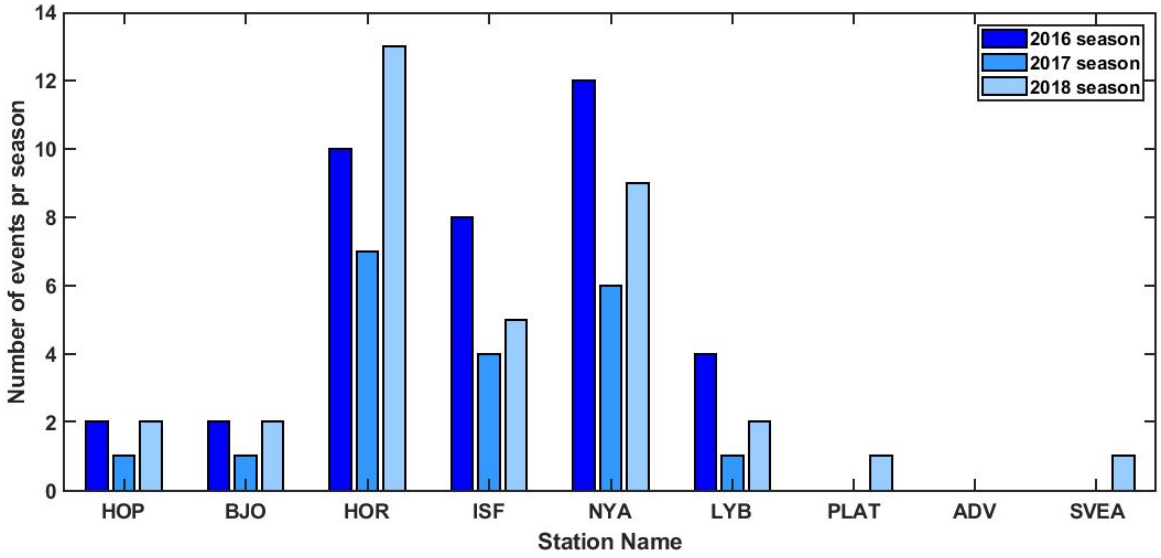

Figure 5.2: *Number of heavy rain events at the MET stations per year.*

To have a sufficient data basis for statistical analysis, only the stations with more than fifteen events in total were chosen for further analysis: Hornsund (30), Isfjord radio (17) and Ny-Ålesund (27). Additionally, Longyearbyen (7) was included since it is the main settlement in Svalbard, but note that the calculated statistics for this station is based on only six data points due to corrupt EC data for one of the events there.

Table 5.1: *The mean, median, maximum values of observed heavy rain events at the four different MET stations. All values, except dates, are given in mm/24hr.*

Station name	Mean value	Median value	Max. value	Date of max. value
Longyearbyen	20 mm	18.3 mm	41.7 mm	08-Nov 2016
Hornsund	22.2 mm	15.3 mm	73.5 mm	19-Sep 2017
Isfjord Radio	20 mm	15.6 mm	47.2 mm	08-Nov 2016
Ny-Ålesund	24.3 mm	19.8 mm	86.8 mm	08-Nov 2016

Summary statistics of the heavy precipitation events for these stations are presented in Table 5.1. Although Hornsund is the station with most heavy rain events (30), Ny-Ålesund had the highest observed 24 hr value in the study period (86.8 mm) and also the highest mean (24.3 mm) and median (19.8 mm) values of the four stations. Isfjord Radio and Longyearbyen have slightly lower mean values (20 mm), but Longyearbyen has the second highest median value (18.3 mm).

5.1.2 Flow Type Statistics

Based on the dataset from Niedźwiedź, described in Section 4.3.5, the synoptic flow type over Svalbard during the observed heavy rain events can be categorized in cardinal and ordinal directions. The flow type indicates where the air mass causing the rain is being advected from.

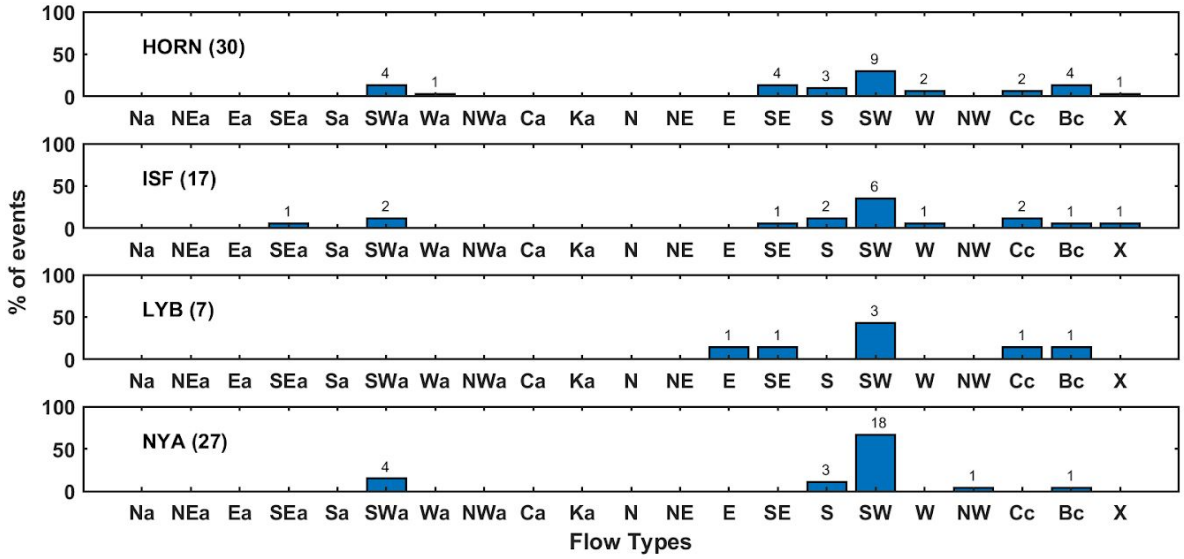

Figure 5.3: *Percentage of all observed heavy rain events with specific flow type at each station, one panel per station. Numbers in brackets behind station names indicate total number of events and Numbers over bars indicate number of events for each flow type. The flow types are described in Section 4.3.5.*

From Fig. 5.3 it is clear that it is the SW synoptic flow type that is the one that caused most heavy rain events at all four stations in this study period. The importance of a southwesterly flow for heavy precipitation events have also been identified by other studies (Førland et al. 1997; Dobler et al. 2019).

5.1.3 Heavy Rain Event Observations Discussion

To summarize, it is obvious that the West-Coast stations (Hornsund, Isfjord Radio, Ny-Ålesund) experience more heavy rain events than the Central Spitsbergen stations (Longyearbyen, Platåfjellet, Adventdalen and Svea) and the Island stations (Hopen and Bjørnøya) in the study period. It is also clear that SW is the most frequent flow type in connection with heavy rain events at the Spitsbergen stations. Nevertheless, there are some exceptions, especially in Hornsund and Longyearbyen, which in total have six heavy rain events with an E or SE flow

type. Ny-Ålesund does not have any rain events with this flow type direction. This can perhaps be explained by Longyearbyen and Hornsund being closer to the East-Coast mountain ranges that would initiate precipitation by orographic lifting, leaving Ny-Ålesund in the rain shadow. This resembles an opposite of some of the SW cases (except the most extreme ones) where precipitation would mostly fall out over the West-Coast stations, but not reach Longyearbyen.

From Table 5.1, many interesting features can be analysed. As mentioned, Ny-Ålesund has the highest 24 hr precipitation observation, despite Ny-Ålesund being located more than 200 km further north than Hornsund. This highlights the importance of location relative to surrounding topography and flow type when it comes to heavy rain events on Svalbard (as these factors are important for orographic precipitation), rather than being located further south in a generally warmer and more moist climate (See section 5.2). Another interesting point is how the median values at the stations most exposed to the open ocean (Hornsund and Isfjord Radio) show lower values of the four stations. This might reflect that these coastal stations are more prone to experience smaller heavy rain events that would not reach the stations further inland. These weak heavy rain events could possibly be caused by weak frontal systems, especially at the southernmost station Hornsund.

5.2 Model Evaluation

Here, a comparison of the AA and EC models against observations of heavy rain events for the Longyearbyen, Isfjorden, Hornsund and Ny-Ålesund stations is performed. First, results from a basic evaluation of both AA and EC using data from the closest model grid points is presented. Subsequently, the sensitivity of the AA model error statistics to the choice of grid points and evaluation metrics is analysed. The methods applied are described in Section 4.3.8. Finally, the ability of AA to capture the duration and intensity of two specific heavy rain events by analysing hourly data from Isfjord Radio is evaluated.

5.2.1 Basic Model Error Statistics Using Closest Grid Point Data

Figure 5.4. presents scatterplots of observed and simulated 24 hr precipitation data for the identified heavy rain events. As explained in Section 4.3.4, EC data is lacking for some events for a few stations and lead times, so only data from events and lead times where both AA and EC have data are included in this evaluation. The total number of events for each of the stations used in this evaluation are indicated in each of the panels in Figure 5.4.

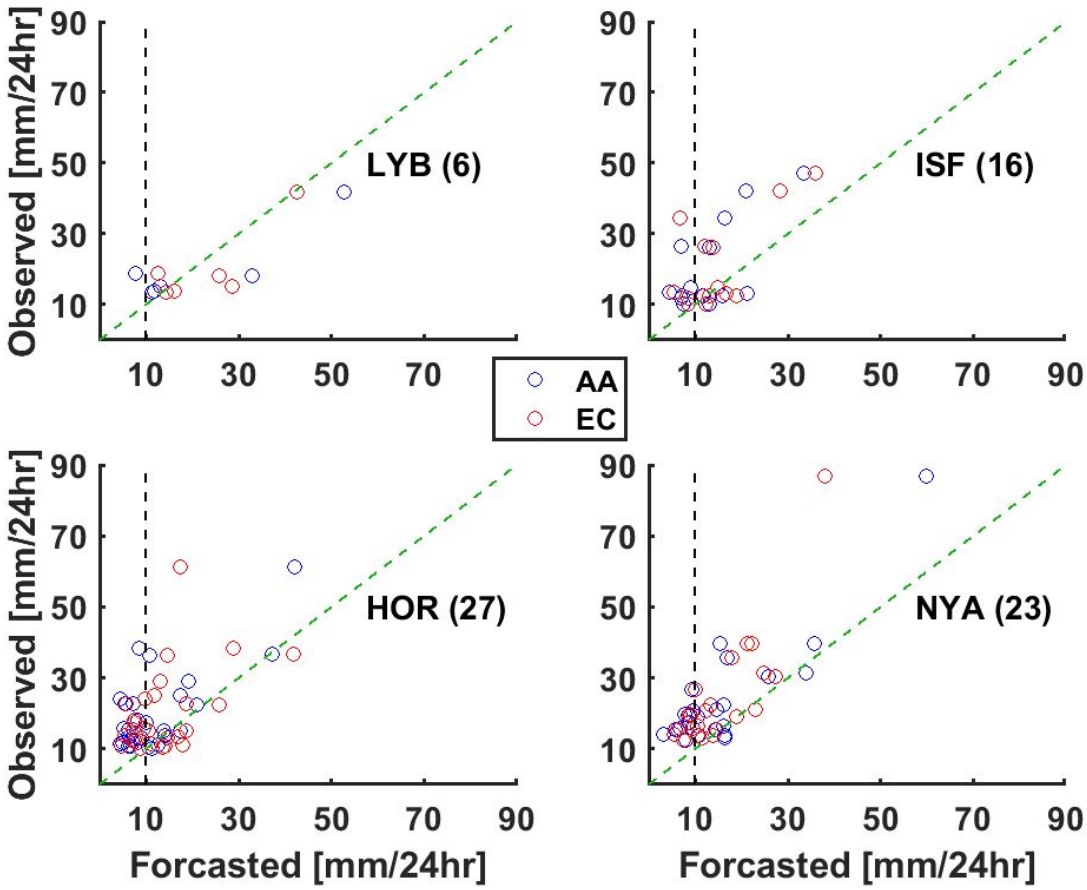

Figure 5.4: *Scatterplots of observed (y-axis) and simulated (x-axis) 24 hr precipitation for heavy rain events at Longyearbyen (LYB), Isfjorden (ISF), Hornsund (HOR) and Ny-Ålesund (NYA). Number of events are given in brackets behind each station name. Blue circles mark AA forecast and red circles mark EC forecast. Black, vertical, dotted line marks the 10 mm/24 hr threshold, while green dotted line marks the one-to-one ratio of forecast and observation. All forecasts are from 00Z runs and have a 6 hour lead time.*

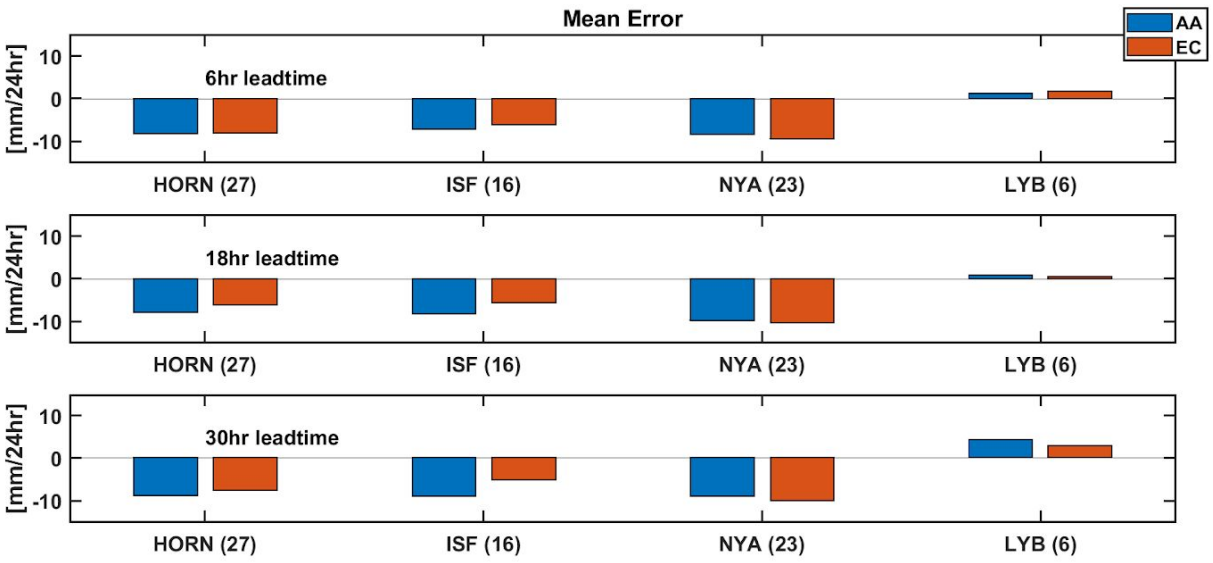

Figure 5.5: *The mean error (forecast - observation) for the closest grid point in AA and EC at each station for observed heavy rain events (> 10 mm/24 hr), given in mm/24 hr. Different lead time in each panel.*

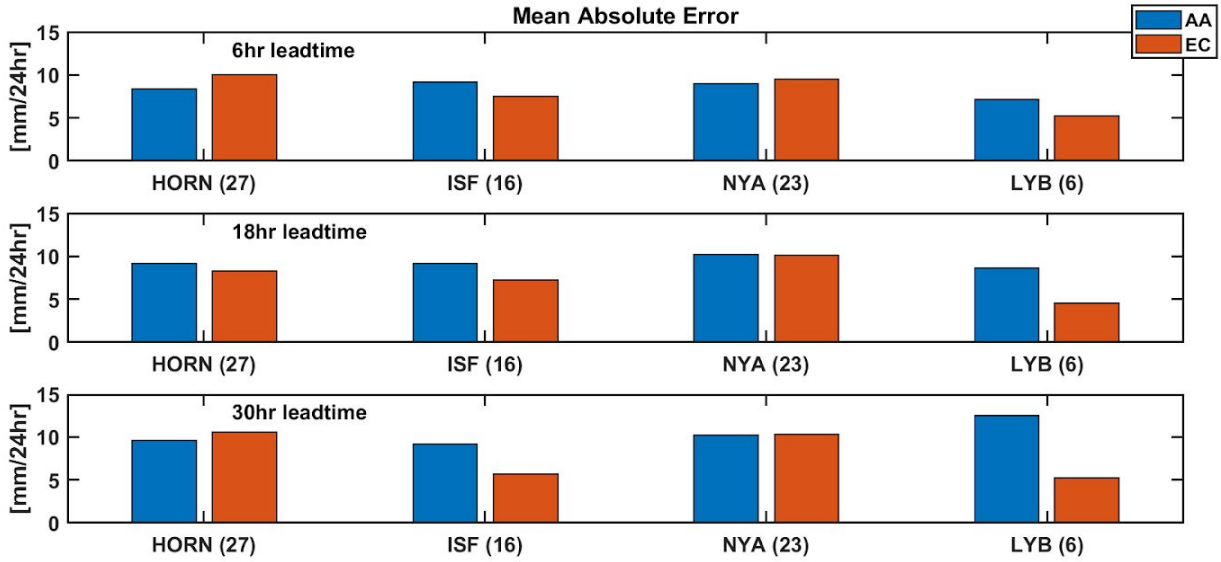

Figure 5.6: *Same as in Figure 5.5, but for the mean absolute error.*

Figure 5.5 and 5.6 show mean error (ME) and mean absolute error (MAE), respectively. The six hour lead time values are calculated with the same data as shown in the scatterplots in Figure 5.4.

On average, both models slightly overestimates heavy rain events for Longyearbyen, and underestimate them for the West-Coast stations (Figure 5.5). This can also be seen in Figure 5.4 where the majority of scatter points are located more above the one-to-one ratio line for the West-Coast stations, than for Longyearbyen. There is no clear increase in ME with increasing lead time in any of the models at any of the stations, with the exception of AA for Longyearbyen, where the ME for 6 hr lead time forecasts (1.3 mm) is smaller than for the 30 hr lead time forecast (4.4 mm).

The MAE is around the same magnitude as the ME for the West-Coast stations (Fig. 5.6, 5-10 mm). For Longyearbyen the MAE is substantially larger than the ME (1-5 mm), especially for the 30 hr lead time forecast (12.5 mm). This is in line with Figure 5.4 where there scattered points for Longyearbyen are distributed somewhat evenly around the one-to-one ratio, and thus cancelling each other out in the ME calculations.

As mentioned in Section 4.3.6, another way to evaluate numerical weather prediction models is to look at their hit rate. It should be noted that this method is sensitive to the threshold values chosen. Additionally, false alarm events (heavy rain forecasted, not observed) are not included in this study, so the results tell us nothing about how often the models are forecasting events that are not occurring.

Table 5.2: *The number of times AA and EC forecasts are above (hits) or below (misses) the 10 mm per 24 hr threshold during observed heavy rain events at the different stations, with 6 hr lead time model data. Last column is hit rate, which is the percentage of all events that were hits.*

Station	Total number of events	Hits AA	Misses AA	Hits EC	Misses EC	Hit rate (AA, EC)
Longyearbyen	7	6	1	7	0	86 %, 100 %
Hornsund	28	14	14	17	11	50 %, 61 %
Isfjord radio	16	8	8	11	5	50 %, 68 %
Ny-Ålesund	25	15	10	17	8	60 %, 68 %

As seen in Table 5.2, with the given threshold for 6 hr lead time forecast, the EC model has a higher hit rate than AA at all the stations. The highest hit rate for any of the models is found in Longyearbyen, where EC captures all the seven events, and AA only misses one. The lowest hit rate is found in Hornsund and Isfjord Radio where AA only forecast half of the heavy rain cases.

5.2.2 AA Model Grid Point Box Error Statistics

The model evaluation has so far been conducted by extracting model data from the closest grid point for each station and comparing these against the observations. Here, model data from geographical boxes centred on each of the stations, as explained in Section 4.3.8, is considered in addition. By including more data points, these boxes allow us to represent the model data by different metrics, like mean, median, minimum and maximum within each box. Also included are the MET high and MET low estimates, calculated from a larger (15 x 15) grid point box as explained in Section 4.3.8. Subsequently, ME and MAE during heavy rain events can be calculated for all these metrics, in a similar way as when considering data only from the closest grid point (Fig 5.5, Fig 5.6). As it turns out, the box metrics are not very sensitive to the forecast lead time, and therefore the focus is only on the 6 hour lead time statistics in the following (See Fig. A3-A4 in Appendix for statistics for all lead times).

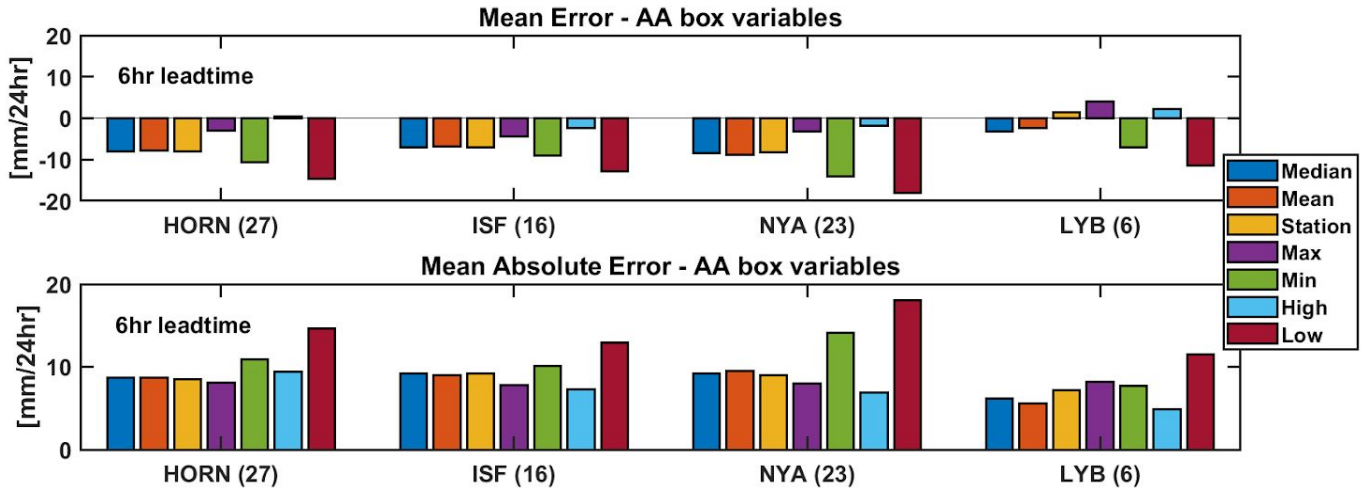

Figure 5.7: *Mean Error (upper panel) and Mean Absolute Error (lower panel) for different metrics from the AA box and the MET high and MET low estimates, for 6 hr lead time at the different stations. Number of events in parenthesis behind station name.*

Figure 5.7 shows ME (upper panel) and MAE (lower panel) for the different AA box metrics and the MET high and MET low estimates. It can be seen that the AA small box metric having the lowest ME for all stations, except Longyearbyen, is the maximum box metric (Max). When considering the MET high (High) and low (Low) estimates, which are computed from a larger grid box, it shows that MET high has a smaller (in the absolute sense) ME than any of the AA box metrics at all stations, except Longyearbyen, where the station grid point (Station) has the lowest ME. The AA small box metric with highest ME is the minimum box metric (Min), and similarly the MET low estimate has the largest ME of any metrics for all the stations. The

median, mean and station metrics have relatively similar ME for all stations.When it comes to MAE, there is more variation between the stations. For Isfjord Radio, Ny-Ålesund and Longyearbyen, the MET High has the lowest MAE, while for Hornsund it is the maximum box metric (Max). The MET low estimate has the highest MAE for all stations. For the small grid box metrics, the maximum box metric (Max) is the one with the lowest MAE for the West-Coast stations, while the minimum box metric (Min) has the highest MAE. In Longyearbyen, mean box metric (Mean) has the lowest MAE, and here the maximum box metric (Max) has the highest MAE of the small grid box metrics.

For the EC grid box shown in Fig 4.11 there is no clear change in ME and MAE for the different box variables or lead times (See Fig. A1 and A2 in Appendix).

Table 5.3: *Elevation values from AA in the 3x3 grid point box around each station.*

Name	Real station height	Model station height	Median box height	Mean box height	Min box height	Max box height
LYB	28	65	65	105	-11	401
HOR	10	39	39	77	-10	277
ISF	7	18	10	40	-3	145
NYA	8	20	20	63	-13	223

One key characteristic within each of the station boxes is varying terrain height. Precipitation in Svalbard is known to depend much on elevation by orographic lifting (Førland et al. 1997), and therefore it is investigated how the terrain varies within each AA box, as summarised in Table 5.3. Indeed, it is obvious that the variation in terrain height in each AA box is rather large, from 390 m (LYB) to 142 m (ISF). In comparison, in the EC model, the station grid point heights are 34 m.a.s.l for Isfjord radio, 137 m.a.s.l. for Ny-Ålesund, 85 m.a.s.l. for Hornsund and 205 m.a.s.l. for Longyearbyen Airport.

In Figure 5.8 (below) the model representation of elevation in the AA grid boxes around the stations are given together with the actual station height. In the same manner, mean forecasted precipitation amounts (6 hr lead time) and the mean observed precipitation level over all the heavy rain events at each station are shown.

The actual station height seems to be well represented in the model (Fig. 5.8 a-d)), while the general underestimation of precipitation at the West-Coast stations shown in Fig 5.4, and Fig 5.5 is also visible when compared to mean observations (Fig. 5.8 f-h)).

From Figure 5.8 it appears that model precipitation during heavy rain event in each grid point seems to depend on the grid points' elevation, especially for the West-Coast stations. For Longyearbyen, however, the connection is not so clear.

From the AA dataset mentioned in Section 4.3.3, a similar precipitation increase with height is seen in AA for the whole of Svalbard. Figure 5.9 shows the mean daily precipitation for a) all days from January 2012 to December 2017, b) heavy rain events in 2016 and 2017, and c) and d) the events with SW and SE synoptic flow type, respectively. It is evident that the mountainous regions close to the coast receive the highest mean daily precipitation in the model (Fig 5.9 a)), and for the SW heavy rain events it is especially the West-Coast mountains that has the highest values (Fig 5.9 c)). SE and E events, shown in Fig 5.9 d), are associated with less precipitation and the connection between the topography and maximum values of precipitation does not appear to be as strong as for the SW cases.

Figure 5.10 is compiled in the same manner as Figure 5.9, but for mean daily 2 m temperature. Despite the different colorbar in Figure 5.10 a) and b-d), it is clear that the mean daily temperature is higher during the extreme events than the overall mean temperature. Additionally, it seems like the mean daily 2 m temperature is higher for all the events (fig 5.10 b)), than for the SW and SE events (Fig 5.10 c) and d)), and that the SW events overall are warmer than the SE events, except for a possible Föhn effect, where subsiding air warms up due to higher ambient pressure, of 1-2°C in the east-west located valleys (Fig 5.10 d)).

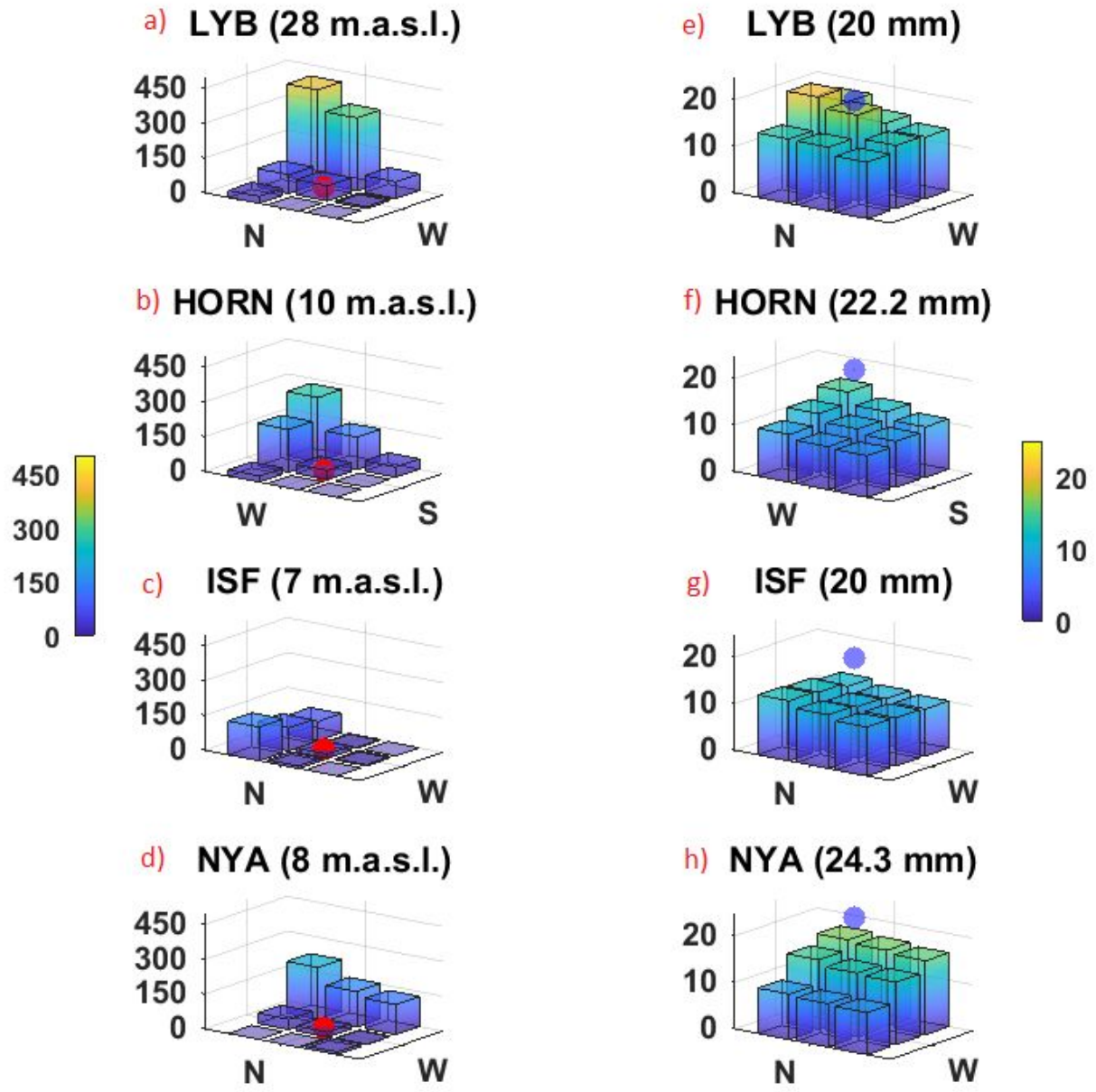

Figure 5.8: ***a-d)*** *AA grid cell elevation in m.a.s.l. (z-axis) around each station. The center cell is the cell closest to the station. Actual station elevation is marked by a red dot, with value (in m.a.s.l.) given in parentheses after the station name.*
e-h) *Mean grid cell precipitation in mm/24hr (z-axis) for chosen events (6 hr lead time). Mean observed precipitation is marked with a blue dot over the station cell, with value given in parentheses (in mm/24hr) after station name. Same grid as the elevation plots (a-d).*
Cardinal directions are given in all panels .

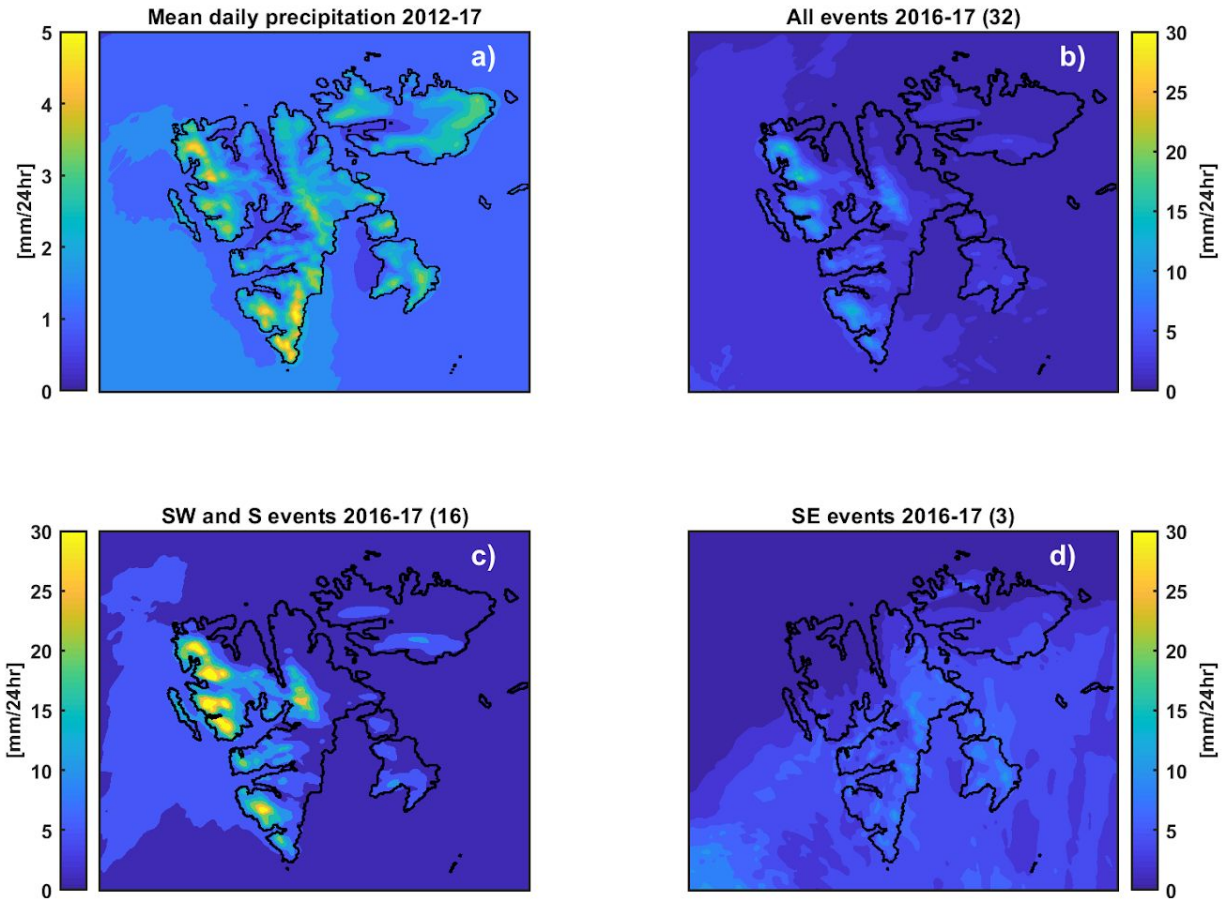

Figure 5.9: *Mean 24hr precipitation in AA for different event types for a) All days from 2012-2017, b) all heavy rain events 2016-2017, c) heavy rain events with SW and S flow type, 2016-17 and d) Heavy rain events with SE flow type, 2016-17. The number of events are included in parentheses behind title for each panel (b-d).*

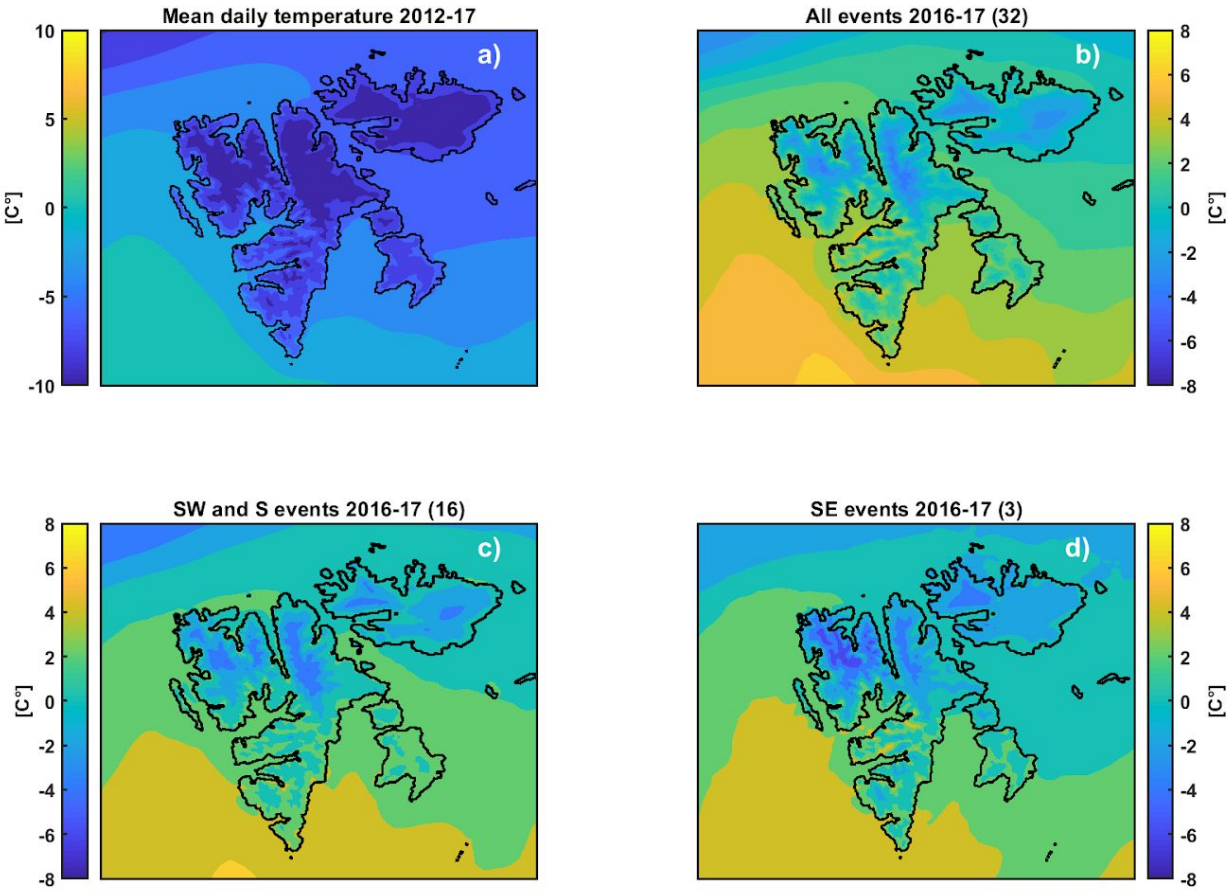

Figure 5.10: *Same as in Figure 5.9, but for the 2 m temperature. Note the different scales in panel a) and the three other panels.*

5.2.3 Analysis of Hourly Values at Isfjord Radio

While the previous section focused on error statistics and how model terrain might influence the precipitation output in the model, here, an analysis of how well AA performs in placing the event correctly in time and with regards to intensity is performed.

As shown in Table 4.1, of the four stations in this analysis, only Isfjord Radio measures precipitation on an hourly basis. In the following parts, hourly observations from Isfjord Radio are compared with hourly precipitation values from AA during the two most intense heavy rain events in the study period.

November 8th 2016 Heavy Rain Event

Isfjord Radio experienced on 8th of November 2016 the strongest heavy rain event in the study period with 47.2 mm/24 hr (Table 5.1). Figure 5.11 shows the hourly measured values from Isfjord Radio (lower panel), and the AA station grid point forecasted precipitation values together with the MET high estimate, which were found to compare the best of the AA box metrics against observations.

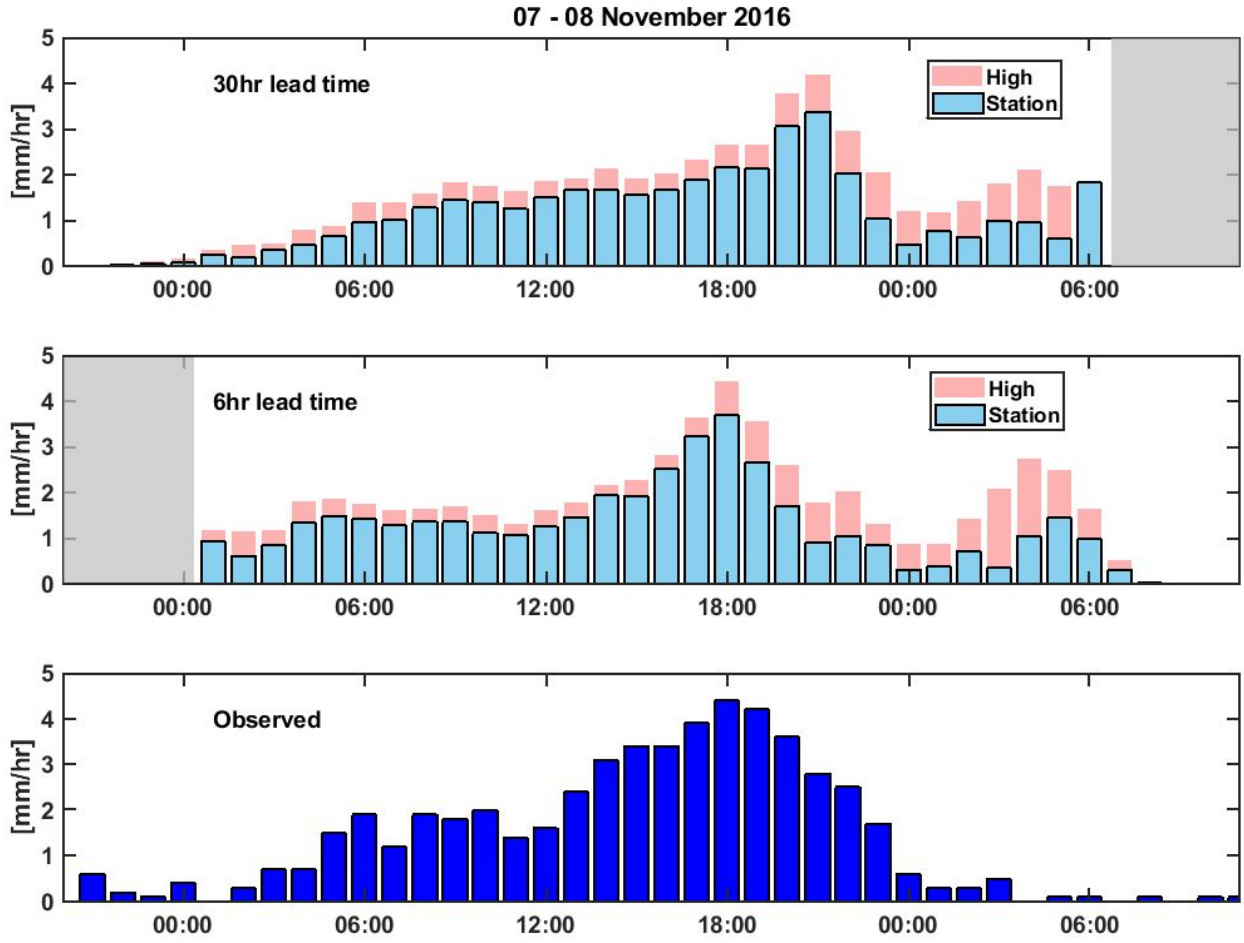

Figure 5.11: *Two upper panels show hourly AA station grid point precipitation values (light blue) and MET high estimate (pink) at Isfjord radio for 30 and 6 hr lead time. Gray areas denote times with no data for the given model runs. Lower panel shows measured values for the same period.*

AA seems to capture the duration and intensity of this event quite well compared to observations at Isfjord Radio (Fig 5.11). The model grid point has a slightly lower maximum hourly value (at 18:00Z) than the observation (AA: 3.8 mm, OBS: 4.3 mm), but the timing is correct for the 6 hr run. For the 24hr accumulated values between 06:00Z and 06:00Z, the model runs are off with 12.7 mm and 10.9 mm (6 hr: 34.5 mm, 30 hr: 36.3 mm), respectively. Both model runs also

balance their general lower hourly intensities by simulating heavier rainfall in the early morning of 08th November when little precipitation was observed.

October 15th 2016 Heavy Rain Event

The second largest event at Isfjord Radio was the 15th October 2016 event with 42.3 mm/24 hr. Figure 5.12 shows the same as Figure 5.11, but for the 15th of October event.

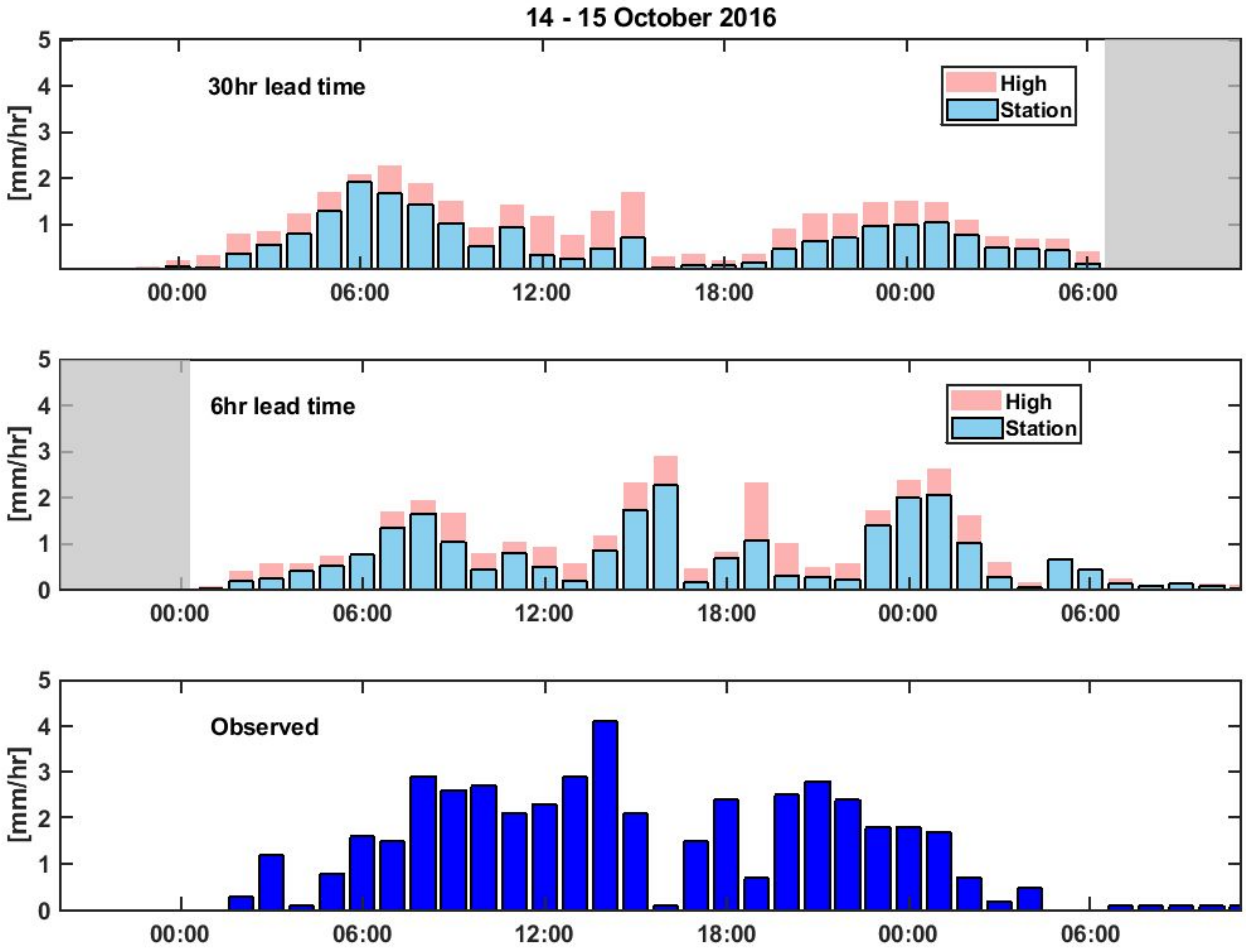

Figure 5.12: *Same as for Fig 5.11, but for the 15 October 2016 event*

The hourly observations from this heavy rain event show stronger and more stable intensities than what is realized in AA. The model simulations fail to capture both the value and timing of the maximum hourly intensity during the event, which in AA (2.2 mm at 16:00 14.Oct) is just slightly more than half of the observed (4.1 mm at 15:00 14.Oct). For the 24hr accumulated values, the 6 hr and 30 hr lead time model runs have 21.3 mm and 14.8 mm for the station grid point, respectively (Fig. A6, Appendix). This is less than half of the observed value. This was indeed the heavy rain event at Isfjord Radio with the highest error in AA 6hr forecast (Figure

5.4). The MET high estimate was best of the box metrics (Fig. A6, Appendix) and has 30.7 mm and 25.5 mm in the 6hr and 30hr lead time runs, respectively.

5.2.4 Discussion of Model Evaluation Results

Based on the results shown in Section 5.2 there are no clear differences between AA and EC in forecasting 24 hr precipitation values of heavy rain events, when evaluating basic statistical quantities like ME, MAE based on observations and data from the nearest model grid point, for the four Svalbard MET stations included in this study. In general, both models are more likely to overestimate heavy rain events in Longyearbyen, and underestimate the heavy rain events at the West-Coast stations. Interestingly, for heavy rain events when the synoptic flow type is from the southeast, like 19.August 2018, the precipitation output in AA is the opposite, with an underestimation in Ny-Ålesund (AA: 16 mm, OBS: 2.6 mm) and an overestimation in Longyearbyen (AA: 8.5 mm, OBS: 19 mm). This might point toward a general bias in AA for heavy rain events where the model is too slow to initiate precipitation upstream of coastal mountain ranges, and subsequently leaves too much precipitation inland or on the leeward side, but more observations would be needed to conclude on this.

From Fig 5.4 it can be seen that the largest differences between model data and observations are found during the major heavy rain events (> 20mm/24hr), and in these most extreme heavy rain episodes it seems like AA is outperforming EC. This is in line with what found by Køltzow (2019a). A good example is 19.September 2017 at Hornsund where 73.5 mm was measured, less than 20 mm was forecasted by EC, while AA forecasted 45 mm (at the station grid point). Such large errors contribute a lot to error statistics based on few data points, and in Hornsund where the largest errors occur, AA has a slightly better performance than EC in both ME and MAE.

However, at the four stations included in the statistical analysis, the majority of events are in the vicinity of 10-15 mm. This is just above the chosen heavy rain event threshold for this study, and as the models do not tend to massively overestimate heavy rain events (Fig 5.4, Fig 5.5), the resulting error in these events is subsequently small and contribute to lowering the ME and MAE, at least for the West-Coast stations. In the end, choosing threshold value is a question of balancing the need of sufficient number of events to do a sound statistical analysis, and avoid including too many small events that obscure model performance error statistics in the strongest rain events.

In the Skill Score (Table 5.2) it appears that EC performs much better than AA. Although a connection between elevation and precipitation output in the EC model has not been investigated as for AA, EC has grid points spanning larger areas (approximately 9.5 km x 2.5 km for the

latitudes of Svalbard) than the AA grid points (2.5 km x 2.5 km). This can make the EC station grid points represent higher elevated areas, causing the grid point elevation value to be higher than the AA model and the real station elevation. According to the numbers shown in Table 5.3 and Section 5.2.2, EC as a higher grid point elevation than both AA and the actual station elevation for all four stations. If there is a similar connection between elevation and precipitation output in the EC model as in AA, this could possibly lead to more precipitation in the EC grid point. Due to this, EC would more often produce precipitation above 10 mm for the smaller heavy rain events of around 10-15 mm, which would result in a better skill score for EC. Nevertheless, this can not be concluded on before a possible precipitation elevation gradient in EC is investigated further.

Both EC and AA have the lowest skill score at the southernmost station Hornsund (AA: 50 %, EC: 61 %). The EC station grid point elevation for Hornsund is 85 m.a.s.l., higher than the actual station height. Thus, a possible underestimation of precipitation, to produce such a low skill score, due to too low elevation in the EC model, is not likely the case. Another possible explanation for the low skill score at Hornsund is that weaker frontal systems play a more important role in heavy rain events here than at the other stations, at least with the given heavy rain event threshold value (10 mm/24 hr). Since weaker events might be more difficult to correctly resolved by the models, this could possibly lower the skill for Hornsund.

In an attempt to evaluate the models in a larger spatial domain than just at the grid points closest to the stations, the grid point box method (Section 4.3.8) is introduced. As shown in Fig. 5.7, the upper box metrics estimates (Max and MET high) indicate better model performance, considering ME and MAE, than the model station grid point at all stations. The only exception is for ME in Longyearbyen, where the model station grid point is slightly better. In general, it is clear that upper estimate box metrics often end up giving a better forecast of heavy rain events than the station grid point cell, but at the same time one should note that the spread between the high/max and the low/min estimates, in the two most extreme cases in this study, exceeds 50 % of the forecasted station grid cell value at Isfjord Radio (Fig. A5 and A6, Appendix). It should also be noted that the Max/Min values tend to have a smaller spread in general between them than MET High/Low values, which most likely due to the smaller geographic areas spanned by the Max/Min boxes. Additionally, false alarm episodes, when the model forecasts a heavy rain event and no heavy rain event is observed, are not included in this study. For these episodes the low estimate and the station grid point box metrics would naturally perform better (closer to the observed values) than the higher metrics, which also probably would induce more false alarm events overall.

As noted, it is clear that topography plays an important role in how much precipitation the model produces during heavy rain events, with more precipitation released over the high elevation grid

points. This is also pointed out by Køltzow (2019a) in his report. Such a strong increase in precipitation with height for the Svalbard region, as seen in Fig 5.9 a), has been pointed out by many studies earlier (Killingtveit et al. 2003). These findings are based on both observation and modelled data. Unfortunately, consistent long term measurements to verify the strength of such an elevation gradient in Svalbard is lacking. (Førland, et al. 1997) estimates 20 % increase in precipitation pr 100 m based on observations. By using linear regression on the model elevation and mean forecasted heavy rain precipitation in the nine model grid points shown in Figure 5.8, the mean precipitation gradient in AA around the stations for heavy rain events are found to be 23.3 %, 14.8 % and 16.9 % per 100 m elevation for Ny-Ålesund, Isfjord Radio and Hornsund, respectively. For Longyearbyen, it seems like the model produces a spill-over effect, where most of the precipitation falls on the leeward side (generally NW) of the dominant topography (Platåfjellet), and thus only has a 4.2 % precipitation increase per 100 m elevation. The mean of the four stations gradients gives a precipitation increase of 14.9 % pr 100 m. This value would indicate that AA is in the middle range of precipitation elevation gradients described by other studies (Killingtveit et al. 2003), although their numbers are based on observations, and not only from heavy precipitation events, in contrast to this study.

When using box metrics to evaluate model performance, or as a tool to improve heavy rain event forecasts, the biggest challenge seems to be optimizing the size of the boxes. In areas where the model generally underestimates precipitation during heavy rain events, expanding the grid point box to include more elevated grid points would be beneficial. Similarly, in Longyearbyen where the model station grid point data in general is overestimating the heaviest rain events (Fig 5.5), the grid point box metrics would benefit from including more lower elevated grid points with less precipitation. Looking at the large and small grid point boxes used in AA around Longyearbyen (Figure 4.11) , and the difference in MAE or ME between the MET high estimate and the maximum box metric (Max), one could speculate that the reason that the MET high estimate is performing better here is that the larger grid point box includes more grid points in low elevated areas such as Isfjorden and Adventdalen, while the small grid point box is biased with a mean elevation of above 100 m.a.s.l., despite Longyearbyen Airport in reality is located at 28 m.a.sl (Table 5.3)

When analysing forecasted and observed hourly values from the two heaviest events at Isfjord Radio, it is shown that the model performs quite well for hourly values when the event is strong enough (8th Nov. 2016), both with regards to timing and maximum hourly intensity. Although the difference might not be so large between MET high and the station grid point values each hour (Fig. 5.11), the accumulated 24hr difference is quite large (Fig. A5 and A6, Appendix). Figure 5.11 also exemplifies one of the pitfalls of evaluating accumulated 24hr rainfall, since AA in this case is ‘catching up’ some of its general underestimation by having too much precipitation in the last hours of the observation period, when nothing is observed. For the 15th Oct. 2016

event, when mudslides were occuring in Longyearbyen (Hanssen-Bauer et al. 2019), there is a clear discrepancy between modelled and observed hourly values at Isfjord radio with regards to intensity (OBS: 4.1 mm, AA: 2.2 mm). The hourly discrepancy during the 15th October rainstorm is also reflected in the 24 hr accumulated values, where the grid point and MET high estimates are off by more than 50 % and 28 % of the total observed value (OBS: 42.3 mm, AA: 14.8mm MET High: 21.3 mm).

5.3 Field Campaign Results

As described in Section 4.3.2, six semi-permanent weather stations with automatic rain gauges were deployed in Central Spitsbergen through the summer of 2018, with the goal of measuring heavy rain events in the interior of Svalbard where there normally are no observations. By the definition used in this study (10 mm/24 hr) only one heavy rain event were measured by the stations during the observation period (19. August, Adventdalen: 13 mm, Bjonapynten 14 mm). Here, results from the field campaign are presented. First, the focus is on the 19th of August heavy rain event, and an extreme hourly value (5 mm/hr) measured at Bjonapynten station that day. After that, measurements of a possible elevation precipitation gradient between Adventdalen and Breinosa is shown. Thereafter, the measurements from Tuna South is presented and compared with AA data. Finally, the observation bias between the field campaign rain gauge and the official MET station in Adventdalen is presented.

5.3.1 18-19th of August 2018 Heavy Rain Event

During the rain gauge station field campaign, only one heavy rain event (> 10 mm/24 hr) was measured. This was the 18-19th of August 2018 event, when the Adventdalen rain gauge measured a total of 13 mm in 24 hrs and Bjonapynten measured 12 mm in the same time period (see section 5.3.2, below). During this event, moist air was advected from the SE in connection with a low pressure system that moved northward toward Spitsbergen on the 17th of August (See Fig. 5.14).

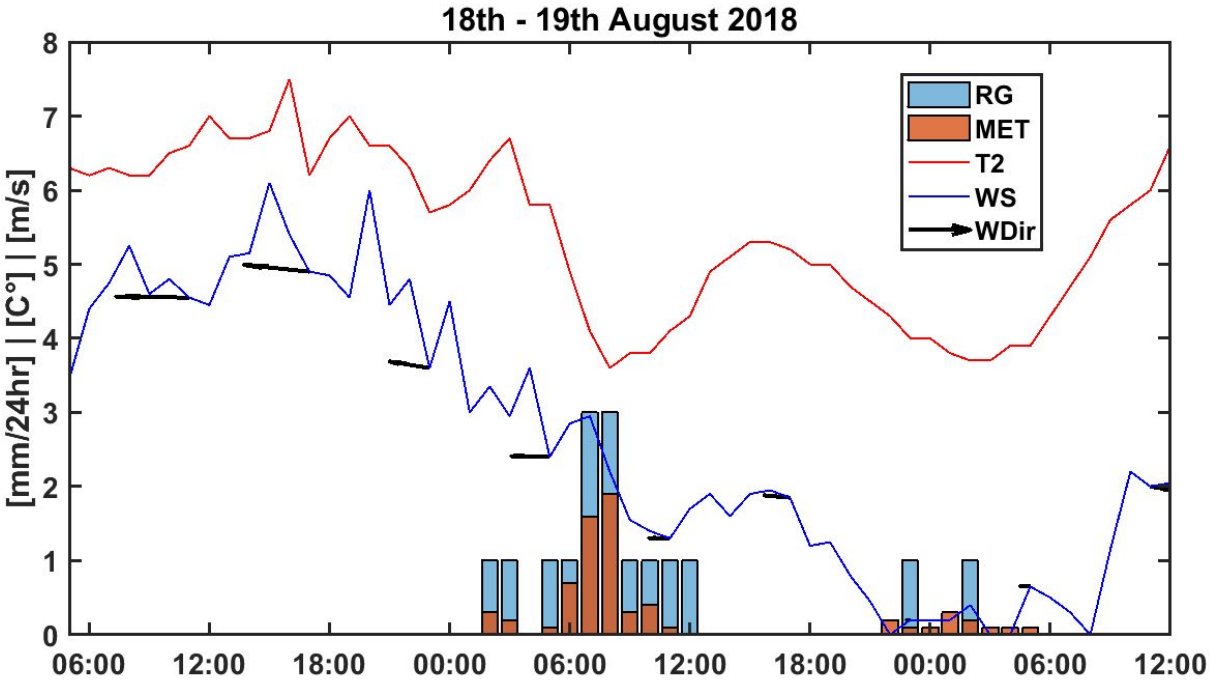

Figure 5.13: *Hourly precipitation values from the Adventdalen ECRN-50 rain gauge (blue bars), the Adventdalen MET Geonor T-200B (red bars) together with 2 m temperature (red line) and wind Speed (blue line) with arrows indicating wind strength and direction every 6hr (arrow pointing left means easterly wind, etc.). Time is UTC.*

The total discrepancies between the Geonor T-200B and the ECRN-50 were relatively big during this event, and this is also evident in the hourly values (Fig. 5.13), where Geonor T-200B never measured more than ⅔ of what ECRN-50 measured. For a more detailed analysis of this difference see Section 5.3.5.

From Figures 5.13 and 5.14, it can be seen how the easterly wind picked up during this heavy rain event as the front passed, before it dropped down again while the low pressure center was located over central Spitsbergen. There is also a clear signal in the temperature with a drop of more than two degrees when the precipitation is at its most intense.

We also see in Fig. 5.13 that the event lasted approximately 11 hours, and crossed a 06:00 'observation time'. Disregarding the standard 06:00-06:00 observational time, the maximum 12 hr intensity measured by ECRN-50 (from 00:00 18.August to 12:00 18.Aug) was actually 14 mm/12 hr. Likewise, the maximum 24 hr intensity (from 02:00 18.August to 02:00 19.August) was in fact 16 mm/24 hr. Additionally, at two successive readings between 02:00 - 03:00 18.Aug, 3 mm/ hr was measured by the ECRN-50 rain gauge, which is slightly higher than the 2.5 mm/hr mudslide threshold found for Longyearbyen (Larsson 1982).

Also the MET stations at Isfjord Radio (12.6 mm), Hornsund (28.9 mm) and the rain gauge station Bjonapynten (12 mm) measured heavy rain events, while Ny-Ålesund only registered 2.6 mm. The AA model predicted 8.5 mm for both the Longyearbyen Airport and Adventdalen grid points, but almost twice the observed amount (16 mm) for Ny-Ålesund. Looking closer at the forecasted hourly precipitation values for Ny-Ålesund (not shown) it seems that the model produces most of the additional precipitation within a few hours around 12:00 18.Aug, with precipitation rates of more than 3 mm/hr. Hence, for this case, it seems that AA overestimates the amount of precipitation falling in Ny-Ålsund with a NE flow. Why the model underestimates the amount in the Longyearbyen area is unclear, but perhaps it produces too much precipitation over the eastern mountain ranges and Edgeøya, and too little water vapour is left for creating precipitation as the air masses reach Central Spitsbergen. At the Bjonapynten rain gauge, which is presumably less shielded by mountains in east and closer to the East-Coast than Longyearbyen, the AA grid point forecast matches the observations much better (AA: 14.5 mm, ECRN-50: 14 mm).

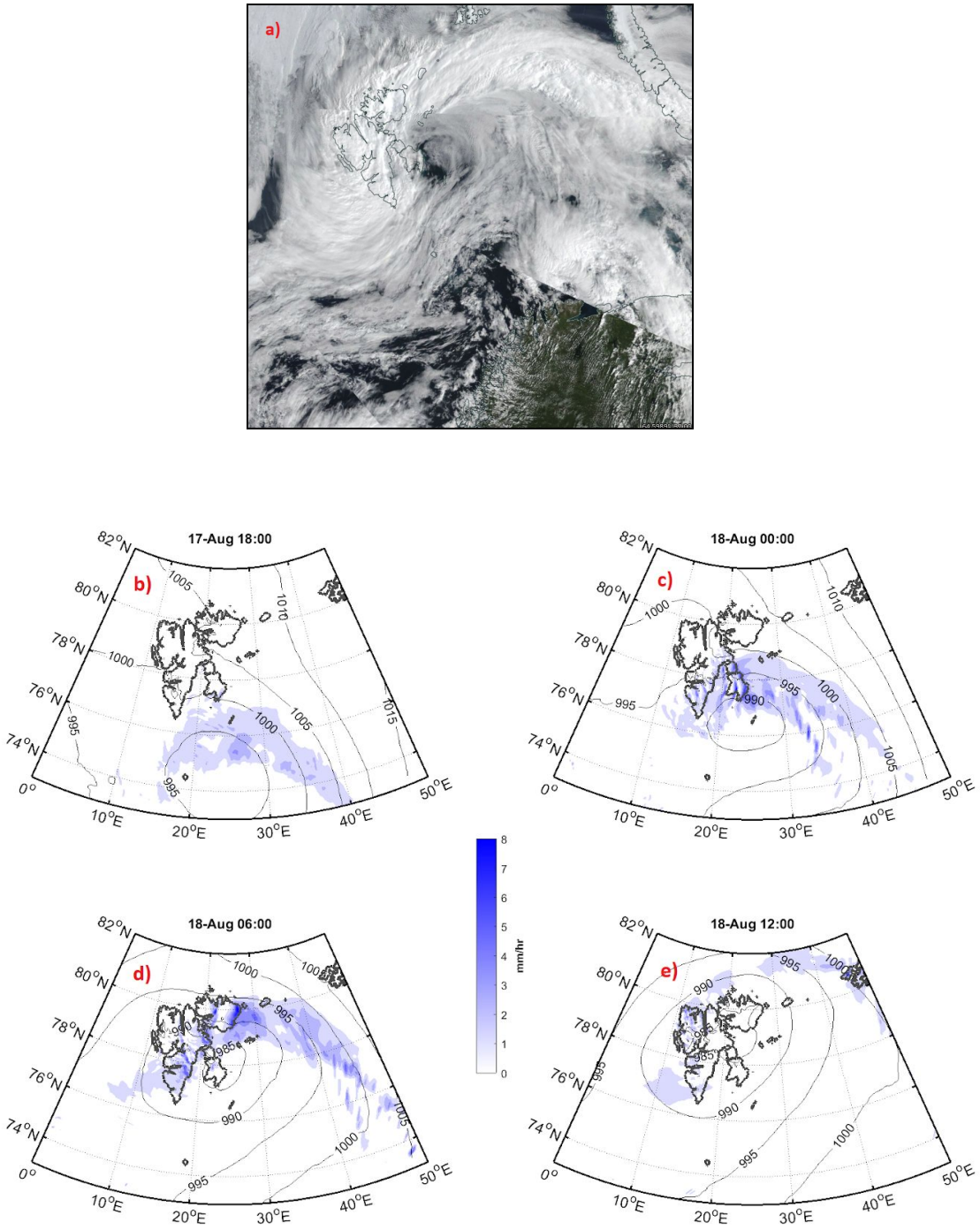

Figure 5.14: ***a)*** *Composite satellite image, from the Soumi-NPP satellite, of the low pressure system located over Svalbard in the morning of 18th August. Credit: NASA Worldview Application (https://worldview.earthdata.nasa.gov)* ***b-e)*** *AA pressure (black, solid lines) and hourly precipitation rates (blue shading) at selected time steps (see panel titles) from the evening of 17 aug (b) until 12 UTC 18 August (e).*

5.3.2 Bjonapynten Intense Hourly Precipitation Rate

During the 19th of August heavy rain event, the Bjonapynten rain gauge station measured a total of 12 mm in 24 hours. Moving the 24 hr measuring period by one hour (from 06Z-06Z to 05Z - 05Z), makes it a total of 14 mm in 24 hours, and the main precipitation in the event (13 mm) happened in only 12 hrs (05Z - 16Z). Measurements from this event are shown in Fig. 5.15 below. Embedded in these 24 hour measurements was a relatively high hourly precipitation rate of 5 mm/hr, measured between 06:00 - 07:00 18.August (Fig. 5.15).

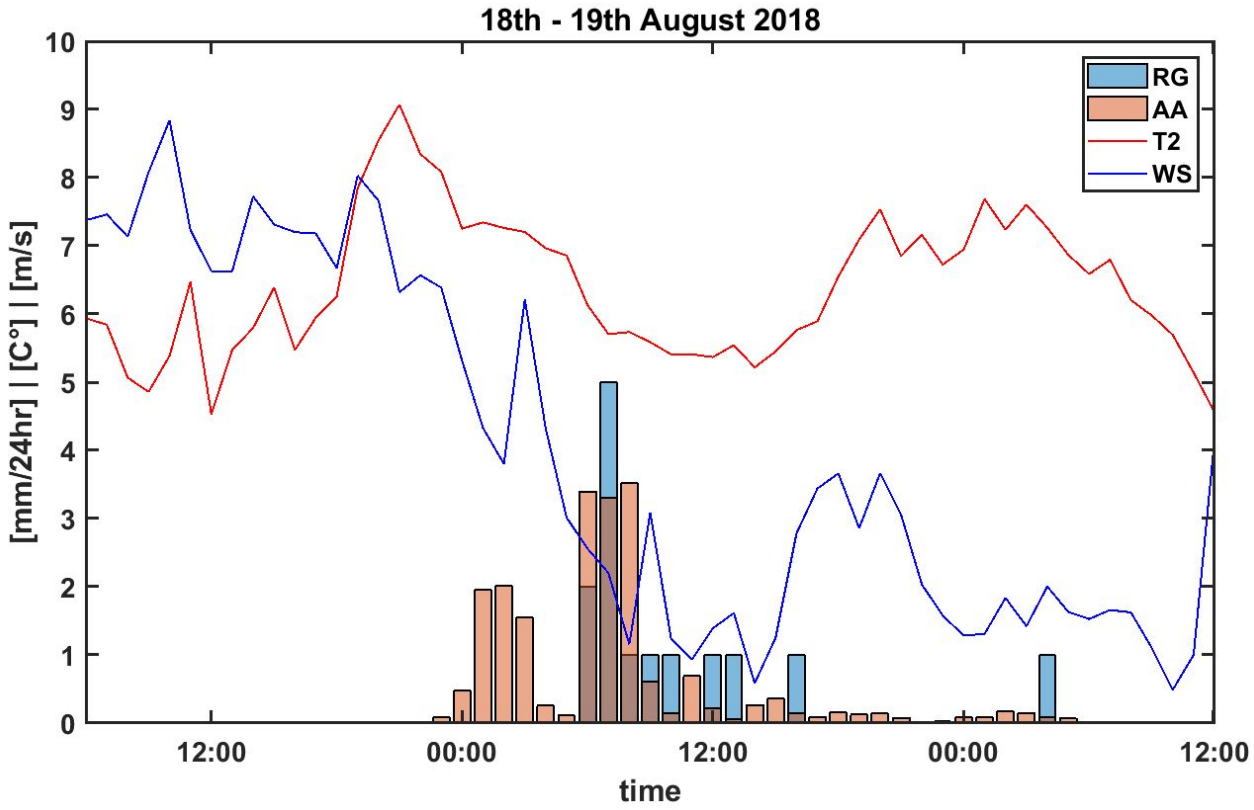

Figure 5.15: *Same as for Fig. 5.13, but for Bjonapynten data (blue bars), and AA forecast (6 hr lead time, red bars). 2 m wind speed (WS, blue line) is taken from the UNIS AWS located ~30m away from the rain gauge station at Bjonapynten. 2 m temperature is obtained from the rain gauge station (T2, red line).*

Similar to the measurements in Adventdalen, the wind was the strongest (up to ~9 m/s) and the temperature the highest (~8 °C) during the day of 17th Aug before rainfall started in the morning of 18.Aug. The rainfall started some hours later at Bjonapynten than in Adventdalen, as the frontal system was moving in from the south (Fig 5.14). When the rainfall occurs, both wind and temperature drop sharply.

The high reading at 07:00 18.Aug (5 mm) alone could possibly be attributed to left-over liquid (rain) in the tipping spoon from previous hours, or very strong winds that can shake the station rig enough to add a “tip”. However, in this case, the gauge measured 2 mm the previous hour, and thus a left-over from last hour is more unlikely. Similarly, the wind speed was relatively low at the time, and no wind gusts (not shown) over 5 m/s were measured at the UNIS AWS. This means that possible erroneous additional precipitation readings, are unlikely to be caused by wind interfering with the instrument.

If deemed trustworthy, it is most likely the first well-documented measurement of an hourly precipitation intensity in central Spitsbergen reaching 5 mm/hr. It might not sound as much, but put in relation to the Svalbard precipitation climate it is higher than the maximum hourly precipitation intensities observed at Isfjord Radio during the record breaking rain storms on 8th November and 15th October 2016 (4.3 mm and 4.2 mm). Additionally, if the hourly data adjacent in time to the 5 mm observation at Bjonapynten are accumulated, the 10 mm heavy rain threshold was reached in a time span of only six hours (05:00 - 11:00).

5.3.3 Breinosa Elevation Gradient

During a week in August-September 2018, both the Breinosa (~500 m.a.s.l.) and Adventdalen (13 m.a.s.l.) rain gauge stations measured precipitation. The events during this period were not intense enough to be classified as heavy rain events, but they are still of interest since the same type of rain gauge instruments measured precipitation at different heights at the same time and less than 8 km apart, in Central Spitsbergen.

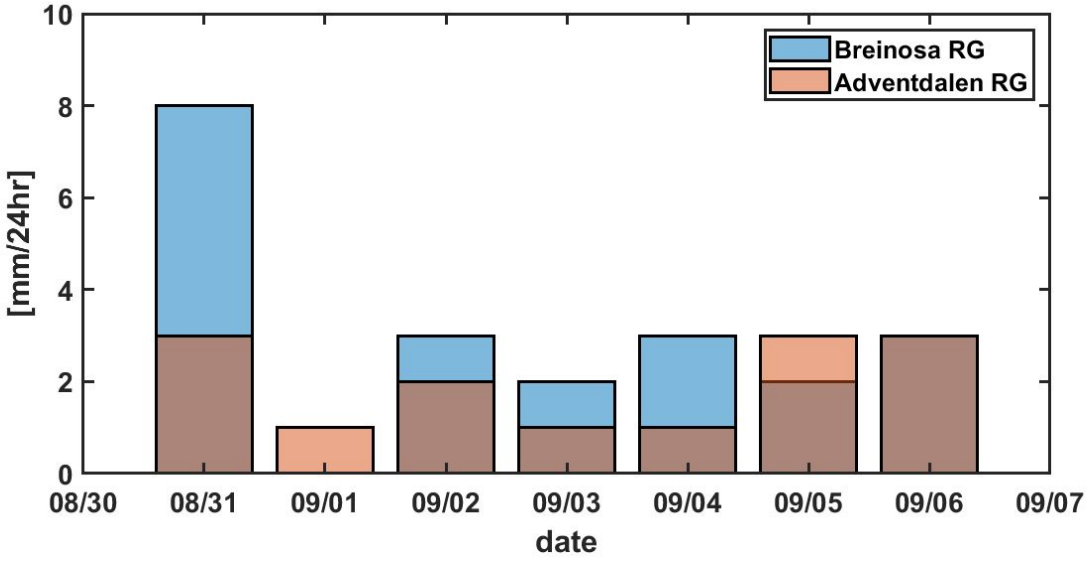

Figure 5.16: *24 hour precipitation measured at Breinosa (blue bars) and Adventdalen (red bars) between 30.Aug and 06.Sep 2018. Both measurements were conducted with ECRN-50 rain gauges.*

In Figure 5.16, it can be seen that the days when both stations measure precipitation (all days except 1.Sep) there is only one day (05.Sep) when more precipitation is measured in Adventdalen than on Breinosa. In the hours included in the 1.Sep measurements, when only Adventdalen measured precipitation, winds were strong at Breinosa (> 10 m/s), and the ECRN-50 at Breinosa was most likely unable to capture any precipitation in these low temperatures and strong winds. The 1.September measurement in the elevation gradient calculation is therefore dismissed.

Using the remaining measurements, the percentage increase (or decrease) in precipitation at Breinosa relative to Adventdalen is then calculated for each day. Since the height difference between the stations is 500 m, the percentage increase (or decrease) in precipitation is further divided by five to get the percentage increase per 100 m elevation. Finally, a mean elevation gradient from these six daily elevation gradients is calculated. Alternatively, the elevation gradient was calculated by using the accumulated (from all six observations) amount of precipitation at each station to find the relative increase (or decrease) in precipitation between the two stations, and then divide it over 500 m. The two methods yield an increase of precipitation per 100m elevation of 8.4 **%** and 12.3 **%**, respectively.

5.3.4 Tuna South Observations Compared to AROME Arctic

The most remote station in this field campaign was the Tuna South station, near Tunabreen (Fig. 4.8, Fig 1.1), that stood unsupervised from 11.June - 10.October. During the field period it was (as far as the author knows) the most easterly precipitation measuring weather station on the whole of Spitsbergen, located roughly 35 km from the East-Coast, separated from it by the Fimbulisen icecap (~800 m.a.s.l) and its adjacent mountains.

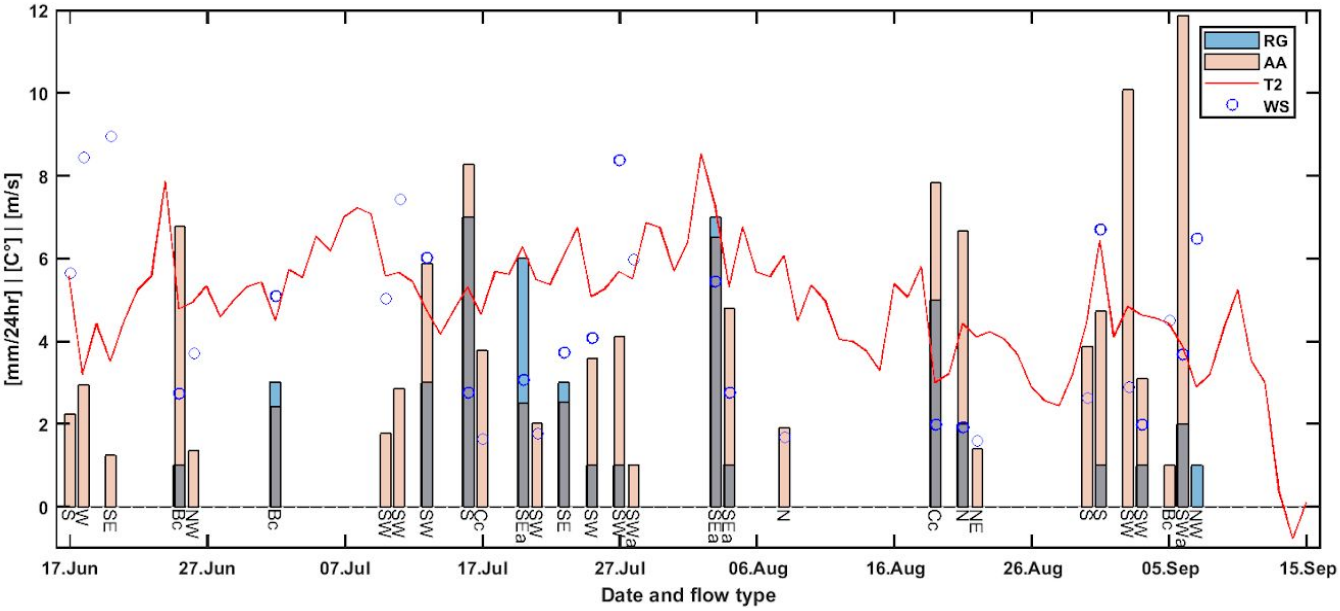

Figure 5.17: *ECNR-50 24 hr precipitation measurements from Tuna South (blue bars), AROME Arctic 24 hr forecast (red bars), where either one is above 1 mm. Mean observed daily wind speed on the days with more than 1 mm forecasted or observed precipitation are indicated as well (blue circles) along with mean observed daily 2 m temperature (red line) and synoptic scale flow type for the days with more than 1mm/24hr forecasted or observed precipitation (Abbreviations underneath bars).*

The Tuna South rain gauge station did not measure any heavy rain event (>10mm/hr) during the summer and early autumn of 2018 (Fig. 5.17). In total, the ECRN-50 rain gauge observed 16 days with precipitation, and a total amount of 45 mm in three months. This was lower than the total of 64 mm that was measured by the Adventdalen ECRN-50, but higher than the total 34 mm measured at Bjonapynten in the same period. The maximum daily precipitation amount at Tuna South was observed two times during the field period with 7 mm in 24 hours (16.July and

03.Aug) Notably, these did not occur on the same date as the maximum daily readings at Adventdalen and Bjonapynten (19.Aug).

On five of the 16 dates when precipitation was observed, AA forecasted less than what was observed. In 14 cases, AA forecasted precipitation, but nothing was observed. There was only one day when there was no precipitation in the model, but precipitation was observed (1 mm, 7.Sept). In general, it appears that AA overestimates the level of precipitation at the station grid point for the days where precipitation over 1 mm either was observed or forecasted. If one assume that the four days with mean wind speed over 7 m/s (18.Jun, 20.Jun, 11.Jul, 27.Jul) can be discarded due to undercatchement likely induced by high winds, the mean error of the AA forecast compared to the observations is 2.6 mm/24hr (as calculated in Section 5.2.1).

Interestingly, it seems like both the amount of daily precipitation, and the sign of the AA forecast error (overestimation/underestimation), is connected to the flow type (Fig. 5.17). In three out of five events where the Tuna South rain gauge measured more than AA forecasted, the synoptic airflow is of SE origin. As, after closer inspection, the synoptic scale through (Bc) that governed the flow type the 02.July, seems to have been northeast of Svalbard (See Fig. A15, Appendix), causing a NW or N flow type over the Tuna South station this day. This means that the two other days, of the five where AA underestimated precipitation, had a NW flow. After dismissal of the high wind cases, there was only one of the eleven days when AA overestimated precipitation that had a SE flow (04.Aug, OBS: 1 mm, AA: 4.5 mm). The flow type that dominates the cases where AA overestimates precipitation, compared to observations, is the SW flow type (SWa included). Out of a total of 21 events for which AA overestimates rainfall (excluded the high wind events), eight events had a SW or SWa flow type, and in total 13 that had either SW, SWa or S flow type. The mean error of the AA forecast compared to the observations are 3.8 mm/24hr for the SW cases and -0.1 mm/24hr for the SE cases, respectively.

Nevertheless, the total amount of observed episodes is one higher for SW flow types (5, SWa included) than for SE flow type (4), but the SE events seems to be more intense (mean SE OBS: 5.7 mm) than the SW events (mean SW OBS: 1.6 mm). It is also noteworthy that there are three events when precipitation is observed (02.July, 07.Sep and 21.Aug) where there is a northerly or northwesterly air flow, which seems to cause precipitation in this area.

5.3.5 Adventdalen Observation Bias

Since the Adventdalen station became an official MET station in 2016, there have been discussions among local meteorologists about the curious differences between Longyearbyen and Adventdalen when it comes to observed precipitation. Installing the field campaign rain gauge station approximately 30 m from the official MET station was initially done with an idea of

validating the ENCRN-50 against official measurements of precipitation. However, as it turned out, it became more an investigation of how correct the official MET measurements were.

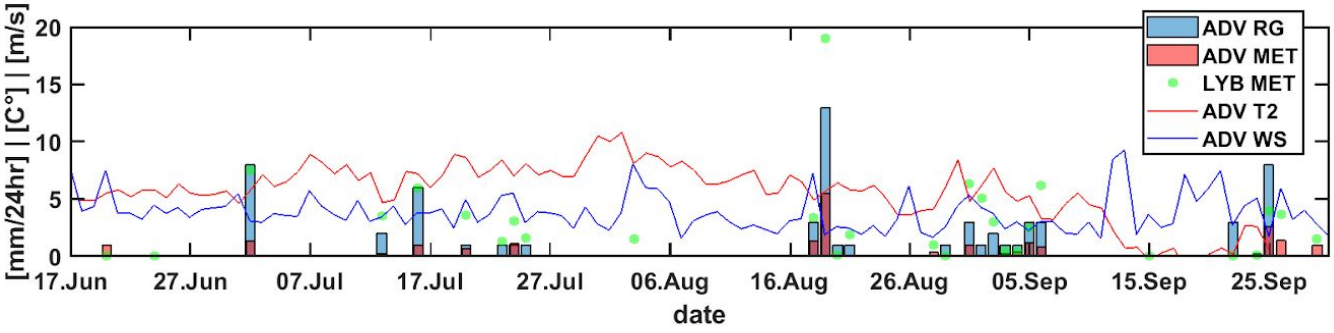

Figure 5.18: *24hr precipitation measured by the ENCRN-50 (blue bars) the Geonor T-200B (red bars) and Longyearbyen airport (green dots), together with Adventdalen daily averaged 2m wind speed (blue line) and Adventdalen 2m daily averaged temperature (red line).*

In Figure 5.18 precipitation observations through summer and autumn of 2018 from the Adventdalen rain gauge (ECRN-50), Adventdalen MET station (Geonor T-200B) and Longyearbyen Airport (manual) are shown together with wind speed and temperature. It is evident that Geonor T-200B did not catch as much precipitation as the ECRN-50 rain gauge through the summer.

Keeping in mind that ECRN-50 is only capable of measuring precipitation in 1 mm steps, there are only three days when Geonor T-200B measured precipitation (20. Jun: 1 mm, 26. Sep: 1.4 mm and 29.Sep: 1 mm) that the ECRN-50 in theory should have been able to measure, but did not. Longyearbyen airport measured 0.0 mm, 3.7 mm and 1.5 mm on these dates, respectively.

Only one time out of the 21 times ECRN-50 measured 1 mm or more, the observations from Geonor T-200B were higher (24.July). There are nine episodes when ECRN-50 measured 1 mm precipitation or more while Geonor T-200B measured only 0.0-0.2 mm. On three of these occasions (23. July, 25. July and 29.Aug) the Geonor T-200B did not register precipitation at all. In seven of these nine events the manual rain gauge at Longyearbyen Airport measured precipitation, and webcam images from Longyearbyen (UNIS) show rainy conditions Adventdalen (See Fig. A7 - A14, Appendix). In as many as 19 of 21 episodes when the ECRN-50 measured precipitation levels above 1 mm in Adventdalen, false readings can most likely be ruled out, as precipitation is indeed registered at Longyearbyen Airport in the same time span.

These small rain events are not the focus of this study, but for climate studies, correct measurements over long time spans are of great importance, since they become accumulated into

monthly or yearly precipitation levels. During the 3.5 months (Jun-Oct) that the ECRN-50 measured precipitation in Adventdalen, it measured a total of 64 mm precipitation. In contrast, the Geonor T-200B measured 22.1 mm, while Longyearbyen airport measured 101.5 mm in the same period.

Table 5.4: *The four events with more than 5 mm measured by any instrument in Adventdalen, with associated synoptic scale flow type of that event.*

Date	Longyearbyen Airport	Adventdalen ENCRN-50	Adventdalen Geonor T-2500B	Flow type
02. Jul	7.5 mm	8 mm	1.3 mm	NW
16. Jul	6.0 mm	6 mm	1.0 mm	S
19. Aug	19 mm	13 mm	5.5 mm	SE
25. Sep	4 mm	8 mm	2.6 mm	N

Given the main focus of this thesis on heavy rain events, less emphasis is put on the 1-3 mm events that the ECRN-50 observed. The four events when the ECRN-50 measured more than 5 mm precipitation in 24 hours are listed in Table 5.4, together with the associated atmospheric flow type (as defined in Section 4.3.5).

Given the doubt cast on the Geonor T-200B measurements in Adventdalen, it is interesting to compare its measurements along with the ECRN-50 measurements in Adventdalen to the nearest manual MET station at Longyearbyen airport (9 km apart). Using the latter as a reference, the difference in rain accumulated over four heavy rain events is 7.5 mm for the Geonor T-200B, while for the ECRN-50 it is 2.6 mm. Expressed in percentages of the accumulated precipitation at Longyearbyen Airport over the four events, the precipitation amount is 70 % and 34 % less for the Geonor T-200B and ECRN-50 than at Longyearbyen airport, respectively. In this context it should be mentioned that some differences in precipitation amounts could be expected between Longyearbyen airport in Adventdalen, e.g. associated with localized showers embedded in the frontal systems. Interestingly, the Geonor T-200B instrument in Adventdalen was visited by MET personnel and underwent a routine check-up after the summer of 2018, without any significant sign of malfunctioning detected, except a more continuous heating of the rain gauge opening than normal for the summer period (Meteorologist at MET Ine-Therese Pedersen, personal communication).

5.3.6 Discussion Field Campaign Results

Despite the broken Murdoch rain gauge station and one of the small deployable stations, the rain gauge field campaign can be deemed a success, by showing that even these low cost and simple rain gauge weather stations are able to make reasonable measurements in a remote high Arctic environment during summer and autumn, given that the mean wind speed is not too strong (~ 7 m/s), or the temperature is too low, causing solid precipitation (Fig. 4.7)

As explained in section 5.3.5, the ECRN-50 rain gauge in Adventdalen was originally placed near the Geonor T-200B, with the goal to validate the ECRN-50 measurements, and subsequently come up with a possible wind adjustment factor applicable to the precipitation measurements from the other rain gauge stations. However, as shown, the precipitation observations from the two instruments in Adventdalen did not match well. The the ECRN-50 was actually closer to the Longyearbyen Airport measurements, both in terms of total rainfall through the summer, and in daily amounts (Table 5.4). Overall, the Geonor T-200B observed just around ⅓ of the total precipitation amount measured by the ECRN-50 through the summer (MET: 22.1 mm, RG: 64 mm).

The discrepancy between the two instruments in Adventdalen can either be caused by the Geonor T-200B undercatching, or the ECRN-50 overcatching precipitation, or a combination of the two. That the ECRN-50 rain gauge should be overestimating the relatively light Arctic precipitation, is rather unlikely. When compared to the manual Longyearbyen Airport measurements, the ECRN-50 in Adventdalen almost always observed less precipitation, although this could also, to some degree, be caused by an actual climatological difference between the two sites (9 km apart). The fact that the Geonor T-200B is undercatching precipitation seems more likely, given the relatively large observed difference between Adventdalen and Longyearbyen Airport, with no clear differences in adjacent topography that could cause such a result. Additionally, the Geonor T-200B is heated around the top (“Geonor T-200B datasheet” n.d.), and during an inspection it turned out that this heating was constantly on, and not periodically as it is supposed to in summer time (Ine Therese Pedersen, MET Meteorologist Longyearbyen, Personal Communication). The warm air caused by this heating could hypothetically create a small updraft or air flow out of the rain gauge opening, making light raindrops miss the rain gauge opening, and subsequently catching less precipitation, but this remains just a theory.

In that aspect, it is interesting to note that despite having evacuated inhabitants, closed off roads and observed mudslides and flooding of roads due to heavy rainfall the last years

(Hanssen-Bauer et al. 2019), currently (2019), in addition to the Adventdalen Geonor T-200B rain gauge there are no other official hourly observations of precipitation in the area around Longyearbyen, except the Platåberget III optical instrument ("Thies Laser Precipitation Monitor datasheet" n.d.).

For this field campaign, that used innovative windshields around a type of rain gauge never used in Arctic conditions before (Fig. 4.7), it is unfortunate that the field period did not yield any opportunity to properly validate the measurements against official precipitation measurements. However, as mentioned, the manual precipitation measurements at Longyearbyen airport is the nearest station, except from the Geonor T-200B in Adventdalen, for validating the Adventdalen ECRN-50 rain gauge, and those measurements yield a possible general undercatchement by the ECRN-50. Although, if this is caused by the different instruments or a climatological difference will remain speculations, due to the distance between the stations (9km).

Because of the uncertainty concerning the precipitation measurements in Adventdalen, no upward adjustments of the values, due to observed wind speeds, was done on the precipitation data before analysing them. As such, it makes it more unlikely that the intense rain observation at Bjonapynten the 18th August was erroneous. As discussed in Section 5.3.2, other reasons for overcatching (wind, leftover rain drops etc.) is also unlikely for this event. This makes the 5mm/hr observation remarkable, as it shows that intense rainfall can be embedded in frontal systems with a SE wind component in Central Svalbard. This event also sets the record for hourly (5 mm), 3-hourly (8 mm) and 6-hourly (10 mm) precipitation measured by the field campaign rain gauges in this study, and thus sets a standard for what can be expected in terms of hourly intensities, from summer rain storms in Central Svalbard. It also shows that despite the SW atmospheric flow type causing the heaviest rain storms in Svalbard, synoptic situations with an SE flow type, should not be ignored, especially for the central and east parts of Spitsbergen. The 18-19th August heavy rain event (19 mm) was in fact not that far from being an event with an estimated return period of 10 years for Longyearbyen (25 mm), and higher than the 99.5 percentile (11 mm) of rain events in Longyearbyen (Dobler et al. 2019).

During this 18-19th of August heavy rain event, Tuna South, 10 km further in Tempelfjorden from Bjonapynten, only measured 5 mm in total, and a maximum hourly intensity of 1 mm. This shows that there can indeed be a difference in precipitation over short distances in Svalbard. But, for the Breinosa-Adventdalen stations (7.5 km apart) shown in Section 5.3.3, it seems more likely that the large elevation gap between the stations (~500 m) caused the difference in precipitation. The observations, although obtained over a short time period, demonstrate that an elevation gradient in precipitation can be present in Central Spitsbergen. In comparison to previous results in the range 4-28 % (Killingtveit et al. 2003) the values found by this field

campaign, 8-12 %, are somewhat in the lower half. But, as mentioned, to make a more reliable estimate of the precipitation elevation gradient, more persistent measurements needs to be done.

One of the reasons for trying to estimate the increasing precipitation with height, is that it is an important variable in glaciology, when estimating mass balance and hydrology for Svalbard glaciers in general (Killingtveit et al. 2003). Indeed, the possible effects of heavy rainfall on the surging glacier Tunabreen's velocities was one of the reasons Tempelfjorden and Tuna South was chosen as a fieldsite in this study. As mentioned, no heavy rain event of the magnitude that struck Svalbard in November 2016 was measured in the field campaign of 2018, and unfortunately there was no time to extract or analyse Tunabreen's velocity from satellite imagery. Instead, the results from Tunabreen became an interesting meteorological dataset from a remote part of Svalbard, that shed some light on precipitation patterns and the performance of AROME Arctic in this area.

The observations from the Tuna South rain gauge station is (as far as the author knows) the first measurements of precipitation in the inner parts of Tempelfjorden. Based on the measurements, shown in Section 5.3.4, the most significant precipitation events in this part of Spitsbergen seems to be caused by SE flow, opposite to the SW flow dependency shown for the West-Coast stations (Section 5.1.1). Although no heavy rain event was measured at this station, which makes it difficult to compare with the AA evaluation in Section 5.2, it is still interesting that the model seem to overestimate precipitation during SW flow. This is somewhat similar to the results found for Longyearbyen (Section 5.2.1), which also is located in central Svalbard, but 40 km further southwest. Noteworthy is also the tendency of AA to underestimate precipitation in the Tuna South station grid point, during SE or NW flow regimes. Although, as already mentioned, it is only possible to say something about these medium-range precipitation events (1 - 8 mm/24hr) that was forecasted or observed.

Interestingly, Tuna South measures lower total amount through the field period (45 mm) than the ECRN-50 in Adventdalen (64 mm), and has it is highest daily measurement of 8 mm/24hr (16.July and 03.Aug) on other days than the field campaign rain gauge in Adventdalen (19.Aug, 01.Jul, 25.Sep). The results from Tuna South is a good example of how the current precipitation measuring station network on Svalbard is biased towards conditions on the West-Coast of Spitsbergen.

Chapter 6
Summary, Conclusions and Outlook

6.1 Summary and conclusions

For the study period of this thesis, June to November 2016-2018, the MET stations in Svalbard that observed the highest number of heavy rain events (> 10 mm/24 hr) were the West-Coast stations Hornsund (30), Isfjord Radio (17) and Ny-Ålesund (27). Of the three seasons (2016-2018), the 2017 season was the season with fewest heavy rain events at most of the available MET stations.

In line with previous work on precipitation in Svalbard, most of the heavy rain events in this study period were connected to a SW atmospheric flow type (Section 5.1), that is likely to induce orographic precipitation when advecting moist air over the West-Coast mountains (Førland et al. 1997; Serreze et al. 2015; Dobler et al. 2019) . The most extreme heavy rain event was the 8th of November 2016 event, with a SW flow. During this event all stations on Spitsbergen measured heavy rain, and Ny-Ålesund measured the highest amount of 87 mm in 24 hours (Table 5.1). Heavy rain events were also found to occur during other atmospheric flow types. Especially SE flow is able to generate heavy rain events at the central Spitsbergen stations, Longyearbyen, the field campaign area, and in Hornsund.

The numerical weather prediction model AROME Arctic (AA) generally underestimates the heavy rain events at the West-Coast stations when comparing the station grid point precipitation data with observations (ME ~ - 5-8 mm/24hr). For Longyearbyen and the central parts of Spitsbergen the picture is more complex with AA generally overestimating precipitation during SW events and underestimating it during SE events, resulting in a ME of 1.3 mm, but a MAE of 7.1 mm for the heavy rain events in Longyearbyen (Fig. 5.5 and Fig. 5.6). These findings are in line with other studies (Køltzow 2019a), but as mentioned, as the error statistics are based on a relatively few number of cases, these conclusions are naturally not very robust.

Especially for the heavy rain episodes with SW flow, precipitation in AA is strongly linked to elevation, i.e. precipitation in general increases with increasing elevation. Elevation precipitation gradients in Svalbard between 4-28% has also been proposed based on observations (Killingtveit et al. 2003). Averaged for the heavy rain events, AA has an estimated precipitation increase of

14.9 % pr 100 m elevation, which is in the middle of the estimates compiled by Killingtveit et al. (2003). The elevation precipitation gradient part of the study would have benefited from more observations of rain events and more stations at different elevations.

In order to take spatial variability of precipitation into account in the model evaluation part, grid point boxes were introduced around the station grid point (explained in Section 4.3.8). The grid point box metrics with high values (Max and MET high) lead to better model performance (in ME and MAE) compared against the observations for the heavy rain events at the West-Coast stations. However, these might also cause more false alarm events (heavy rain forecasted in model but not observed), which were not analysed in this study. Additionally, the MET high and MET low estimates (based on a 15 x 15 grid box size) show a large spread between them for the two events studied closer for Isfjord Radio (8.Nov: 23mm and 15.Oct: 18mm, Fig. A5 and A6 Appendix). Simultaneously, the spread between the smaller Max and Min box metrics (based on 3 x 3 grid box size) are not as big (8.Nov: 17 mm and 15.Oct: 12 mm, Fig. A5 and A6 Appendix), most likely due to the smaller size of the boxes.

The number of MET stations with hourly measurements are few. The measurements that do exist from Isfjord Radio however, indicate that hourly model precipitation output seems to fit observations relatively well in intensity and timing during the very strong 8th November 2016 event, but less so during the 15th October 2016 event. For at least one event (8.Nov 2016) the model also compensates for an underestimation of the total daily precipitation, by producing precipitation in periods where none was observed (Fig. 5.11). Also the differences in maximum hourly intensity is noteworthy, as this variable can play an important role in triggering mud slides (Larsson 1982). For the 15. October 2016 event, the maximum forecasted hourly intensity is as low as 50 % of the observed, with 2.2 mm forecasted by AA and 4.1 mm observed.

When comparing AA to the ECMWF IFS HRES (EC) model, there is no clear difference in performance when it comes to forecasting the heavy rain events that occurred in the study period. The ME and MAE (~ 5-10 mm) values at the four stations considered are relatively similar for both models (Fig. 5.5 and Fig. 5.6). Though EC is more likely to likely to actually forecast precipitation above 10 mm for the heavy rain events, and subsequently has a higher hit rate at all stations (Table 5.2). This hit rate result must be treated cautiously, since ‘false alarm’ events are not included in this study, and the hit rate result is likely dependent on the heavy rain event threshold value chosen. Nevertheless, there are occasions where AA greatly outperforms EC. One example is 19.September 2017 at Hornsund where 73 mm was observed, AA forecasted 45 mm while EC forecasted less than 20 mm.

The second main goal of this thesis was to study in more detail heavy precipitation events and general precipitation patterns in central Spitsbergen by conducting a field campaign in the

summer of 2018. Like the rest of Svalbard, this is a particularly climate sensitive region with amongst others several marine terminating glaciers. Simultaneously, the region is not as logistically challenging to reach as most parts of the archipelago, which makes it ideal for shorter field campaigns like the one that was designed as part of this study for the summer of 2018. During this campaign, several rain gauges were installed in strategic locations, including Bjonapynten, Tuna South and Breinosa (Fig 4.8), providing a unique dataset of precipitation from central Spitsbergen. In addition, a rain gauge was installed in Adventdalen to compare it against the MET Geonor T-200B rain gauge there. Although the resulting dataset spans a relatively limited timeframe, the campaign can be deemed a success, as it gives new insight into summer and early autumn rainfalls in both populated, and more remote parts of Spitsbergen where few or no such observations have been made before.

Firstly, the field campaign results yielded a heavy rain event with a SE flow type reaching the 10 mm threshold in only six hours, and hourly precipitation intensity of 5mm/hr measured during the event at Bjonapynten station. This is possibly the most intense hourly precipitation rate measured in central Spitsbergen, and the observation gives an indication of what can be expected of hourly rainfall rates in heavy rain events on Svalbard, both now and in the coming years.

Secondly, the field campaign also demonstrated that it is possible to measure and estimate a precipitation elevation gradient in central Spitsbergen, as other studies have been doing on the West-Coast around Ny-Ålesund in the 90's (Killingtveit et al. 2003). By utilizing the fact that two identical instruments were measuring precipitation at different elevations in central Spitsbergen (Adventdalen 13 m.a.s.l., Breinosa 500 m.a.s.l.) during the field campaign, an elevation gradient of 8-12 % increase in precipitation per 100 m was found, based on six 24 hr measurements taken during a week in August-September 2018. This is somewhat in the lower half of the range of estimates from 4-28% that has been found in other studies (Killingtveit 2003).

Based on the precipitation measurements taken at the Tuna South station in summer 2018 (Section 5.3.4), there is shown to be a clear difference in synoptic flow type for when AA underestimates or overestimates precipitation in the station model grid point. For rain events with a southwest synoptic (SW) flow type, AA tend to overestimate the precipitation amount (3.8 mm/24 hr), while events with southeast (SE) or northwest flow (NW) type is underestimated in the model (-0.1 mm/24 hr). In general, the SE events are also stronger (5.7 mm/ 24 hr) than the SW events (1.7 mm/24 hr) at this station.

Finally, field campaign results show that the Adventdalen Geonor T-200B rain gauge from MET most likely was undercatching precipitation during the summer and autumn of 2018, which means that data from this MET station should be thoroughly quality checked if used by others.

The Adventdalen ECRN-50 data highlights the importance of trustworthy hourly observations to better understand and monitor heavy rain events in the area around Longyearbyen, a settlement vulnerable to mudslides and avalanches (Larsson 1982; Hanssen-Bauer et al. 2019).

Overall, the field campaign part of this thesis has demonstrated how a small, low cost, field campaign can be conducted in summertime in central Spitsbergen to help improve the understanding of heavy rain events in Svalbard. Currently, this is a most important topic, as the Svalbard 2100 report clearly states that these events are likely to be more frequent and more intense in the coming decades (Hanssen-Bauer et al. 2019)

6.2 Outlook

There has already been done studies that have focused on evaluating and improving the ability of AROME Arctic (AA) to forecast precipitation on Svalbard (Køltzow 2019a, Køltzow et al 2019b), and more studies can be expected in the future. It would be interesting for future studies to do more specific case studies on the heavy rain events when models have large errors in precipitation amount (e.g. 19.September 2017 in Hornsund), in an attempt to better understand why the model might be so erroneous in these cases. By focusing on a selection of events, it should be possible to get a clearer idea of what is causing the errors in the models, e.g. wrong positioning of extratropical cyclones and fronts in time or space, some parameterization scheme or perhaps the boundary conditions.

In the coming years, there will most likely be more heavy rain events in Svalbard (Dobler, A. Førland, E.J. Isaksen, K. 2019), which can be further used to evaluate and improve AA's performance in more detail. To achieve this in the best way possible, an effort to obtain continuous and accurate precipitation measurements with high temporal resolution, and to obtain observations from other locations in Svalbard than the West-Coast and areas around Longyearbyen, should be made by MET and other research institutions doing research in Svalbard.

In a climate science perspective, many of the changes that are attributed to climate change are already taking place in Svalbard (Førland et al. 2011; Serreze et al. 2011), and it is therefore crucial to maintain the current long term measurement series of precipitation and temperature (Nordli 2010). Additionally, with more effort put into introducing continuous observations in areas where few measurements are taken to day, more observations of possible extremes, and a better understanding of the spatial and temporal variability that might be present, would be possible to achieve.

As mentioned in Section 2.1, and in most scientific papers on Arctic precipitation, the problem of undercatchement due to blowing snow and wind is substantial for this region. A shift from this apologetic attitude, towards a more opportunistic style of measuring precipitation in the summertime when conditions allow it, would largely benefit the precipitation research in Svalbard. As previous results (e.g. Førland et al. 1997), and this thesis, show: It is possible to carry out field campaigns that measure precipitation in the form of rain, through the summer season in Svalbard.

Other studies (e.g. Wolff 2015), have calculated, and implemented an adjustment factor to balance for undercatchement of precipitation due to wind during precipitation events, but this is not done in this study. This is mostly since the ECRN-50 rain gauges have quite a different shape than the Geonor-T200B or the manual rain gauge, which could cause different small scale turbulent effects around the rain gauge than the adjustment factor has been calibrated for. Additionally, there was no successful measurements by the ECRN-50 rain gauge close to the official Longyearbyen Airport manual rain gauge to make corrections from. Future studies that might use the ECRN-50 rain gauge, should do comparison measurements over a longer time close to a manual rain gauge or Geonor T-200B instrument, and in windy conditions, to attempt calculating an adjustment or correction factor for the precipitation measurements done by this specific type of rain gauge.

Future field campaigns measuring summer precipitation could also possibly focus more on the interesting topic of how heavy rain events might increase glacier velocities, by reducing the glacier bed friction (Kehrl et al. 2015), in Svalbard. In other regions such as Greenland (Doyle et al. 2015), New-Zealand (Kehrl et al. 2015), Switzerland (Sugiyama and Gudmundsson 2004) and Himalaya (Kääb et al. 2018), such effects have been investigated, but (as far as the author knows) this has not been done for the Svalbard region. Another glaciology relevant number that could be estimated more precisely from persistent summer field campaigns is the precipitation elevation gradient. As glaciers gain mass from snowfall, may lose mass from rainfall, and in Svalbard span altitudes from sea level up to 1700 m.a.s.l., it makes the elevation gradient an important tool for estimating the mass balance and hydrological regimes of Svalbard glaciers. Although thorough work has been done in trying to estimate a precipitation elevation gradient for Svalbard (e.g. Førland et al. 1997), the results are mostly based on observations around Ny-Ålesund and at the West-Coast, and few follow-up studies from other areas on Spitsbergen have been conducted to evaluate the results.

Finally, a phenomenon that is relevant in the context of heavy rain events, is that of Atmospheric Rivers (AR). AR's, which there was no time to include a thorough analysis of in the context of this thesis, can be considered the largest freshwater 'rivers' on earth, with an average water transport of more than double of the Amazon river. They are located in the lower troposphere

and are typically associated with the cold front of extratropical cyclones ("Atmospheric River Definition" n.d.). Newell coined the term AR in the early 90's (Zhu and Newell 1998), but it was not until the last decade that the topic started receiving a lot of scientific interest.

In Svalbard, the most extreme heavy rain events seems to show similarities with AR (Serreze et al. 2015). There is nevertheless a wide range in intensity, shape and duration when it comes to ARs. An analysis to check if the most extreme heavy rain events in Svalbard fit in this AR framework, could be done with for example reanalysis data, or observations from the daily balloon soundings in Ny-Ålesund. A quick calculation using the balloon sounding data from Ny-Ålesund at 12Z, 7th November 2016, hours before the most heavy rain event in the study period started, gives an integrated water vapor transport (IVT) of 138 kg/m/s. The lower threshold used to detect a possible AR is an IVT above 250 kg/m/s (Ralph et al. 2019), so the 8th November 2016 does not reach AR conditions, based on this one sounding. This might suggest that a new and lower threshold should be set to identify 'Arctic Atmospheric Rivers', but more data from heavy rain events must be analysed before concluding on this. Using a type of AR classification could nevertheless be useful, both as an additional climatological framework for heavy rain events, and perhaps in the future, as an aid in forecasting heavy rain events in Svalbard.

Reference list

Atmospheric River Definition, 2019. (n.d.). Retrieved from http://glossary.ametsoc.org/wiki/Atmospheric_river

Batrak, Y., Kourzeneva, E. & Homleid, M., 2018. Implementation of a simple thermodynamic sea ice scheme, SICE version 1.0-38h1, within the ALADIN-HIRLAM numerical weather prediction system version 38h1. *Geoscientific Model Development Discussions*, pp.1–30. Available at: http://dx.doi.org/10.5194/gmd-2018-22.

Bengtsson & coauthors, 2017. The HARMONIE–AROME Model Configuration in the ALADIN–HIRLAM NWP System. *Monthly Weather Review*, 145(5), pp.1919–1935. Available at: http://dx.doi.org/10.1175/mwr-d-16-0417.1.

Bintanja, R. & Andry, O., 2017. Towards a rain-dominated Arctic. *Nature Climate Change*, 7(4), pp.263–267. Available at: http://dx.doi.org/10.1038/nclimate3240.

Boone, A., Calvet, J.-C. & Noilhan, J., 1999. Inclusion of a Third Soil Layer in a Land Surface Scheme Using the Force–Restore Method. *Journal of Applied Meteorology*, 38(11), pp.1611–1630. Available at: 2.0.co;2">http://dx.doi.org/10.1175/1520-0450(1999)038<1611:ioatsl>2.0.co;2.

Borstad, C., 2017. Tunabreen may be surging decades earlier than expected. *UNIS*. Retrieved from https://www.unis.no/tunabreen-may-surging-decades-earlier-expected/ [Accessed August 12, 2019].

Campbell Wind Sentry datasheet. (n.d.). Retrieved from https://www.campbellsci.com/03002-wind-sentry

CR 10 logger datasheet. (n.d.). Retrieved from https://www.campbellsci.com/cr10

CR 200 logger datasheet. (n.d.). Retrieved from https://www.campbellsci.com/cr200

Dee, D.P. & coauthors, 2017. The ERA-Interim reanalysis: configuration and performance of the data assimilation system. *Quarterly Journal of the Royal Meteorological Society*, 137, pp.553–597. Available at: https://doi.org/10.1002/qj.828

Dobler, A., Førland, E.J. Isaksen, K., 2019. *Present and future heavy rainfall statistics for Svalbard - Background report for Climate in Svalbard 2100*, Norsk klimaservicesenter. Available at: https://cms.met.no/site/2/klimaservicesenteret/rapporter-og-publikasjoner/_attachment/14513?_ts=168f0e62a92. [Accessed August 12, 2019].

Douville, H., Royer, J.-F., Mahfouf, J.-F., 1995. A new snow parameterization for the Météo-France climate model. *Climate Dynamics*, 12(1), pp.21–35. Available at: http://dx.doi.org/10.1007/bf00208760.

Doyle, S.H. & coauthors, 2015. Amplified melt and flow of the Greenland ice sheet driven by late-summer cyclonic rainfall. *Nature Geoscience*, 8(8), pp.647–653. Available at: http://dx.doi.org/10.1038/ngeo2482.

Eckerstorfer, M. & Christiansen, H.H., 2011. The "High Arctic Maritime Snow Climate" in Central Svalbard. *Arctic, Antarctic, and Alpine Research*, 43(1), pp.11–21. Available at: http://dx.doi.org/10.1657/1938-4246-43.1.11.

ECMWF, Part IV : Physical processes. In ECMWF, ed. *IFS Documentation CY45R1*. IFS Documentation. ECMWF. Available at: https://www.ecmwf.int/en/elibrary/18714-part-iv-physical-processes [Accessed August 12, 2019].

ECRN-50 datasheet. (n.d.). Retrieved from http://ictinternational.com/pdf/?product_id=261

Eklima data portal. (n.d.). Available at: www.eklima.no [Accessed August 12, 2019].

Ericson, Y., Falck, E., Chierici, M., Fransson, A., Kristiansen, S., 2019. Marine CO2 system variability in a high arctic tidewater-glacier fjord system, Tempelfjorden, Svalbard. *Continental Shelf Research*, 181, pp.1–13. Available at: http://dx.doi.org/10.1016/j.csr.2019.04.013.

Fleming, E.J., Lovell, H., Stevenson, C.T., Petronis, M., Benn, D., Hambrey, M., Fairchild, I., 2013. Magnetic fabrics in the basal ice of a surge-type glacier. *Journal of Geophysical Research: Earth Surface*, 118(4), pp.2263–2278. Available at: http://dx.doi.org/10.1002/jgrf.20144.

Flink, A.E., Noormets, R., Kirchner, A., Benn, D., Luckmann, A., Lovell, H., 2015. The evolution of a submarine landform record following recent and multiple surges of Tunabreen glacier, Svalbard. *Quaternary Science Reviews*, 108, pp.37–50. Available at: http://dx.doi.org/10.1016/j.quascirev.2014.11.006.

Fylkesvis oversikt over høyeste registrerte nedbørmengde (mm) for ulike varigheter. (n.d.). Retrieved from https://klimaservicesenter.no/faces/desktop/article.xhtml?uri=klimaservicesenteret/dimensjonerende-nedbor [Accessed August 12, 2019].

Førland, E.J., Benestad, R., Hanssen-Bauer, I., Haugen, J.E., Skaugen, T.E., 2011. Temperature and Precipitation Development at Svalbard 1900–2100. *Advances in Meteorology*, 2011, pp.1–14. Available at: http://dx.doi.org/10.1155/2011/893790.

Førland, E.J., Hanssen-Bauer, I., Nordli, P.Ø., 1997. *Orographic precipitation at the glacier Austre Brøggerbreen, Svalbard*, MET report. Available at: https://www.met.no/publikasjoner/met-report/met-report-1997 [Accessed August 12, 2019].

Geonor T-200B datasheet. (n.d.). Retrieved from https://geonor.no/wp-content/uploads/2014/11/GeonorBrosj4siderAug_10-Lav.pdf

Hanssen-Bauer, I., and coauthors, 2019. *Climate in Svalbard 2100 - A knowledge base for climate adaptation*, Norsk Klimaservicesenter. Available at: https://www.miljodirektoratet.no/globalassets/publikasjoner/m1242/m1242.pdf [Accessed August 12, 2019].

Heiberg, H., Kristiansen, S., Mamen, J., Szewczyk-Bartnicka, H., 2016. *Været i Norge, Klimatologisk månedsoversikt November og høstsesongen 2016*, MET report. Available at: https://www.met.no/publikasjoner/met-info/met-info-2016 [Accessed August 12, 2019].

How, P. & coauthors, 2019. Calving controlled by melt-under-cutting: detailed calving styles revealed through time-lapse observations. *Annals of Glaciology*, 60(78), pp.20–31. Available at: http://dx.doi.org/10.1017/aog.2018.28.

Humlum, O., 2002. Modelling late 20th-century precipitation in Nordenskiold Land, Svalbard, by geomorphic means. *Norsk Geografisk Tidsskrift - Norwegian Journal of Geography*, 56(2), pp.96–103. Available at: http://dx.doi.org/10.1080/002919502760056413.

Isaksen, K., Nordli, Ø., Førland, E.J., Lupikasza, E., Niedźwiedź, T., 2016. Recent warming on Spitsbergen-Influence of atmospheric circulation and sea ice cover. *Journal of Geophysical Research: Atmospheres*, 121(20), pp.11,913–11,931. Available at: http://dx.doi.org/10.1002/2016jd025606.

Ivanov, B.V., Sviashchennikov, P.N., Zhuravkiy, D., Pavlov, A., Førland, E.J., 2014. Metadata for a long-term climate series from the Russian meteorological station "Pyramiden" (1948-1957) at Svalbard (Short Communication). *CPR population research*, 4(1), pp.57–62. Available at: http://dx.doi/org/10.5817/CPR2014-1-6

Kääb, A. & coauthors, 2018. Massive collapse of two glaciers in western Tibet in 2016 after surge-like instability. *Nature Geoscience*, 11(2), pp.114–120. Available at: http://dx.doi.org/10.1038/s41561-017-0039-7.

Kehrl, L.M., Horgan, H.J., Anderson, B.M., Dadic, R., Mackintosh, A.N., 2015. Glacier velocity and water input variability in a maritime environment: Franz Josef Glacier, New Zealand. *Journal of Glaciology*, 61(228), pp.663–674. Available at: http://dx.doi.org/10.3189/2015jog14j228.

Killingtveit, Å., Pettersson, L.E., Sand, K., 2003. Water balance investigations in Svalbard. *Polar Research*, 22(2), pp.161–174. Available at: http://dx.doi.org/10.1111/j.1751-8369.2003.tb00105.x.

Køltzow, M., 2019a, Strengths and limitations of state-of-the-art weather and climate prediction systems in the Arctic. The APPLICATE project (applicate.eu); Deliverable No. 5.2. Preliminary version provided by M. Køltzow Jan. 2019, MET-Norway, final version will be available at: https://applicate.eu/outreach/documents/category/5-deliverables?start=0

Køltzow, M., Casati, B., Bazile, E., Haiden, T., Valkonen, T.M., 2019b. An NWP Model Intercomparison of Surface Weather Parameters in the European Arctic during the Year of Polar Prediction Special Observing Period Northern Hemisphere 1. *Weather and Forecasting*, 34(4), pp.959–983. Available at: https://doi.org/10.1175/WAF-D-19-0003.1

Larsson, S., 1982. Geomorphological Effects on the Slopes of Longyear Valley, Spitsbergen, after a Heavy Rainstorm in July 1972. *Geografiska Annaler: Series A, Physical Geography*, 64(3/4), pp.105–125. Available at: https://doi.org/10.1080/04353676.1982.11880059

Masson, V. & coauthors, 2012. The SURFEXv7.2 land and ocean surface platform for coupled or offline simulation of Earth surface variables and fluxes. *Geoscientific Model Development Discussions*, 5(4), pp.3771–3851. Available at: http://dx.doi.org/10.5194/gmdd-5-3771-2012.

Milne, R. & Wallmann, J., 2007. *Forecasting Lee-Side Precipitation in the Central and Northern Sierra - Part II: Narrow Cold Frontal Rainbands*, Weather forecast office Reno NV. Available at: https://www.weather.gov/media/wrh/online_publications/TAs/ta0702.pdf. [Accessed August 12, 2019]

Müller, M., Batrak, Y., Kristiansen, J., Køltzow, M., Noer, G., 2017. Characteristics of a Convective-Scale Weather Forecasting System for the European Arctic. *Monthly Weather Review*, 145(12), pp.4771–4787. Available at: http://dx.doi.org/10.1175/mwr-d-17-0194.1.

Neiman, P.J., Ralph, F.M., Moore B.J., Hughes, M., Mahoney, K.M., Cordeira, J.M., Dettinger, M.D., 2013. The Landfall and Inland Penetration of a Flood-Producing Atmospheric River in Arizona. Part I: Observed Synoptic-Scale, Orographic, and Hydrometeorological Characteristics. *Journal of Hydrometeorology*, 14(2), pp.460–484. Available at: http://dx.doi.org/10.1175/jhm-d-12-0101.1.

Nordli, Ø., 2010. The Svalbard Airport Temperature Series. *Bulletin of Geography. Physical Geography Series*, 3(1), pp.5–25. Available at: http://dx.doi.org/10.2478/bgeo-2010-0001.

Ralph, F.M. & coauthors, 2019. A Scale to Characterize the Strength and Impacts of Atmospheric Rivers. *Bulletin of the American Meteorological Society*, 100(2), pp.269–289. Available at: http://dx.doi.org/10.1175/bams-d-18-0023.1.

Serreze, M.C., Barrett, A.P. & Cassano, J.J., 2011. Circulation and surface controls on the lower tropospheric air temperature field of the Arctic. *Journal of Geophysical Research*, 116(D7). Available at: http://dx.doi.org/10.1029/2010jd015127.

Serreze, M.C., Crawford, A.D., Barrett, A.P., 2015. Extreme daily precipitation events at Spitsbergen, an Arctic Island. *International Journal of Climatology*, 35(15), pp.4574–4588. Available at: https://doi.org/10.1002/joc.4308

Sevestre, H., Benn, D.I, Hulton, N.R., Bælum, K., 2015. Thermal structure of Svalbard glaciers and implications for thermal switch models of glacier surging. *Journal of Geophysical Research: Earth Surface*, 120(10), pp.2220–2236. Available at: http://dx.doi.org/10.1002/2015jf003517.

Shahrban, M., Walker, J.P, Wang, Q.J., Seed, A., Steinle, P., 2016. An evaluation of numerical weather prediction based rainfall forecasts. *Hydrological Sciences Journal*, 61(15), pp.2704–2717. Available at: http://dx.doi.org/10.1080/02626667.2016.1170131.

Sugiyama, S. & Gudmundsson, H.G., 2004. Short-term variations in glacier flow controlled by subglacial water pressure at Lauteraargletscher, Bernese Alps, Switzerland. *Journal of Glaciology*, 50(170), pp.353–362. Available at: http://dx.doi.org/10.3189/172756504781829846.

Teigen, S.H., Nilsen, F. & Gjevik, B., 2010. Barotropic instability in the West Spitsbergen Current. *Journal of Geophysical Research*, 115(C7). Available at: http://dx.doi.org/10.1029/2009jc005996.

Thies Laser Precipitation Monitor Datasheet. (n.d.). Retrieved from: https://www.thiesclima.com/pdf/en/Products/Precipitation-Electrical-devices/?art=774 [Accessed August 12, 2019].

Thredds data server. (n.d.). Available at https://thredds.met.no/thredds/catalog.html [Accessed August 12, 2019].

Tiedtke, M., 1993. Representation of Clouds in Large-Scale Models. *Monthly Weather Review*, 121(11), pp.3040–3061. Available at: 2.0.co;2">http://dx.doi.org/10.1175/1520-0493(1993)121<3040:rocils>2.0.co;2.

TinyTag Sensor datasheet. (n.d.). Retrieved from http://gemini2.assets.d3r.com/pdfs/original/3242-tgp-4500.pdf [Accessed August 12, 2019].

Vikhamar-Schuler, D., Førland, E.J., Lutz, J., Gjelten, H.M., 2019. *Evaluation of downscaled reanalysis and observations for Svalbard - Background report for Climate in Svalbard 2100*, Norsk Klimaservicesenter. Available at: https://cms.met.no/site/2/klimaservicesenteret/rapporter-og-publikasjoner/_attachment/14514?_ts=168f0e505b7. [Accessed August 12, 2019].

Wallace, J.M. & Hobbs, P.V., 2006. Cloud Microphysics. *Atmospheric Science*, pp.209–269. Available at: http://dx.doi.org/10.1016/b978-0-12-732951-2.50011-9.

Wolff, J.K., Harrold, M., Fowler, T., Gotway, J.H., Nance, L., Brown, B.G., 2014. Beyond the Basics: Evaluating Model-Based Precipitation Forecasts Using Traditional, Spatial, and Object-Based Methods. *Weather and Forecasting*, 29(6), pp.1451–1472. Available at: http://dx.doi.org/10.1175/waf-d-13-00135.1.

Wolff, M.A., Isaksen, K., Petersen-Øverleir, A., Ødemark, K., Reitan, T., Brækkan, R., 2015. Derivation of a new continuous adjustment function for correcting wind-induced loss of solid precipitation: results of a Norwegian field study. Hydrol. Earth Syst. Sci., 19, pp.951-967. Available at: https://doi.org/10.5194/hess-19-951-2015

Zhu, Y. & Newell, R.E., 1998. A Proposed Algorithm for Moisture Fluxes from Atmospheric Rivers. *Monthly Weather Review*, 126(3), pp.725–735.

Appendix

Table A1: *The AA grid point box metrics and how they were calculated.*

Box Metric Name	**Calculated by**	**Box size**
Maximum	The maximum value of the nine 24 hr accumulated grid box points	3 x 3
Minimum	The minimum value of the nine 24 hr accumulated grid box points	3 x 3
Mean	The mean of the nine 24 hr accumulated grid box points	3 x 3
Median	The median of the nine 24 hr accumulated grid box points	3 x 3
Station	The central grid point in the box, covering the real station location	3 x 3
MET high	The upper 85th percentile of the 225 grid points in the box. Accumulated over 24hr	15 x 15
MET low	The lower 25th percentile of the 225 grid points in the box. Accumulated over 24hr	15 x 15

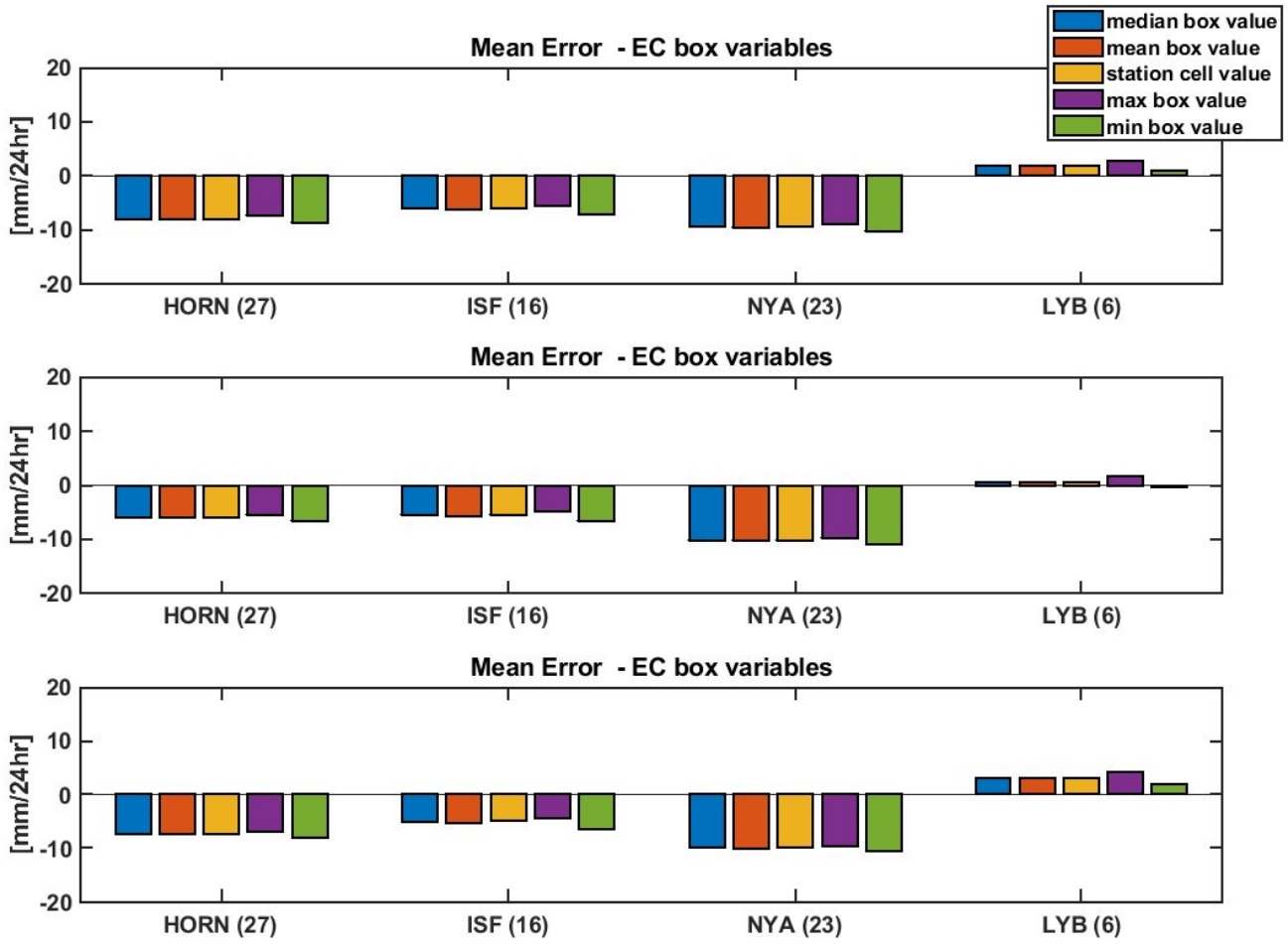

Figure A1: *ME, here is the figure for EC box values for different lead times. Upper panel 6 hr leadtime, middle panel 18hr, lower panel 30 hr leadtime.*

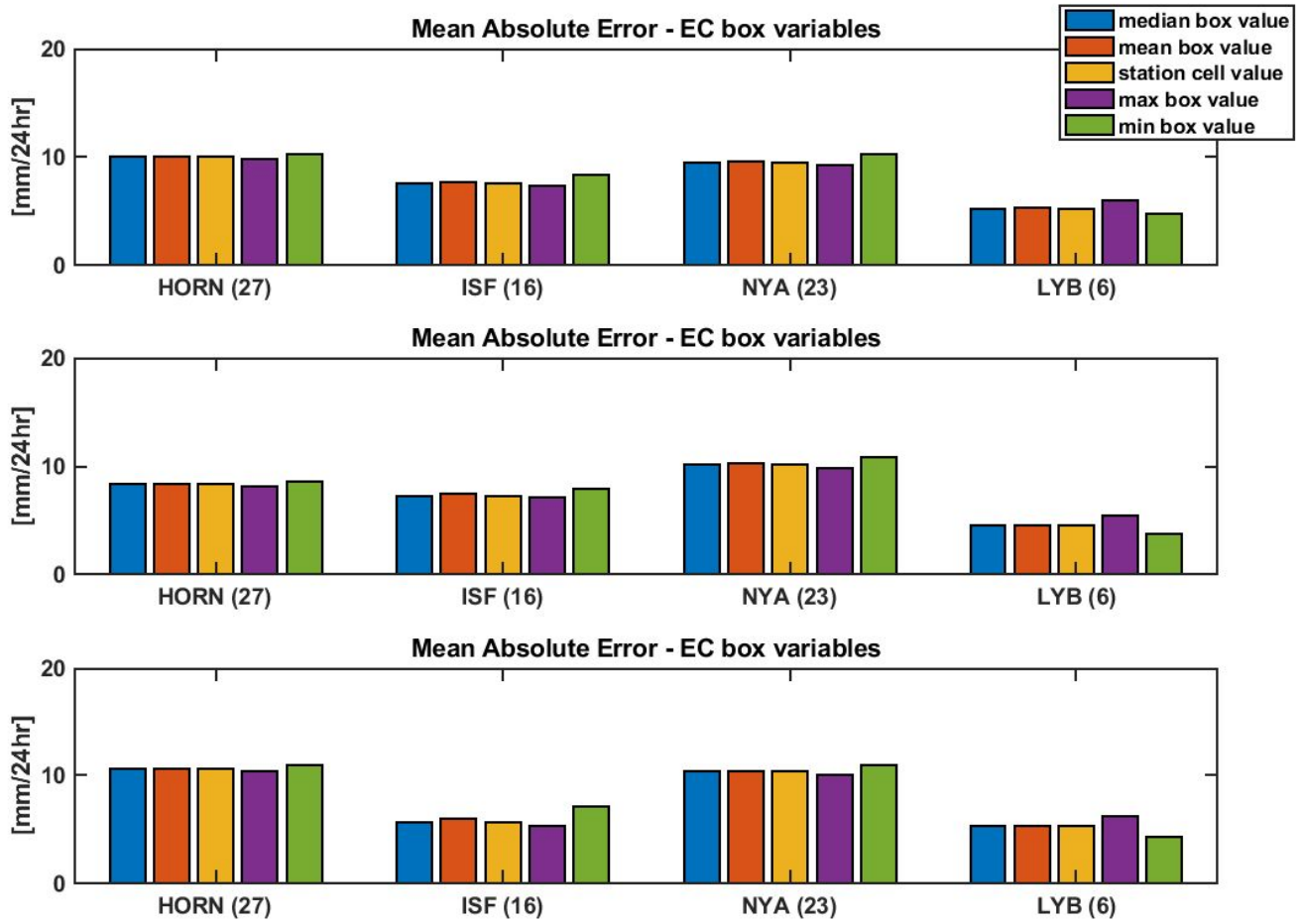

Figure A2: *MAE for EC box values at different lead times. Upper panel 6 hr leadtime, middle panel 18hr, lower panel 30 hr leadtime.*

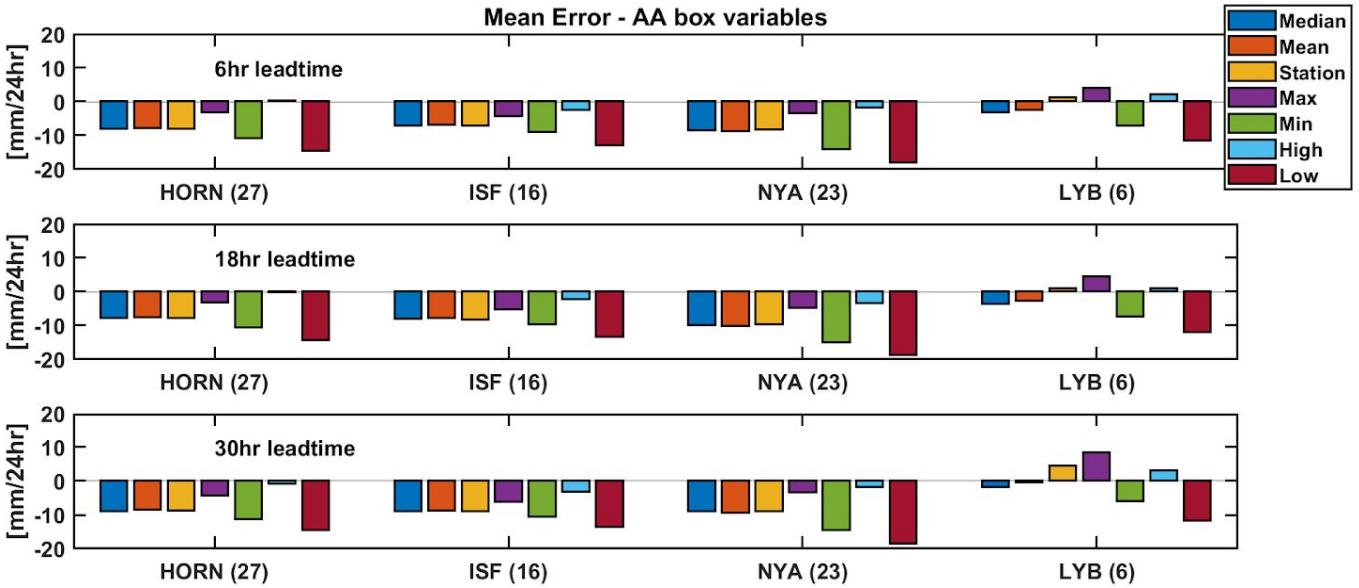

Figure A3: *ME for AA box values for different lead times. Upper panel 6 hr leadtime, middle panel 18hr, lower panel 30 hr leadtime.*

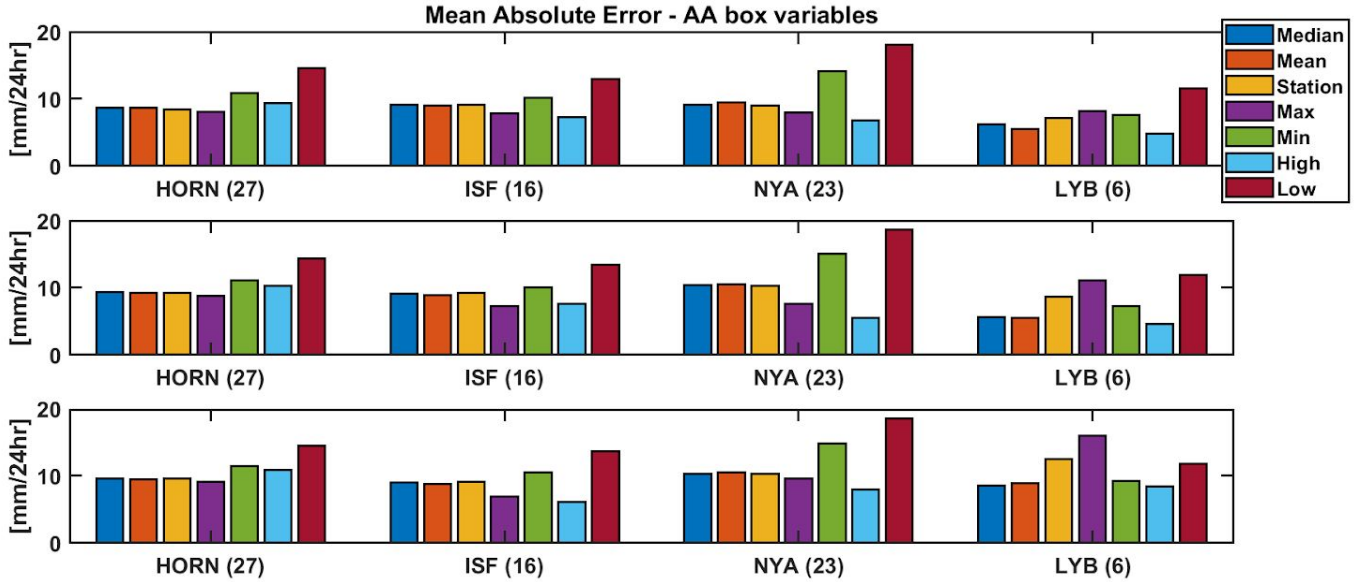

Figure A4: *MAE for AA box values for different lead times. Upper panel 6 hr leadtime, middle panel 18hr, lower panel 30 hr leadtime.*

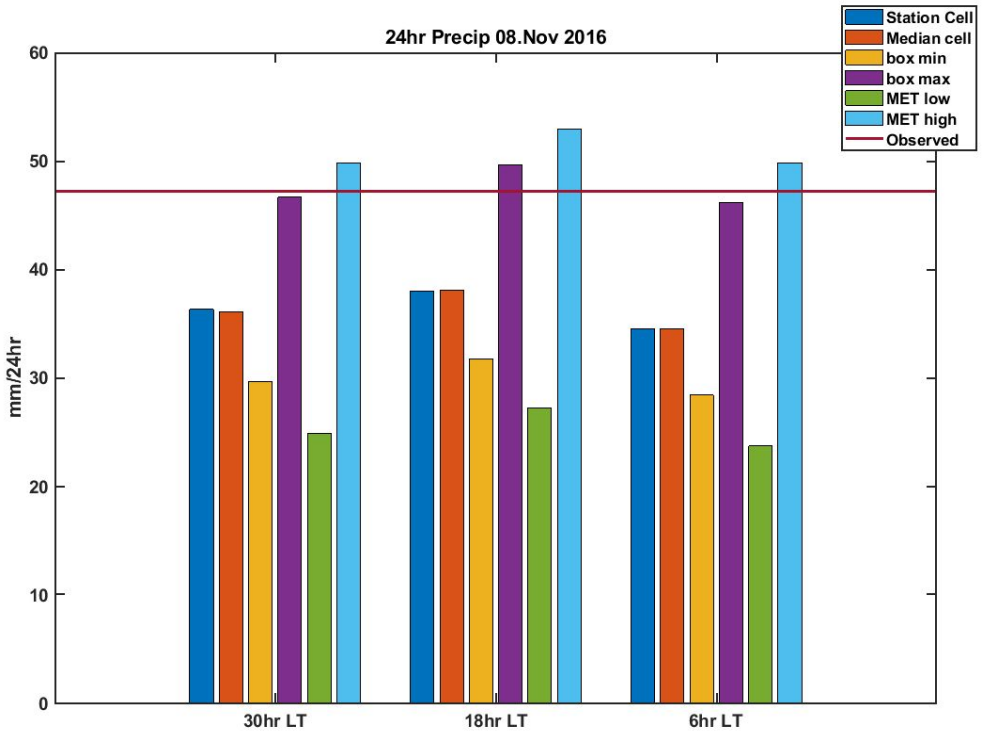

Figure A5: *Total Accumulated 24 hr precipitation at Isfjord Radio during the 8.November event 2016, different box variables (bars) and observation (horizontal line).*

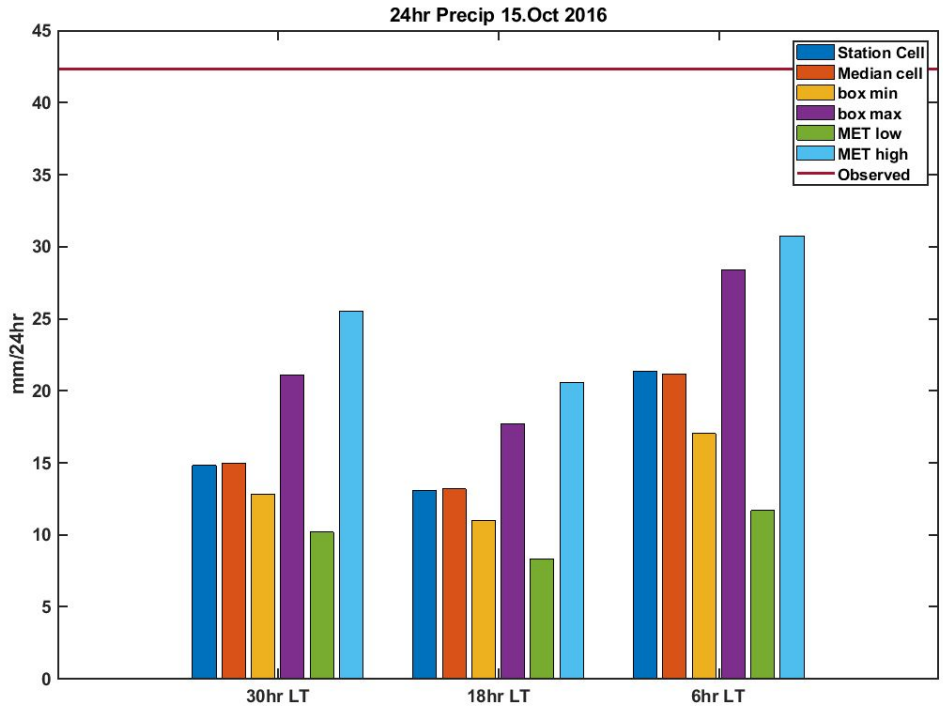

Figure A6: *Same as for fig A5, but for the 15.Oct event at Isfjord Radio.*

Figure A7: *Image from UNIS towards Adventdalen, one of the days where the manual rain gauge at Longyearbyen and Adventdalen ECRN-50 measured 1mm or more of precipitation, but not the Adventdalen Geonor-200. Date and time in image. Note the wet asphalt close to the camera. Credit: Eiliv Leren, Borealis Panorama, longyearbyen.kystnor.no*

Figure A8: *As Fig A7, for another day. Credit: Eiliv Leren, Borealis Panorama, longyearbyen.kystnor.no*

Figure A9: *As Fig A7, for another day. Credit: Eiliv Leren, Borealis Panorama, longyearbyen.kystnor.no*

Figure A10: *As Fig A7, for another day. Credit: Eiliv Leren, Borealis Panorama, longyearbyen.kystnor.no*

Figure A11: *As Fig A7, but for another day. Credit: Eiliv Leren, Borealis Panorama, longyearbyen.kystnor.no*

Figure A12: *As Fig A7, for another day. Credit: Eiliv Leren, Borealis Panorama, longyearbyen.kystnor.no*

Figure A13: *As Fig. A7, for another day. Credit: Eiliv Leren, Borealis Panorama, longyearbyen.kystnor.no. Note the dry asphalt close to the camera in this image.*

Figure A14: *Image from the hour in the 18-19.Aug 2018 heavy rain event where ECRN-50 in Adventdalen measured 3mm, and ECRN-50 at Bjonapynten 5mm.*

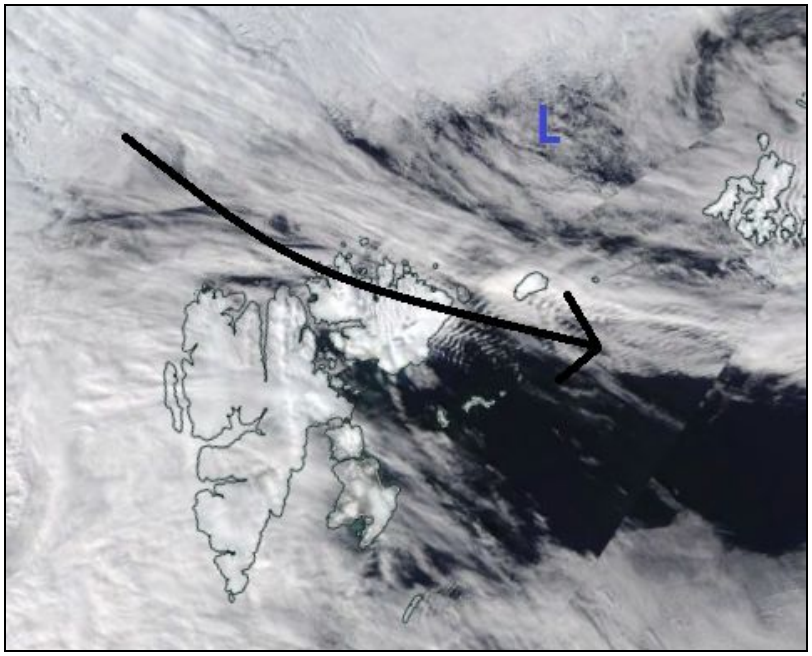

Figure A15: *Composite satellite image, from the Soumi-NPP satellite, of the low pressure through (blue L) located northeast of Svalbard the 01.July August 2018. General airflow is denoted with black arrow. Credit: NASA Worldview Application (https://worldview.earthdata.nasa.gov).*

Figure A16: *Image from Bjonapynten 03.August 2018 04:03 UTC, showing Bjonapynten rain gauge station and Tempelfjorden in rainy conditions This day Bjonapynten measured 3 mm and Tuna South measured 7 mm precipitation in 24 hr.*

Rain gauge station overview

Tempelfjorden stations

Tuna South

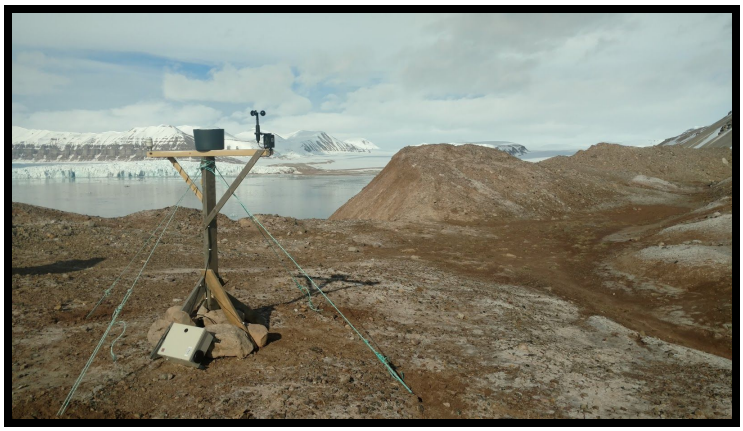

Image towards north east, Tunabreen in the background left.

Location: N78 24.898’ E17 15.271’
Date set up: 11.June
Measurements: *ECRN-50:* Precipitation
Wind-Sentry: Wind speed max and avg. (hourly values)
Tiny Tag: Temperature, Relative Humidity (hourly values)
Logger: CR200
Location details: Located 24 m.a.s.l. it stands on a ridge (see map). Can be spotted from afar, but not from landing site. Land on the beach west of the ridge top and then go up on the ridge and to the left (north east) when at the highest point of the ridge it should be easy to spot.

Murdoch

Picture taken towards north east, Tunabreen in the background.

Location: N 78 25.715' E17 04.715'
Date set up: 15.August
Measurements: *ECRN-50:* Precipitation, (hourly values)
Tiny Tag: Temperature air (white) and ground (black) (hourly values)
Logger: CR10
Location details: Located approx. 40m from the shore on the north eastern parts of the Murdoch fan, south west of Kapp Murdoch itself. Broken by animals 18.August.

Bjonapynten

Picture taken towards east, Tempelfjorden in the background

Location: N 78 23.138' E16 50.775'
Date set up: 11.June
Measurements: *ECRN-50:* Precipitation (hourly values)
Tiny Tag: Temperature, Relative Humidity (all hourly values)
Logger: CR10
Location details: Located approx 30 m east (further out) from the UNIS weather station mast.

Longyearbyen stations

Adventdalen

Location: N78 12.134', E15 49.817'
Date set up: 11.June
Measurements: *ECRN-50:* Precipitation
Wind-Sentry: Wind speed max and avg. (hourly values)
Tiny Tag: Temperature, Relative Humidity (hourly values)
Logger: *CR200*
Location details: Located approx 50 m west, towards old Aurora station, from the UNIS weather station mast.

Longyearbyen Airport

Location: N 78 14.818', E 15 30.205'
Date set up: 23. Aug
Measurements: *ECRN-50:* Precipitation, (hourly values)
Logger: *CR10*
Location details: Located approx 10 m north (further out) from the MET manual rain gauge. Removed for field work at Kapp Linne from 13.Sep to 21.Sep in the AGF-213 course. Broken by animals.

Breinosa

No Image

Location: N 78 08.798'N, E 16 02.286'
Date set up: 23..Aug
Measurements: *ECRN-50:* Precipitation, (hourly values)
Logger: *CR10*
Location details: Located approx. 5m north of the UNIS AWS at Breinosa by the Kjell Henriksen Observatory. Removed for field work at Kapp Linne from 13.Sep to 21.Sep in the AGF-213 course.